

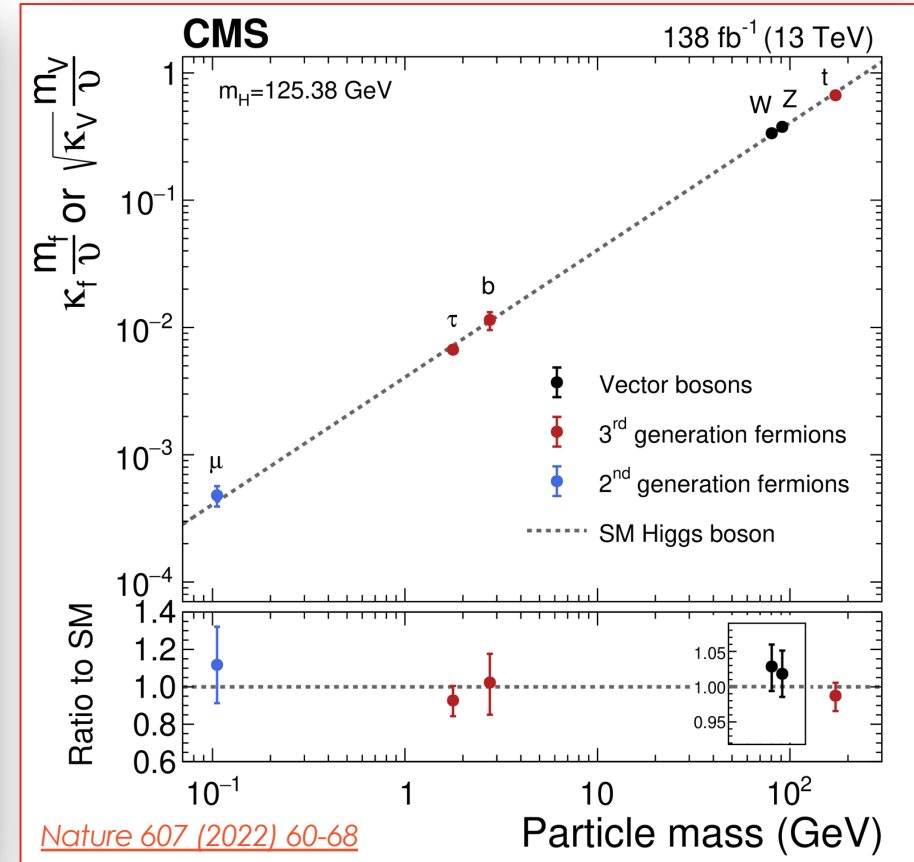
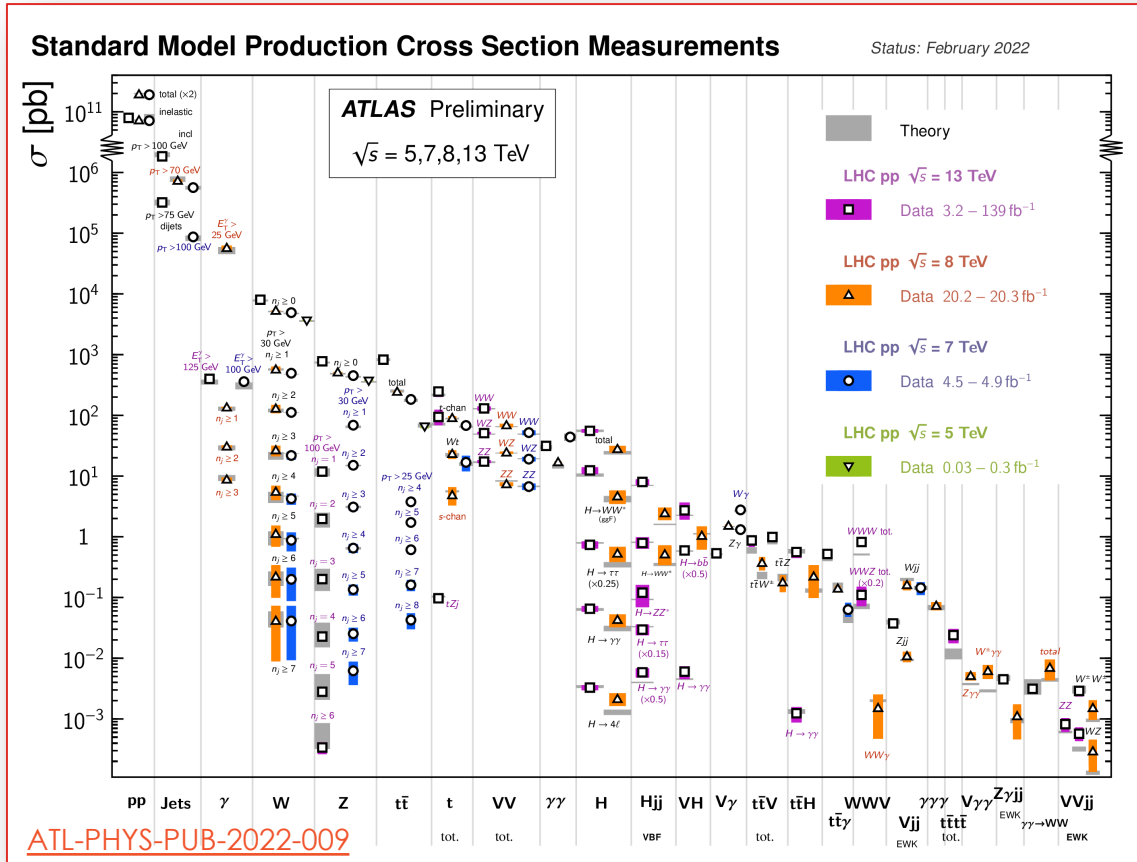


New Physics Searches in an Effective Field Theory context

Valentina Maria Martina Cairo

On behalf of the
ATLAS & CMS collaborations

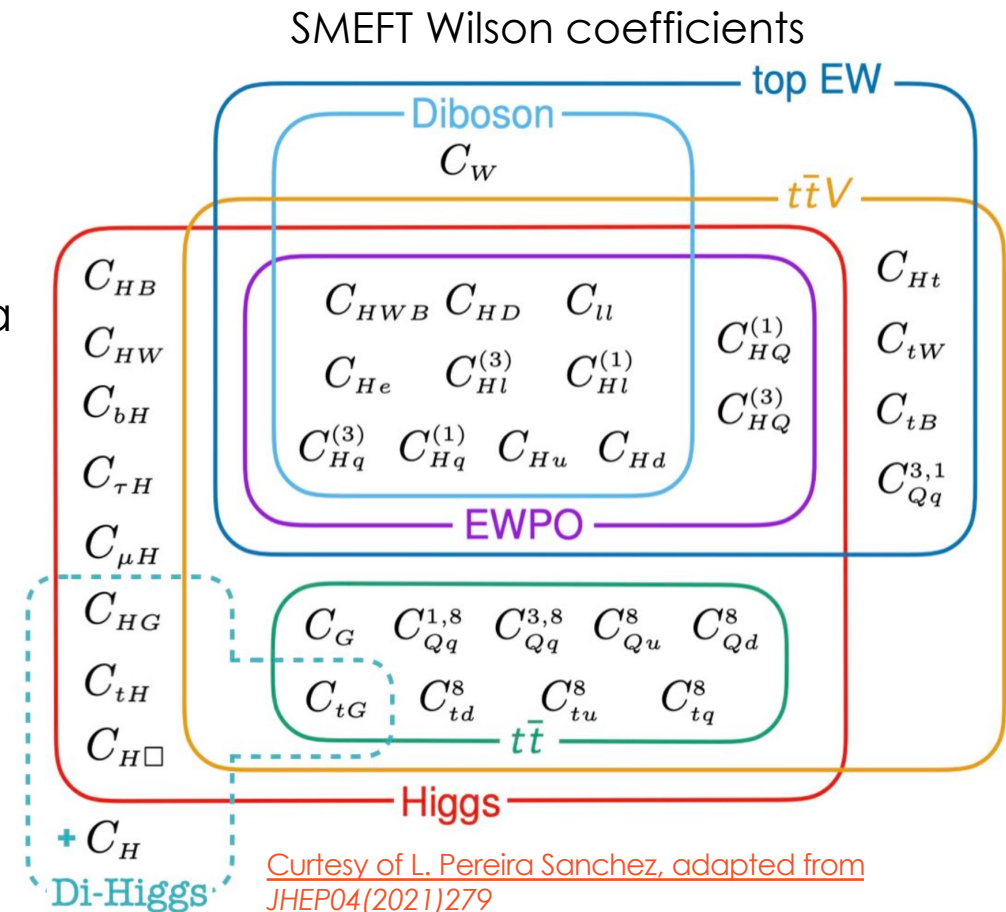
THE STANDARD MODEL: A STORY OF SUCCESS



So far, the *Standard Model* rules, but we know it has its shortcomings and the exploration has just begun...

EFFECTIVE FIELD THEORIES AT THE LHC

- Searching for **physics Beyond the Standard Model (BSM)**
major goal of particle physics
- **Higgs, Top and electroweak precision measurements** benefit from a global approach in the framework of **Effective Field Theories (EFT)**
 - Different operators sensitive to different phenomena
- **SMEFT (SM EFT, Higgs fields as doublets)** or **HEFT (Higgs EFT, physical Higgs boson)**
- SMEFT typically expanded to dim. 6 operators, dim. 8 included to probe certain couplings
- HEFT more general than SMEFT, certain coefficients become independent



DIRECT VS INDIRECT PROBES

Direct

BSM effect **fully simulated**
Analyses optimized for EFT parameters

Potentially **better sensitivity** to a **smaller set of operators**

- More difficult to combine due to overlap

Optimal Observables based on Matrix Element Method (MELA) or on parameterized classifiers optimized with ML

Indirect

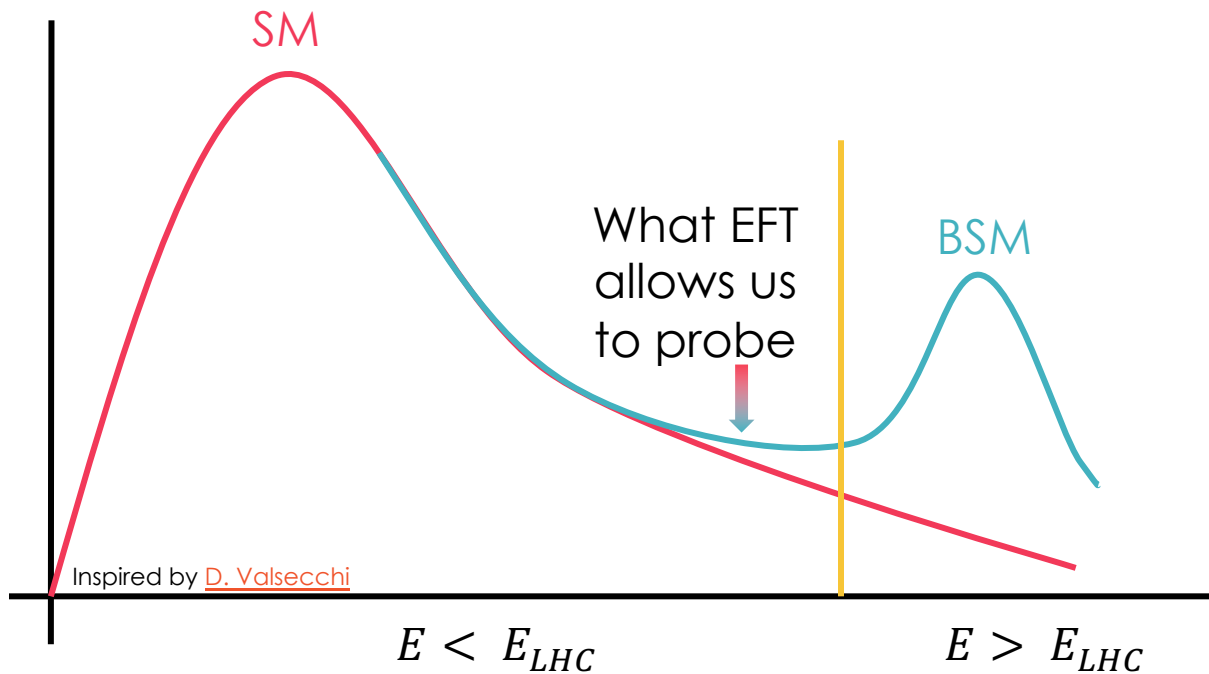
Reinterpretation of existing measurements
(e.g STXS in the Higgs)

Access to **more operators** but with potentially **reduced sensitivity**

- Power comes from combinations

Acceptance effects may be difficult to model

EXPERIMENTAL OBSERVABLES



$$\mathcal{L}_{SMEFT} = \mathcal{L}_{SM} + \mathcal{L}^5 + \mathcal{L}^6 + \mathcal{L}^7 + \mathcal{L}^8 + \dots,$$

Odd dim. neglected (1/b number violations)

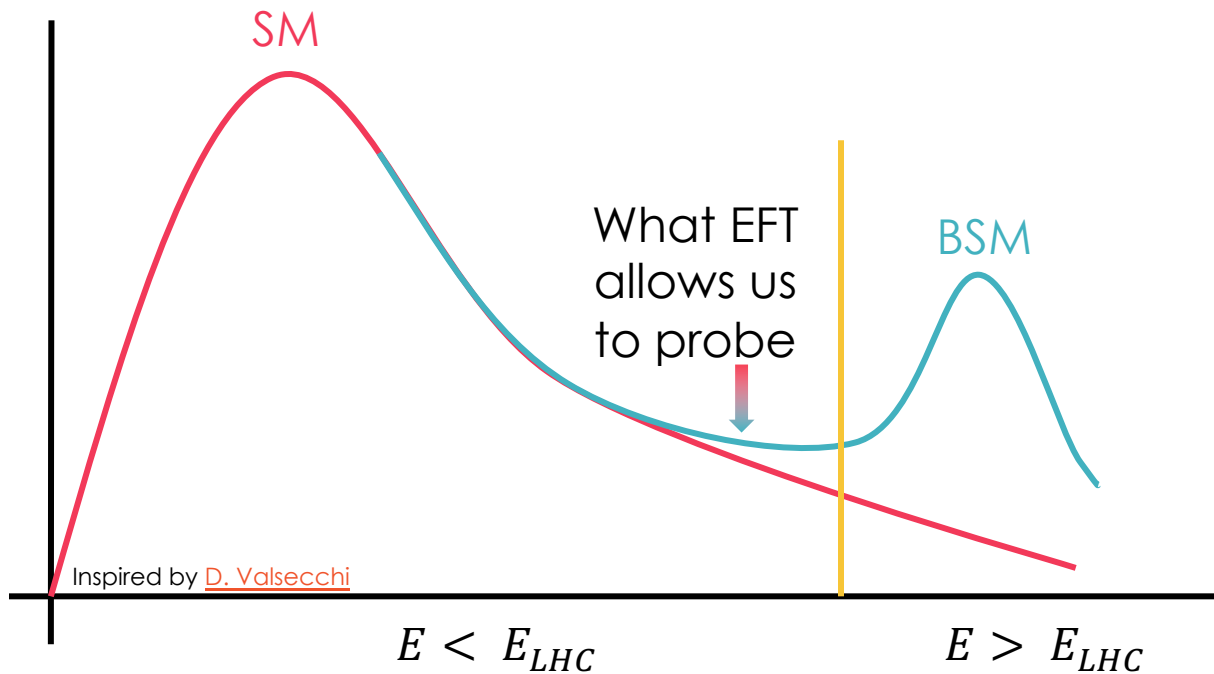
$$\mathcal{L}^{(d)} = \sum_{i=1}^{n_d} \frac{C_i^{(d)}}{\Lambda^{d-4}} Q_i^{(d)} \quad \text{for } d > 4$$

Wilson Coefficient

Scale of BSM physics

Operator (indicated also with O)

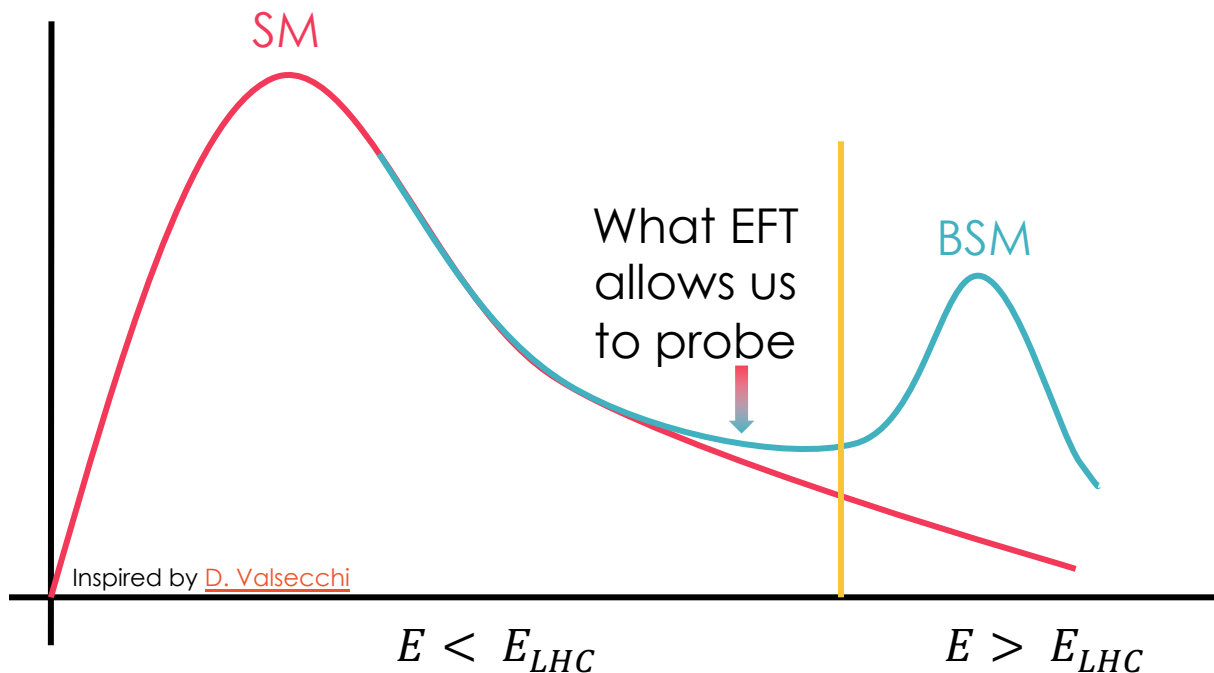
EXPERIMENTAL OBSERVABLES



$$\mathcal{L}_{SMEFT} = \mathcal{L}_{SM} + \mathcal{L}^6 + \mathcal{L}^8 + \dots \Rightarrow$$

$$\sigma_{SMEFT} = \sigma_{SM} + \underbrace{\sigma_{int,6}}_{\substack{\text{linear} \\ (1/\Lambda^2)}} + \underbrace{\sigma_{BSM,6} + \sigma_{int,8} + \dots}_{\substack{\text{quadratic} \\ (1/\Lambda^4)}}$$

EXPERIMENTAL OBSERVABLES



High energy **tails of kinematic observables** enhance experimental sensitivity to SM deviations

- Lin. vs Lin.+Quad. to probe higher order effects

Differential & precise measurements are key

Great complementarity between **SM**, **Top** and **Higgs** sectors to address fundamental physics questions...

$$\mathcal{L}_{SMEFT} = \mathcal{L}_{SM} + \mathcal{L}^6 + \mathcal{L}^8 + \dots \Rightarrow$$

$$\sigma_{SMEFT} = \sigma_{SM} + \underbrace{\sigma_{int,6}}_{\text{linear } (1/\Lambda^2)} + \underbrace{\sigma_{BSM,6} + \sigma_{int,8} + \dots}_{\text{quadratic } (1/\Lambda^4)}$$

7/17/23

8

STANDARD MODEL MEASUREMENTS

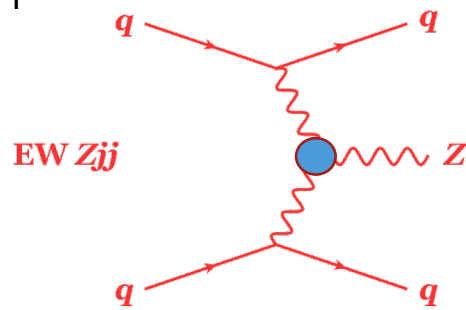
More in [Li Yuan](#), [Shu Li](#),
[W. Hopkins](#), [M. Vos](#)



CP TESTS WITH V-BOSONS

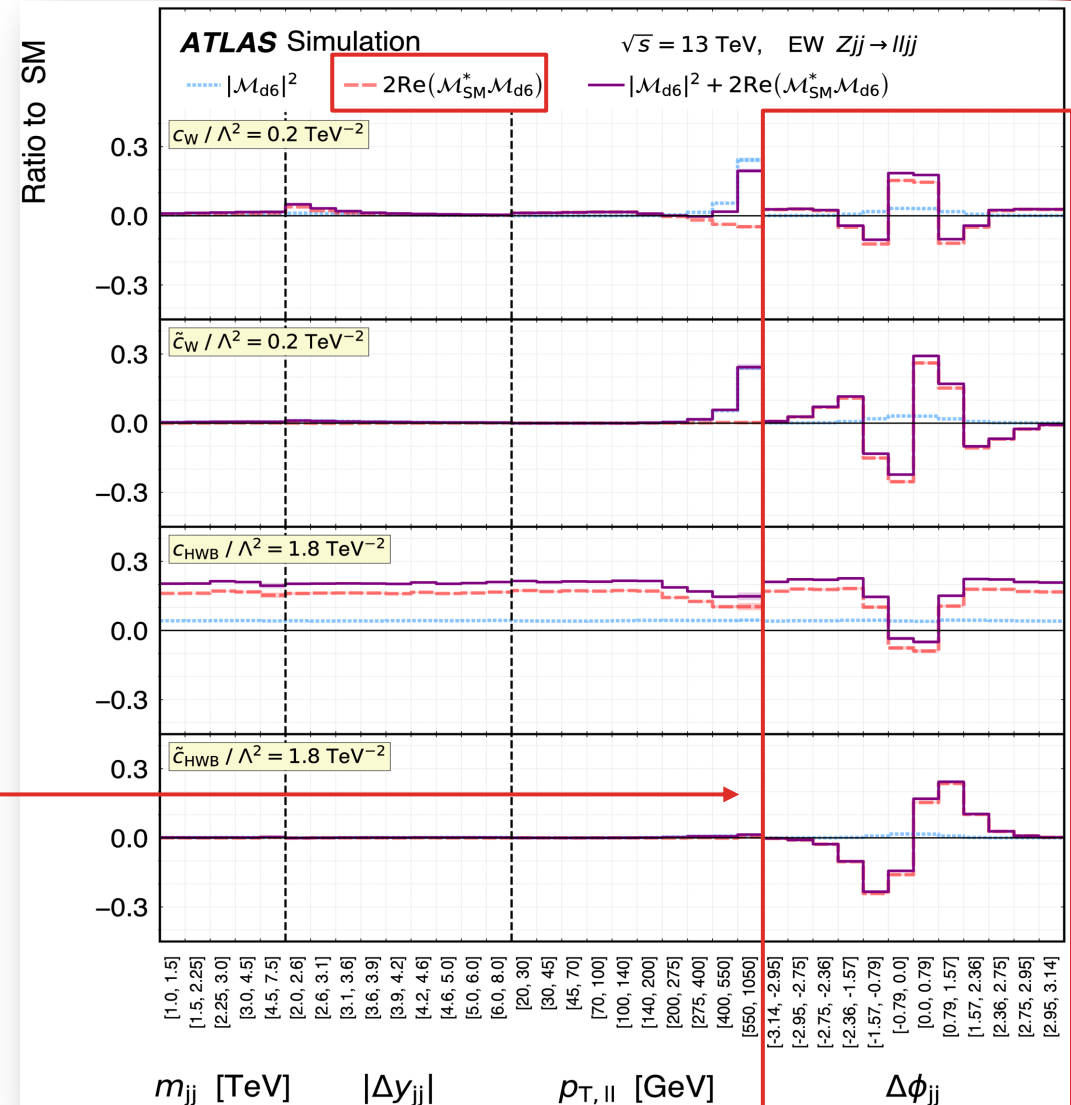
Eur. Phys. J. C 81 (2021) 163

- Additional sources of **CP-violation** required to **explain the matter-antimatter asymmetry** in the Universe \rightarrow can manifest as anomalous Higgs/multiboson interactions
- E.g. ATLAS EW **Zjj Run 2** differential cross-section



- m_{jj} , $|\Delta y_{jj}|$, $p_{T,\parallel}$, $\Delta\phi_{jj}$ sensitive to SM and BSM interference, direct CP test
- Constraints placed on 0_W , 0_{HWB} (CP-even) and $\tilde{0}_W$, $\tilde{0}_{HWB}$ (CP-odd), which produce **anomalous WWZ interactions**, e.g. c_W obs [-0.19,0.41]

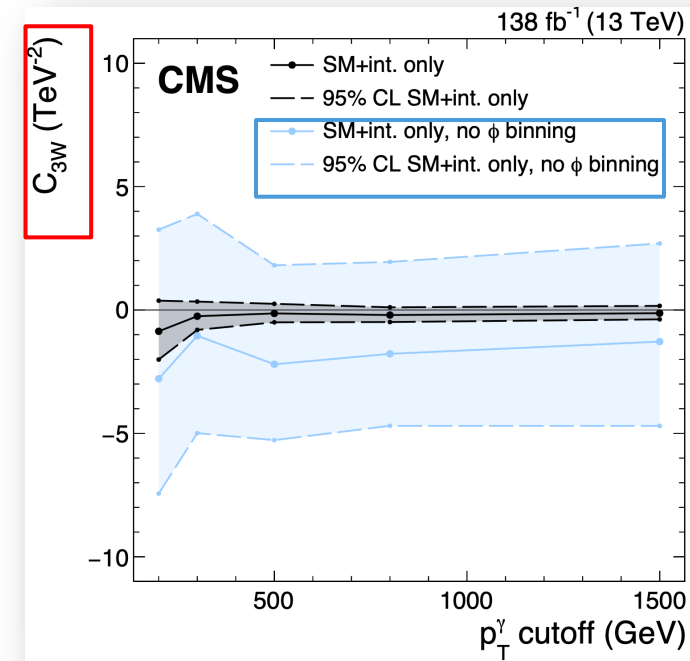
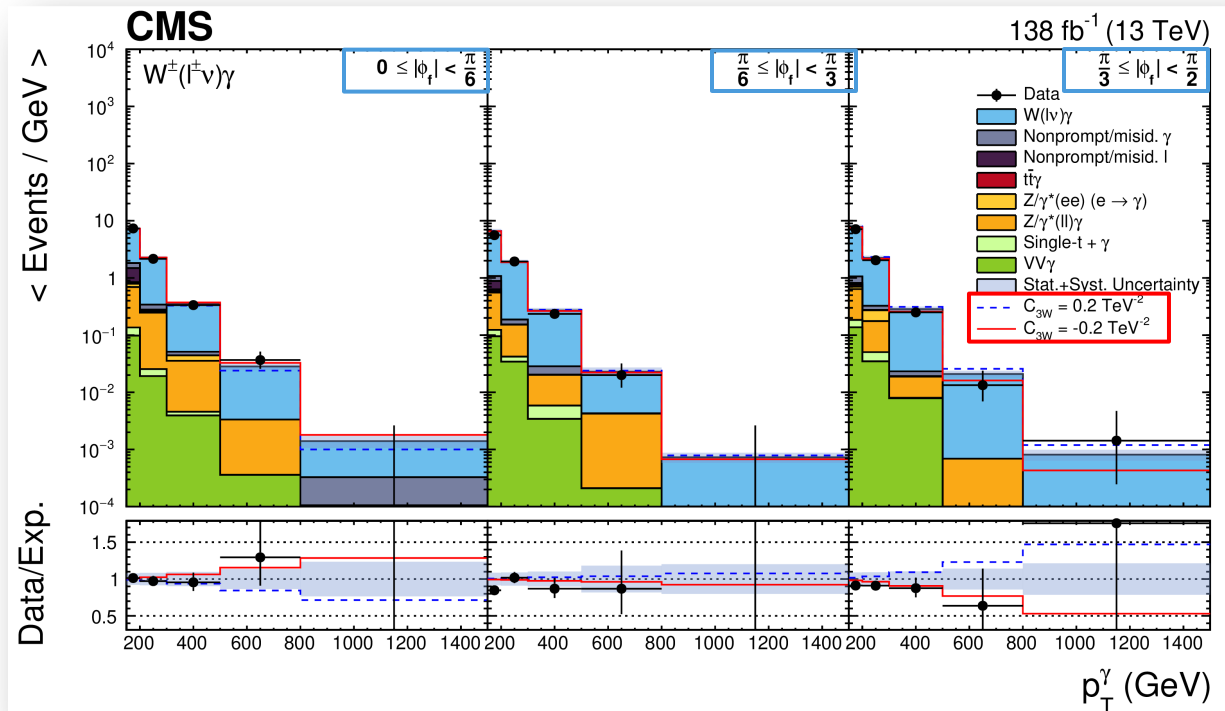
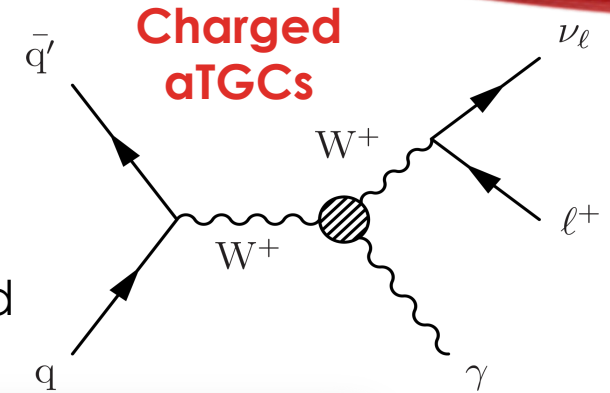
V.M.M.CAIRO



DI-BOSONS AS TESTS OF $aTGC$

Phys. Rev. D 105 (2022) 052003

- $V\gamma$ and VV production sensitive to **anomalous triple gauge couplings (aTGCs)**
- **CMS Run 2 analysis uses p_T^γ and ϕ_l in $W\gamma$ events** to enhance sensitivity to interference between SM and \mathcal{O}_{3W} $\mathcal{O}_{3W} = \epsilon^{ijk} W_\mu^{iv} W_\nu^{j\rho} W_\rho^{k\mu}$
- Similar approach in ATLAS WW +jets ([STDM-2018-34](#)) previously unexplored

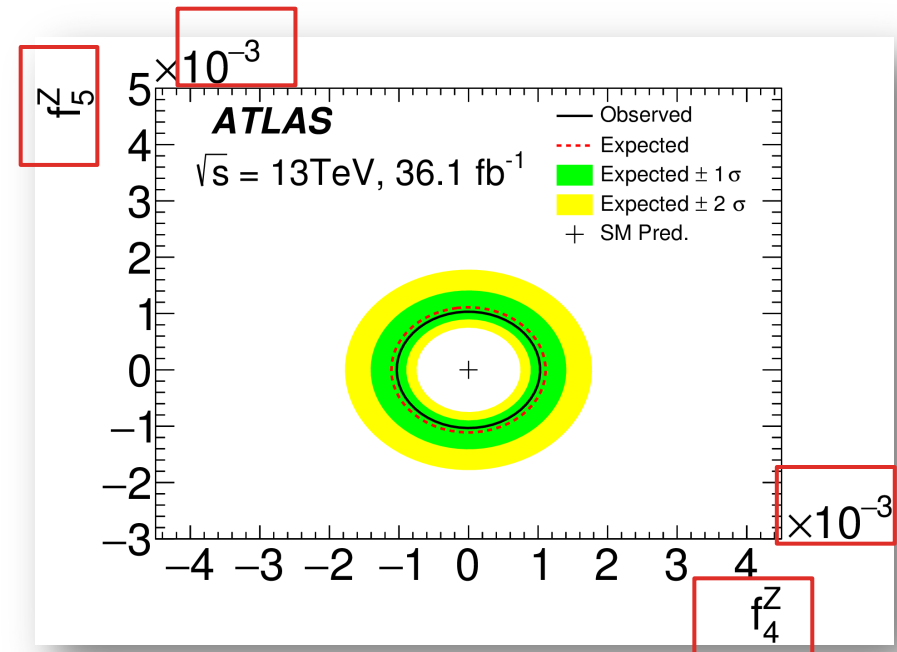
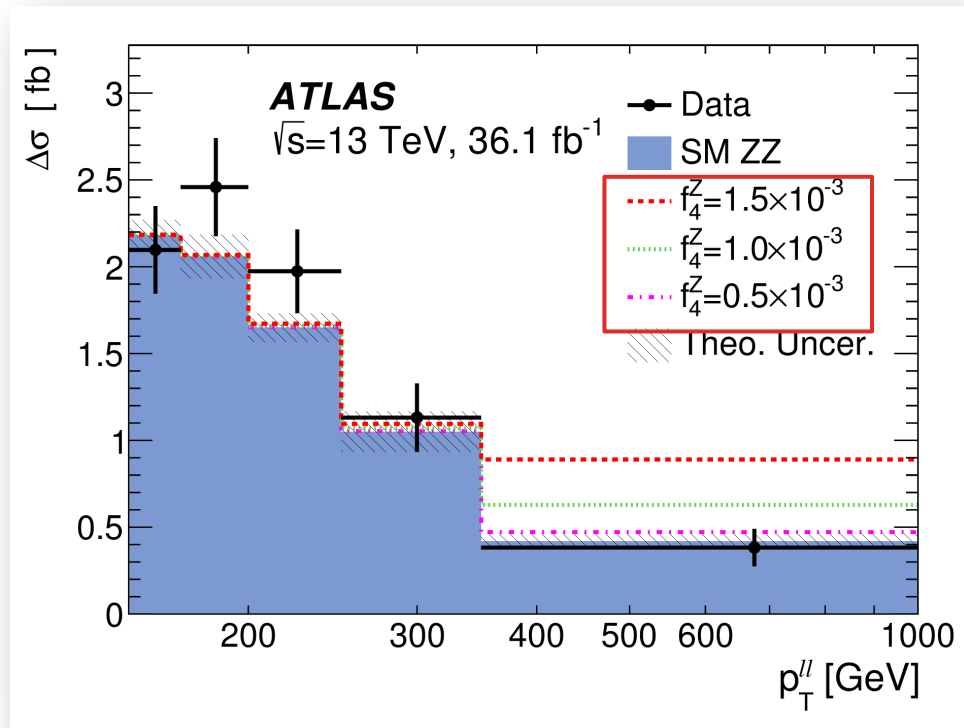
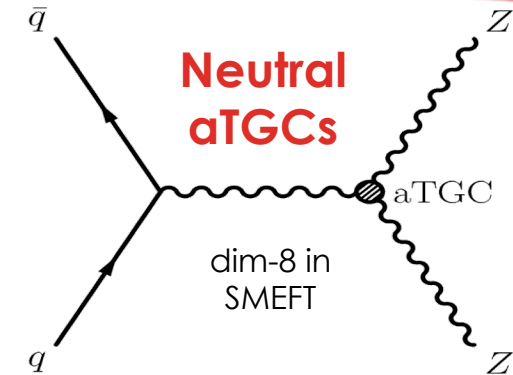


Up to x10 impr. due to ϕ bins

DI-BOSONS AS TESTS OF $aTGC$

[JHEP 10 \(2019\) 127](#)

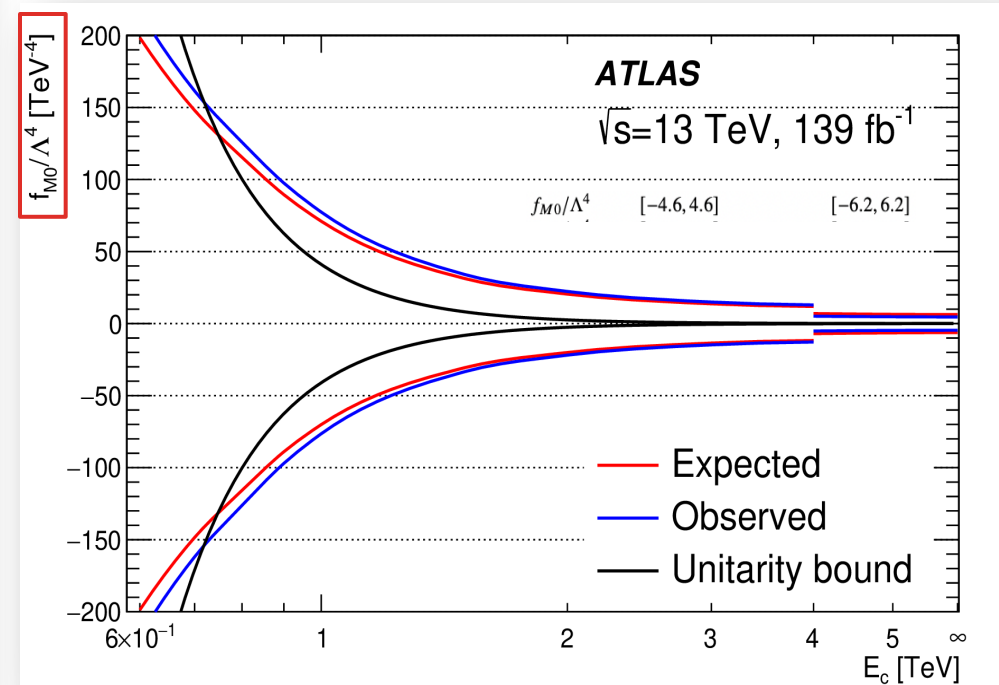
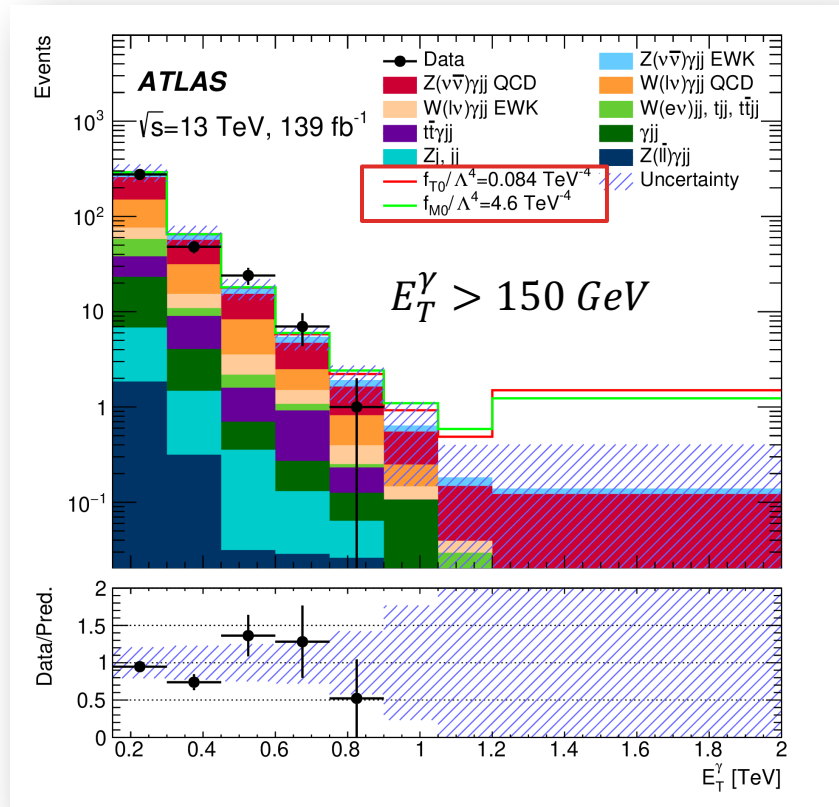
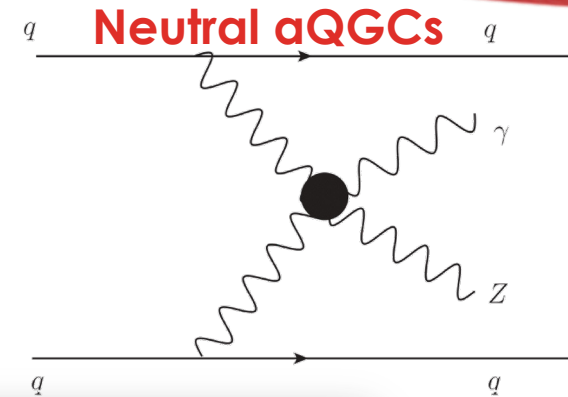
- $V\gamma$ and VV production sensitive to **anomalous triple gauge couplings (aTGCs)**
- ATLAS Run 2 analysis examines high-energy tails of $p_T^{\prime\prime}$ in $ZZ(ll\nu\nu)$ events** (Z boosted against the other in the transv. plane) to test aTGCs in an *effective vertex function* approach
 - f_4^Y and f_4^Z (CP violating), f_5^Y and f_5^Z (CP conserving)



DI-BOSONS AS TESTS OF a QGC

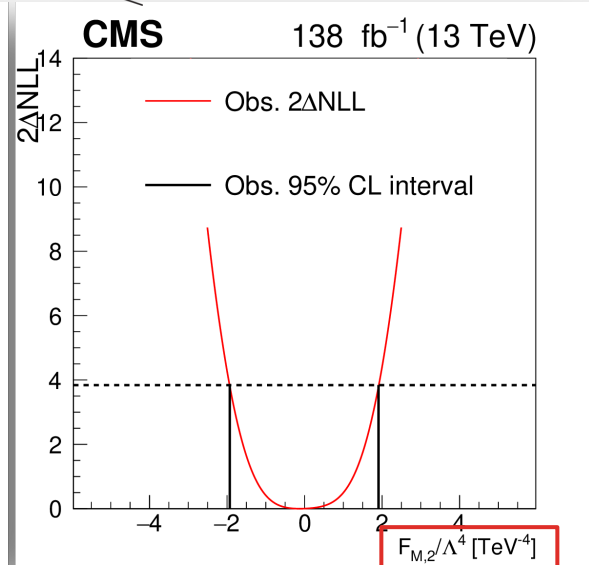
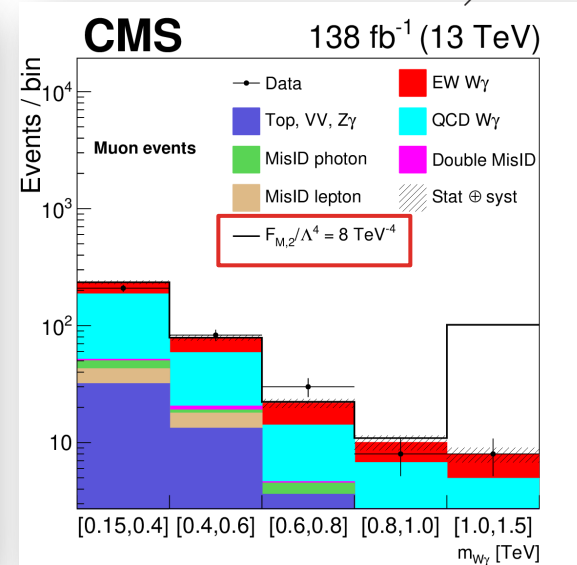
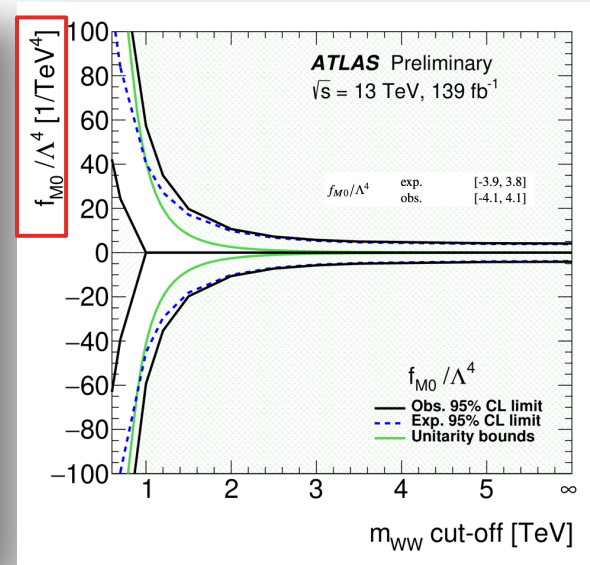
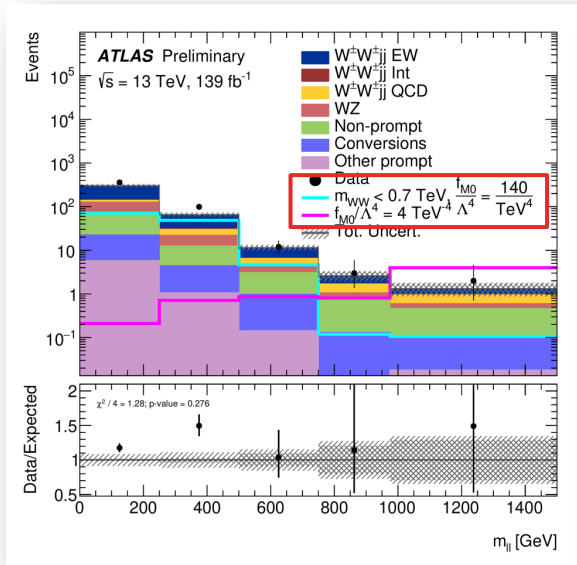
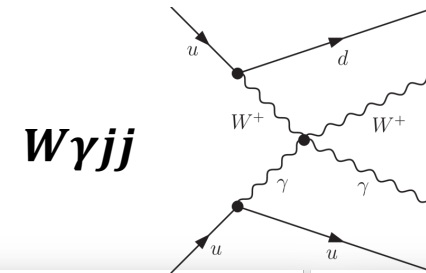
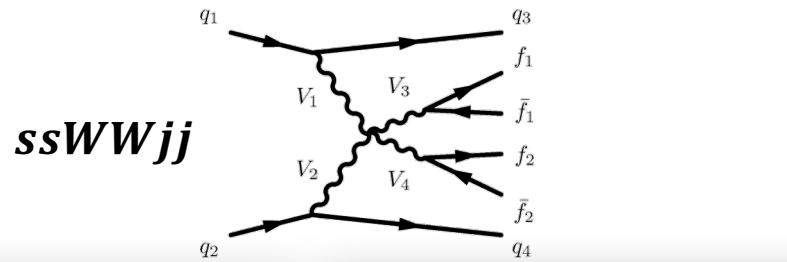
CMS: [2212.12592](#),
 ATLAS: [ATLAS-CONF-2023-023](#), [JHEP 06 \(2023\) 082](#), [ATLAS-CONF-2023-024](#)

- $V\gamma$ or VV plus jets used by CMS and ATLAS to test **anomalous quartic gauge couplings (aQGCs)** (dim. 8 EFT operators)
 - 4 covariant derivatives Higgs field ($O_{S0,1,2}$, scalar type)
 - 2 Higgs covariant derivatives, 2 field strength tensors ($O_{M0,1,2,3,4,5,7}$ of mixed scalar/tensor type)
 - 4 field strength tensors ($O_{T0,1,2,5,6,7,8,9}$ of tensor type)



DI-BOSONS AS TESTS OF a QGC

CMS: [2212.12592](#),
 ATLAS: [ATLAS-CONF-2023-023](#), [JHEP 06 \(2023\) 082](#), [ATLAS-CONF-2023-024](#)



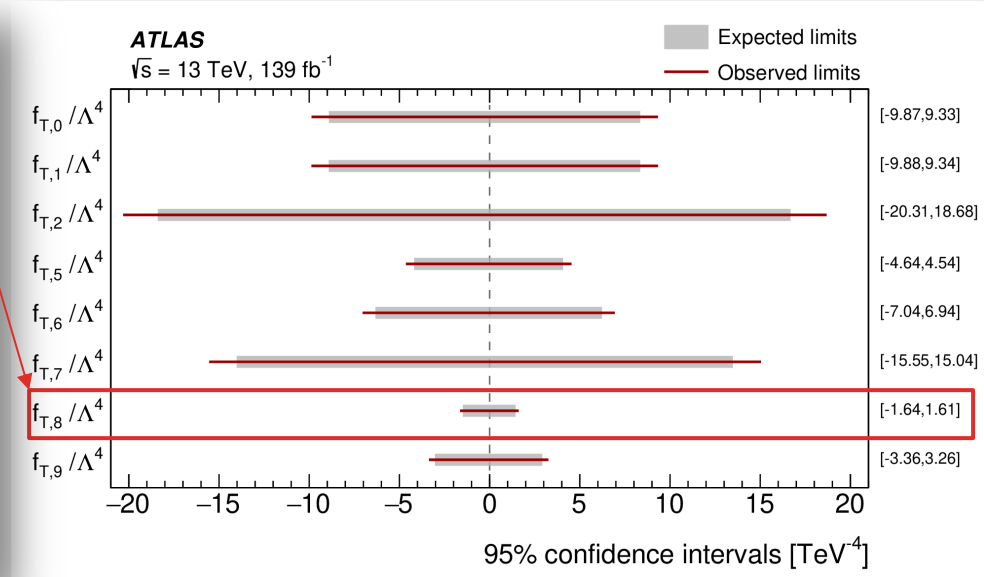
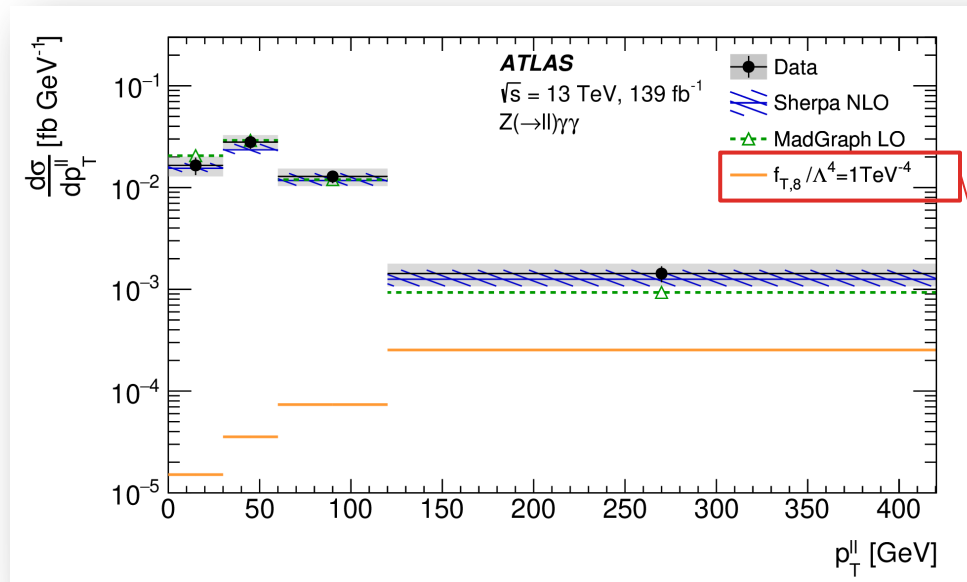
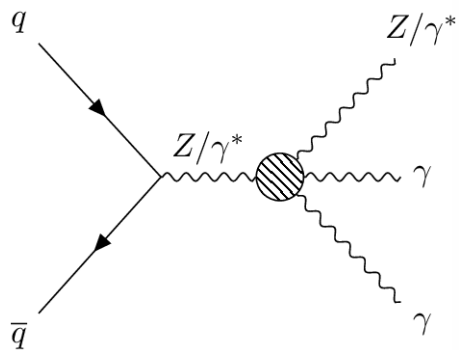
First efforts from ATLAS at combining a QGC results [ATL-PHYS-PUB-2023-002](#)

TRI-BOSONS AS TESTS OF a QGC

Eur. Phys. J. C 83 (2023) 539

- $V\gamma\gamma$ also studied in ATLAS & CMS to test **aQGCs**
- Resent **ATLAS $Z\gamma\gamma$** inclusive and differential cross-section measured
- Sensitive to field strength tensors, with p_T^{ll} distributions providing the highest sensitivity

$$\sigma_{fid}^{Z(\rightarrow\ell\ell)\gamma\gamma} = 2.45 \pm 0.20(\text{stat}) \pm 0.22(\text{syst}) \pm 0.04(\text{lumi}) \text{ fb}$$



CMS' results on $W\gamma\gamma$ and $Z\gamma\gamma$ can be found here: [JHEP 10 \(2021\) 174](#)

TOP MEASUREMENTS

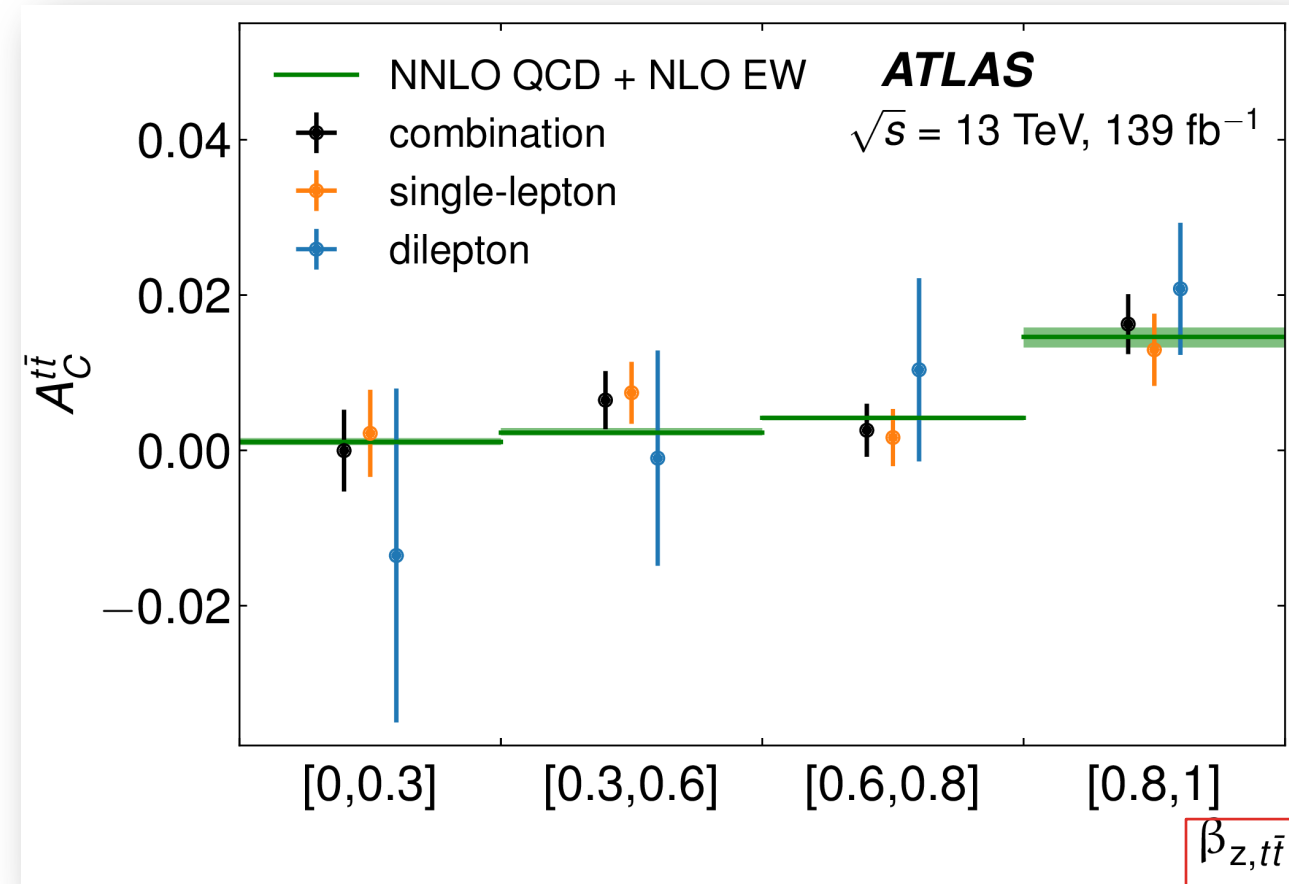
More in [T. Barillari](#), [D. Dobur](#)



$t\bar{t}$ CHARGE ASYMMETRY [2208.12095](#)

$$A_C^{t\bar{t}} = \frac{N(\Delta|y_{t\bar{t}}| > 0) - N(\Delta|y_{t\bar{t}}| < 0)}{N(\Delta|y_{t\bar{t}}| > 0) + N(\Delta|y_{t\bar{t}}| < 0)}$$

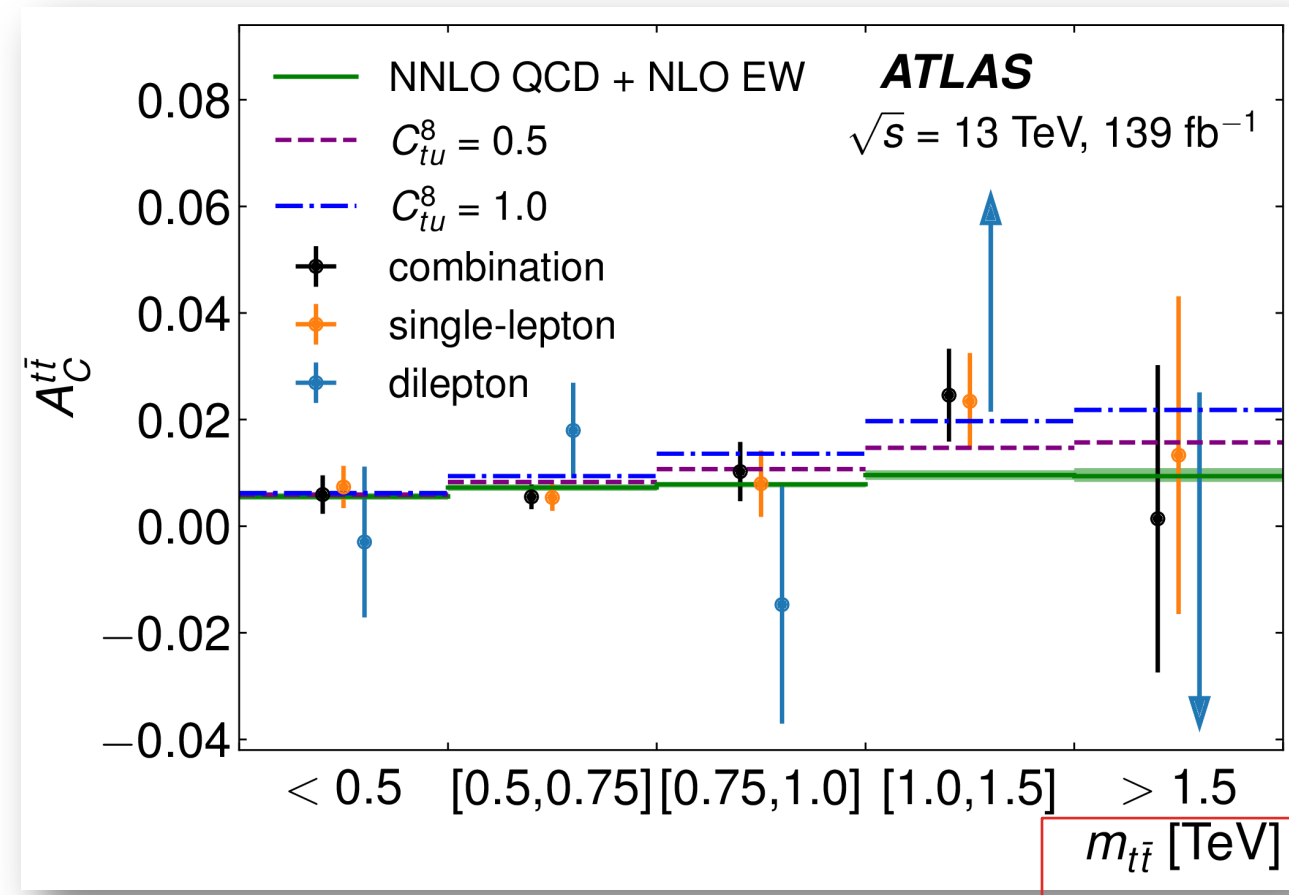
- $\sim O(1\%)$ (symmetric ggF production dominates over asymmetric $q\bar{q}$ and gq)
- Effects can vary with $m_{t\bar{t}}$, $p_{T,t\bar{t}}$, $\beta_{z,t\bar{t}}$
- Full Run 2 ATLAS results report **evidence of $t\bar{t}$ charge asymmetry**
- Combined inclusive $A_C^{t\bar{t}} = 0.0068 \pm 0.0015$, which **differs from zero by 4.7 standard deviations.**



$t\bar{t}$ CHARGE ASYMMETRY 2208.12095

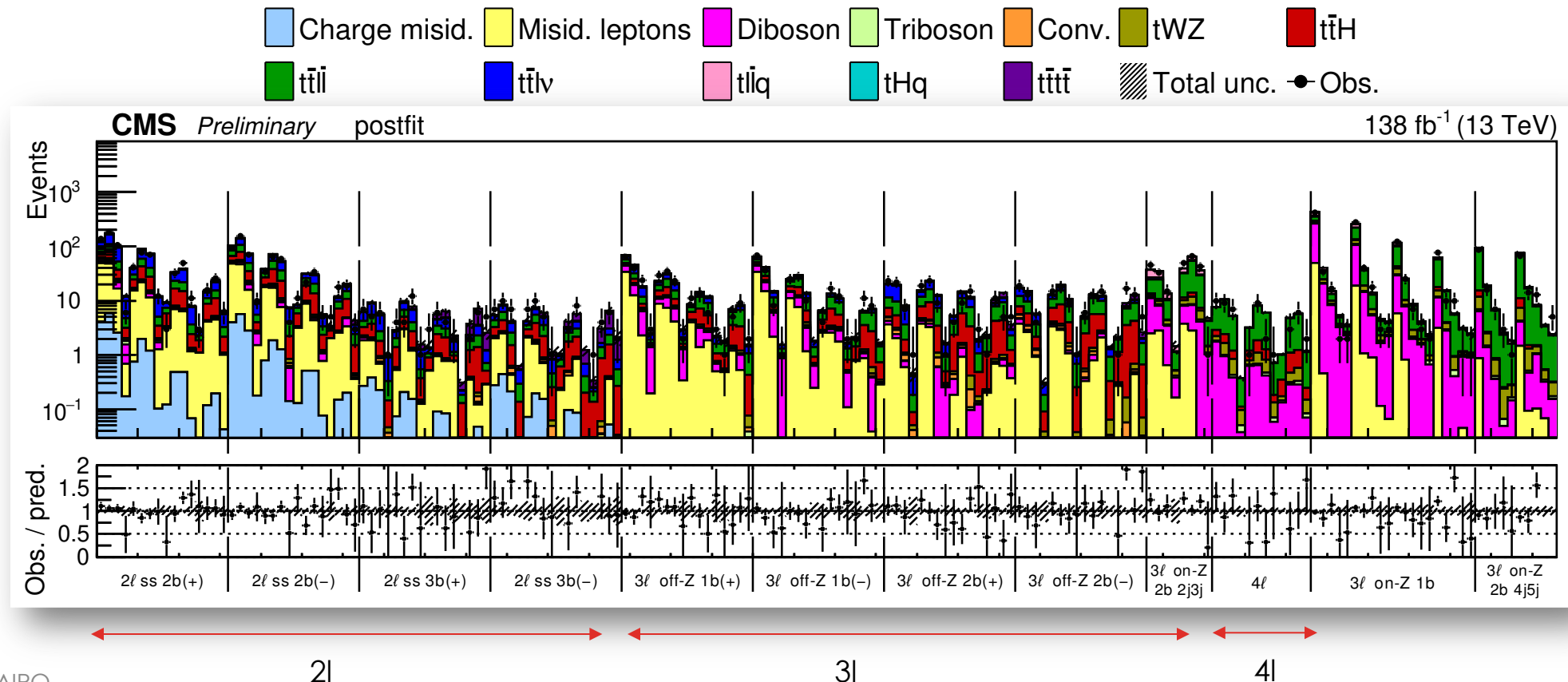
- BSM predicts charge asymmetry varying with $m_{t\bar{t}}$, $p_{T,t\bar{t}}$, $\beta_{z,t\bar{t}}$
- Results are **interpreted in SMEFT**
 - 14 four-fermion operators and 1 top-gluon operator
- **Differential distributions** allow for up to **x2 better** constraints on WCs
- Complementary info to charge asymmetry (see extra slides)

$$O_{tu}^8 = (\bar{t}\gamma_\mu T^A t)(\bar{u}_i\gamma^\mu T^A u_i)$$



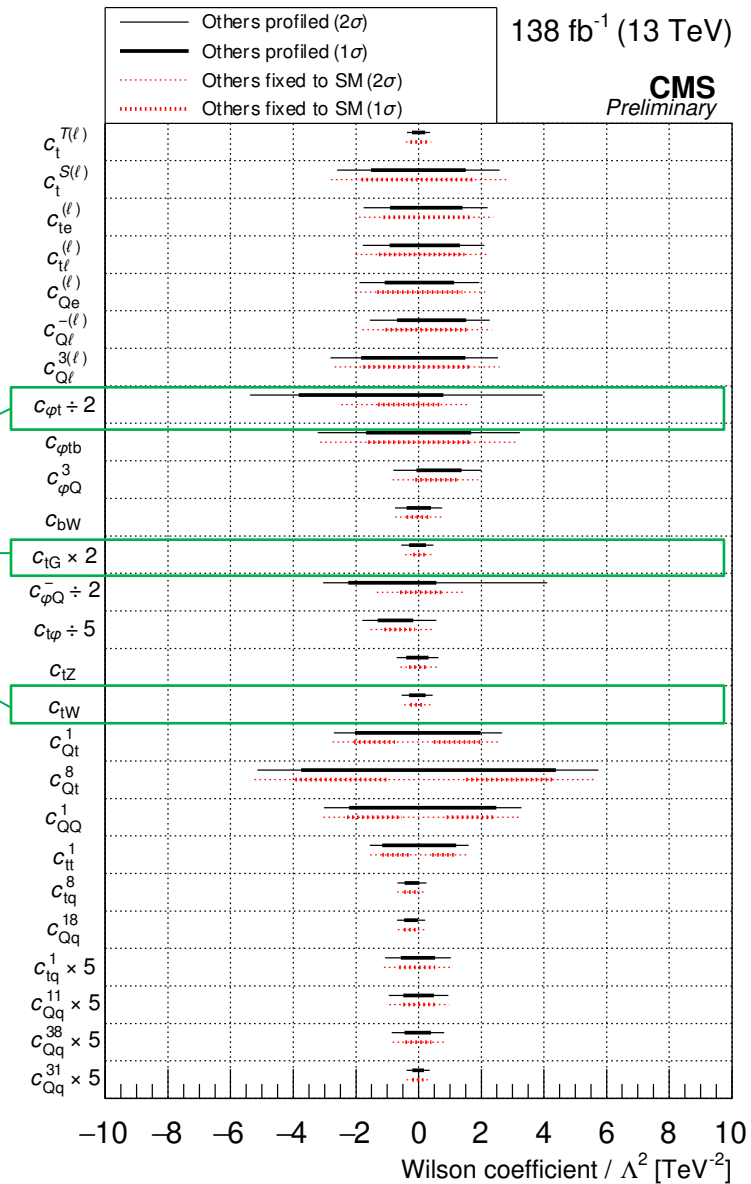
$t\bar{t} + X$ [TOP-22-006](#)

- **Most comprehensive** CMS EFT analysis about top-related operators (top to leptons, bosons, and other heavy quarks)
- Run 2 data, **categories based on lepton, jet, b-jet multiplicity & total lepton charge**
- Targeting ttH , ttZ , ttW , tHq , tZq , $tttt$ processes with **26 WCs** fitted together, **178 analysis bins**

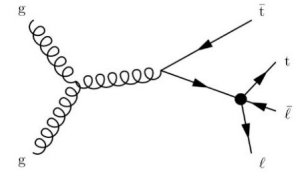


$t\bar{t} + X$ TOP-22-006

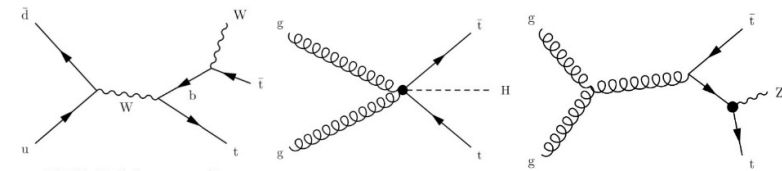
Two heavy with bosons, impact from many processes



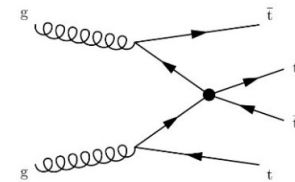
Two heavy two leptons



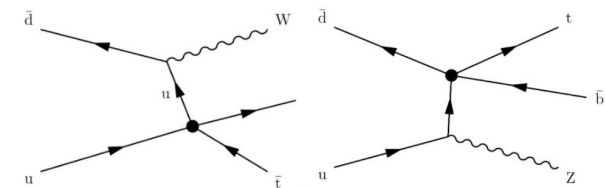
Two heavy with bosons



Four heavy

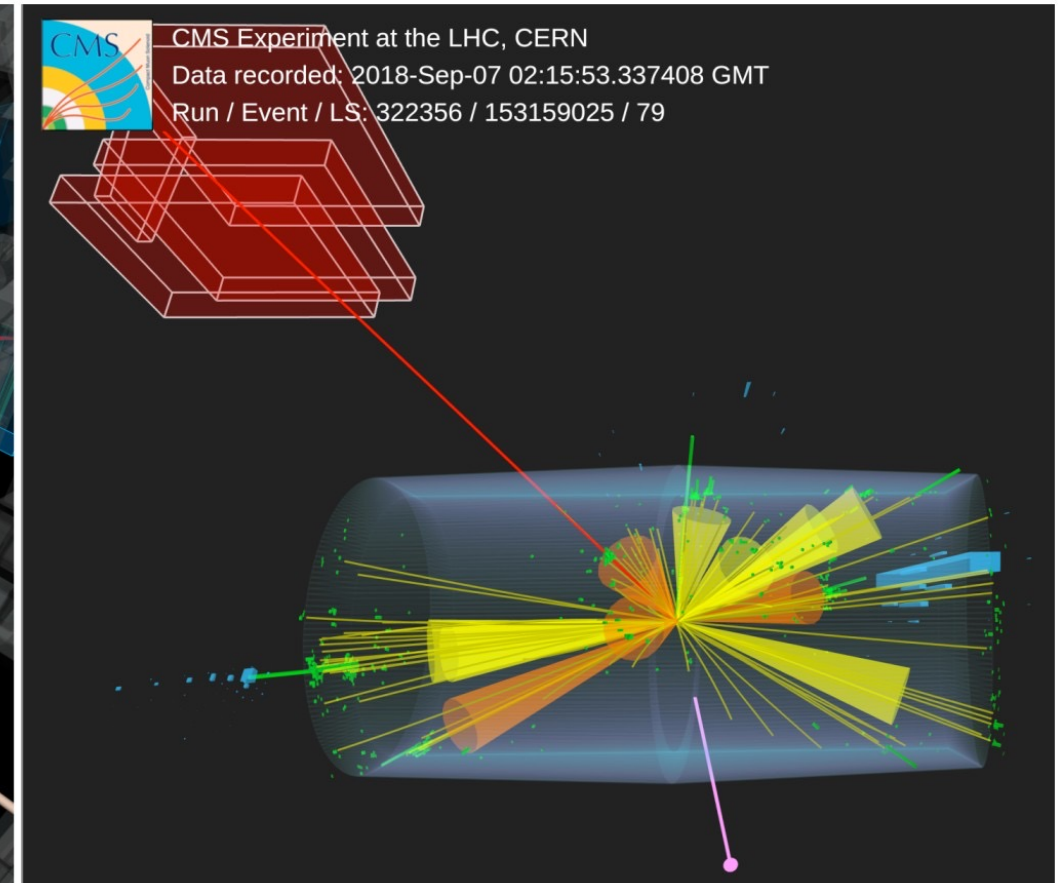
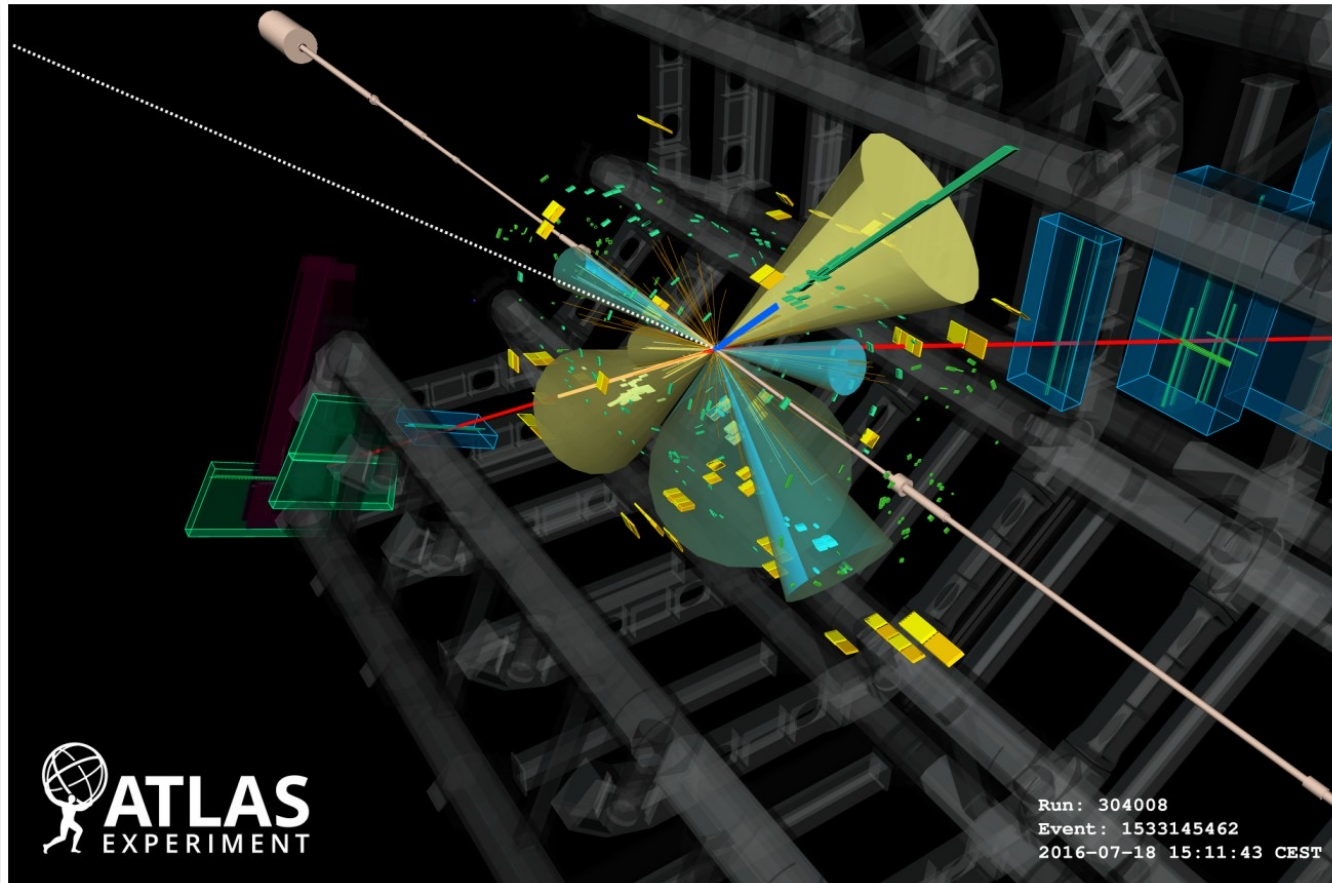


Two heavy two light



4 TOP OBSERVATION *Eur. Phys. J. C 83, 496 (2023), 2305.13439*

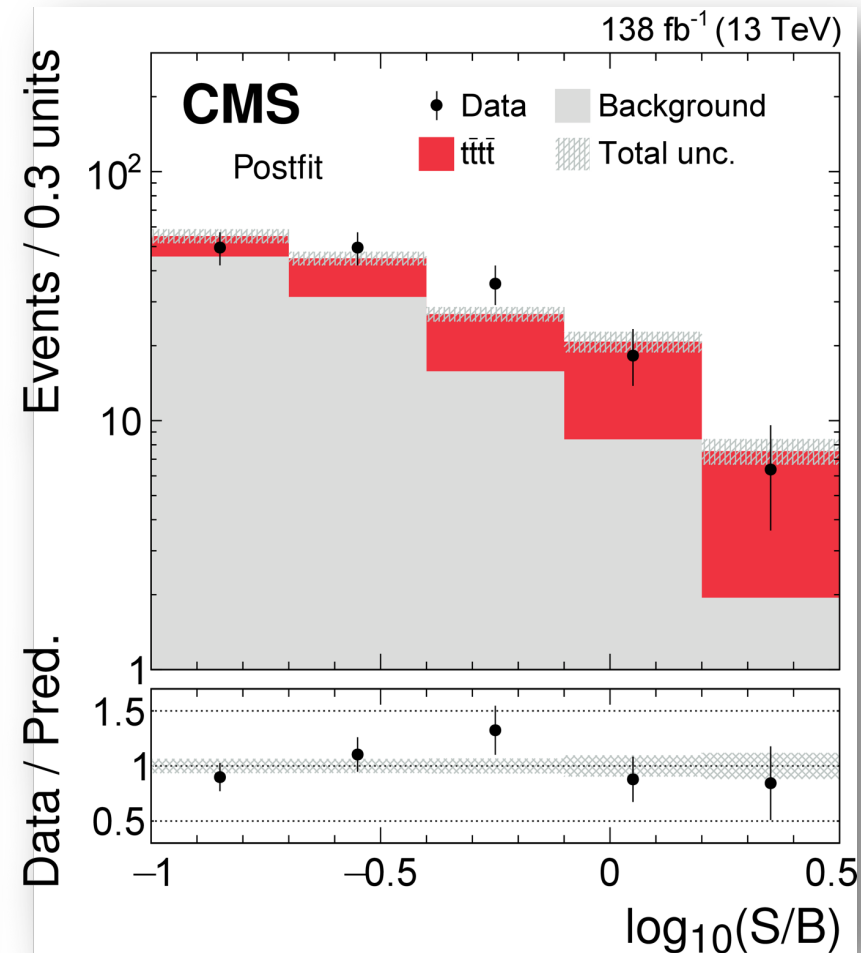
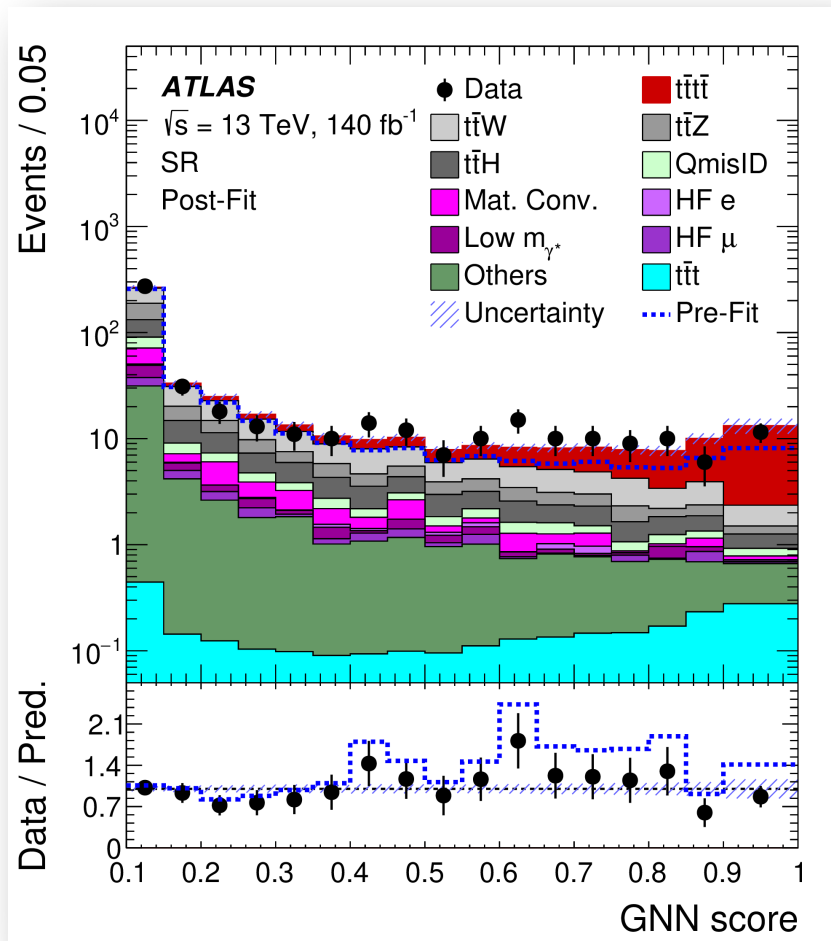
- **4 top observed by ATLAS (6.1σ) and CMS (5.6σ)**, announced during Moriond earlier this year
- Final state contains from zero to four charged leptons (results require at least 2) and up to 12 jets



4 TOP OBSERVATION

Eur. Phys. J. C 83, 496 (2023), 2305.13439

- 4 top observed by ATLAS (6.1σ) and CMS (5.6σ), announced during Moriond earlier this year
- Final state contains from zero to four charged leptons (results require at least 2) and up to 12 jets



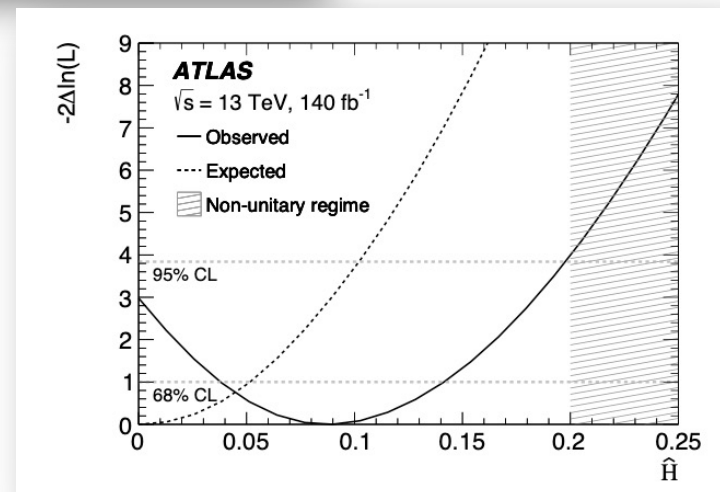
4 TOP OBSERVATION *Eur. Phys. J. C 83, 496 (2023)*

- ATLAS provides **EFT interpretations** (CMS's provided before observation, included in top + X combination)
- 4top sensitive to heavy-flavour fermion operators $O_{QQ}^1, O_{tt}^1, O_{Qt}^1, O_{Qt}^8 \rightarrow$ probe BSM that enhances interactions between third-generation quarks

Operators	Expected C_i/Λ^2 [TeV ⁻²]	Observed C_i/Λ^2 [TeV ⁻²]
O_{QQ}^1	[-2.4, 3.0]	[-3.5, 4.1]
O_{Qt}^1	[-2.5, 2.0]	[-3.5, 3.0]
O_{tt}^1	[-1.1, 1.3]	[-1.7, 1.9]
O_{Qt}^8	[-4.2, 4.8]	[-6.2, 6.9]

Fit one parameter at the time

- Sensitive to Higgs oblique parameter \hat{H}
ATLAS' limit coincides with the largest value that preserves unitarity in the perturbative theory
CMS' is at 0.12

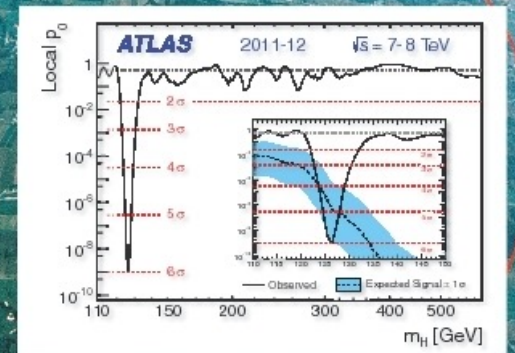
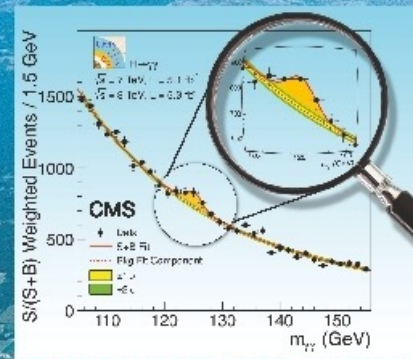


HIGGS MEASUREMENTS AND SEARCHES

More in [A. Mehta](#)



First observations of a new particle
in the search for the Standard
Model Higgs boson at the LHC



CP TESTS IN $H \rightarrow \tau\tau$ 2205.05120

- CMS full Run 2 analysis dedicated to studying anomalous couplings in ggF, VBF and VH $H \rightarrow \tau\tau$
 - Combined with $H \rightarrow \gamma\gamma$ and $H \rightarrow 4l$
- Measure effective cross-section ratios (reduce uncertainties)

$$A(Hff) = -\frac{m_f}{v} \bar{\psi}_f (\kappa_f + i \tilde{\kappa}_f \gamma_5) \psi_f,$$

CP-even

CP-odd

$$f_{CP}^{Hff} = \frac{|\tilde{\kappa}_f|^2}{|\kappa_f|^2 + |\tilde{\kappa}_f|^2} \text{sgn} \left(\frac{\tilde{\kappa}_f}{\kappa_f} \right)$$

$$A(HVV) = \frac{1}{v} \left[a_1^{VV} + \frac{\kappa_1^{VV} q_{V1}^2 + \kappa_2^{VV} q_{V2}^2}{(\Lambda_1^{VV})^2} + \frac{\kappa_3^{VV} (q_{V1} + q_{V2})^2}{(\Lambda_Q^{VV})^2} \right] m_{V1}^2 \epsilon_{V1}^* \epsilon_{V2}^*$$

$$+ \frac{1}{v} a_2^{VV} f_{\mu\nu}^{*(1)} f^{*(2),\mu\nu} + \frac{1}{v} a_3^{VV} f_{\mu\nu}^{*(1)} \tilde{f}^{*(2),\mu\nu},$$

SM

CP-even

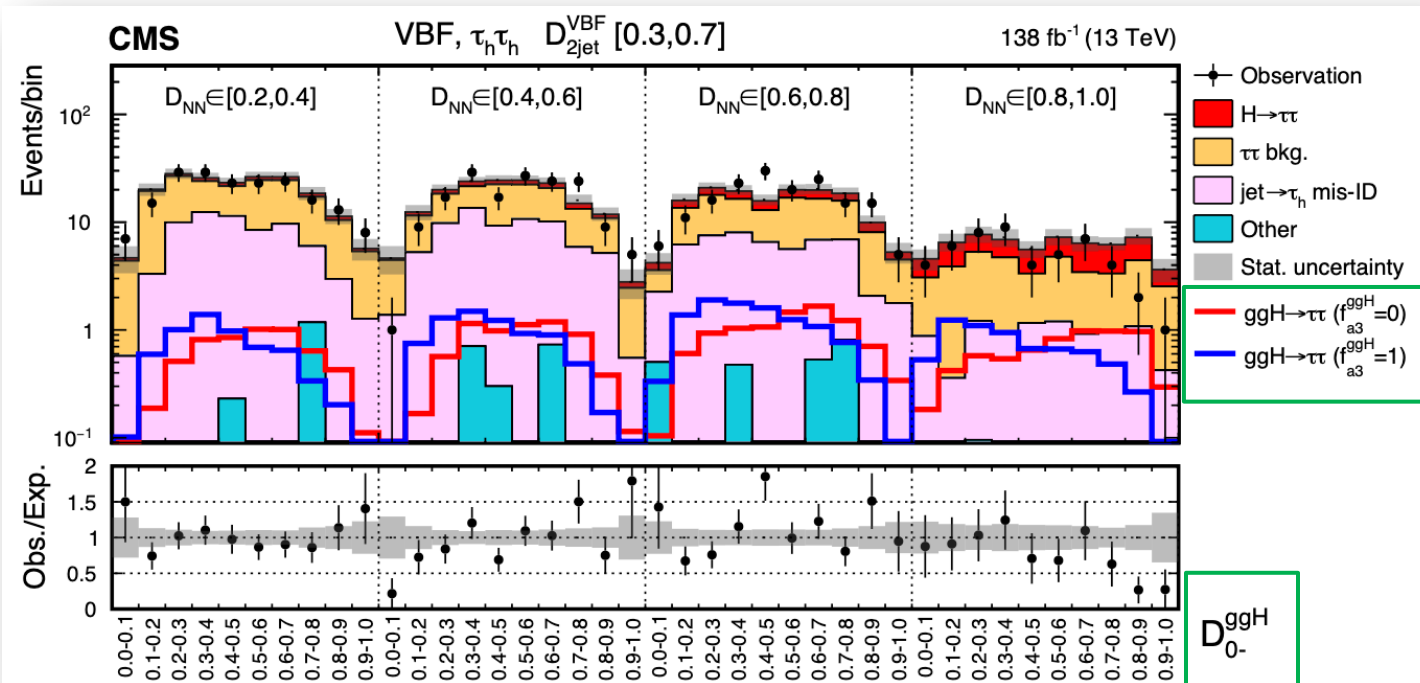
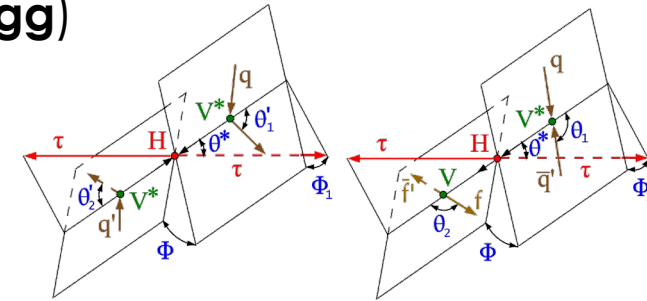
CP-odd

$$f_{ai} = \frac{|a_i|^2 \sigma_i}{\sum_{j=1,2,3\dots} |a_j|^2 \sigma_j} \text{sign} \left(\frac{a_i}{a_1} \right)$$

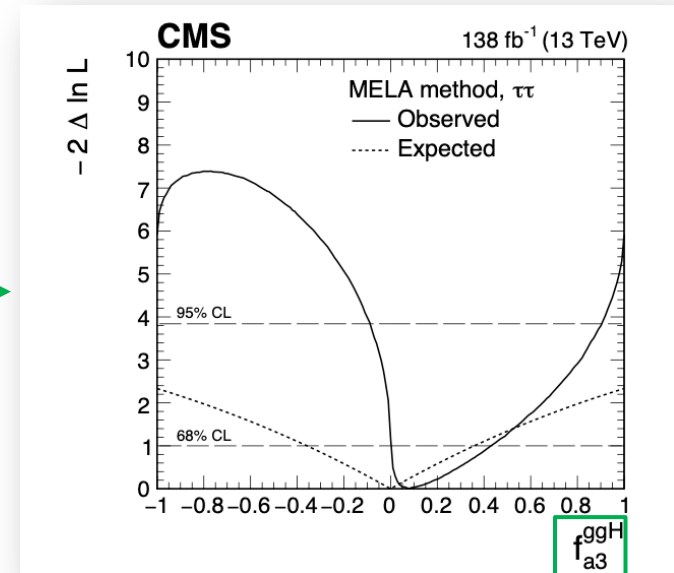
Courtesy [D. Valsecchi](#)

CP TESTS IN $H \rightarrow \tau\tau$ 2205.05120

- Access CP-violating effects using reconstructed $H \rightarrow \tau\tau$ events
 - correlation of H and two quark jets or leptons in VBF and VH production (**anomalous HVV**)
 - correlation of H and two quark jets in ggH production (**anomalous Hgg**)
- Use a matrix element likelihood approach (MELA) and neural networks
 - Build optimal discriminants, e.g. $D_{0^-}^{ggF}$ ($J^P = 0^-$ is the BSM hypothesis)



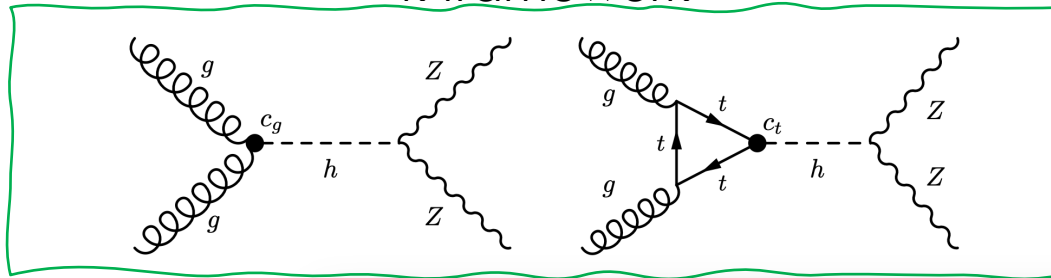
CP even
CP odd



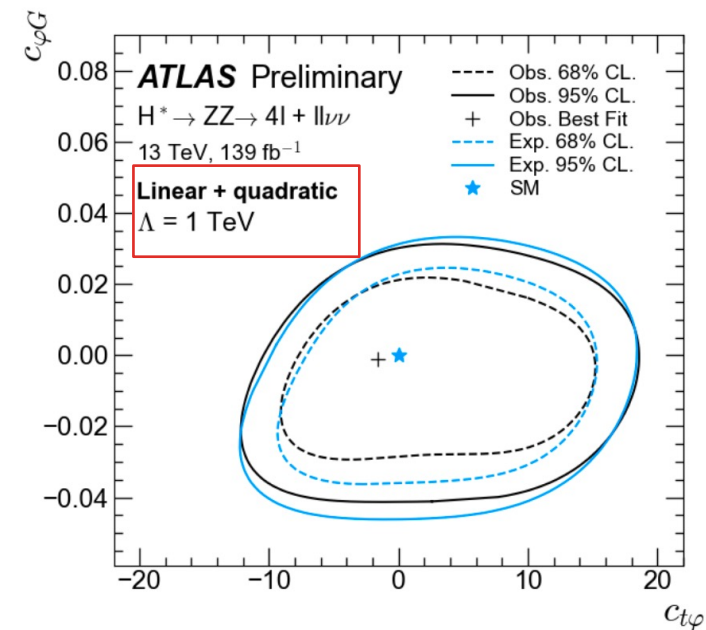
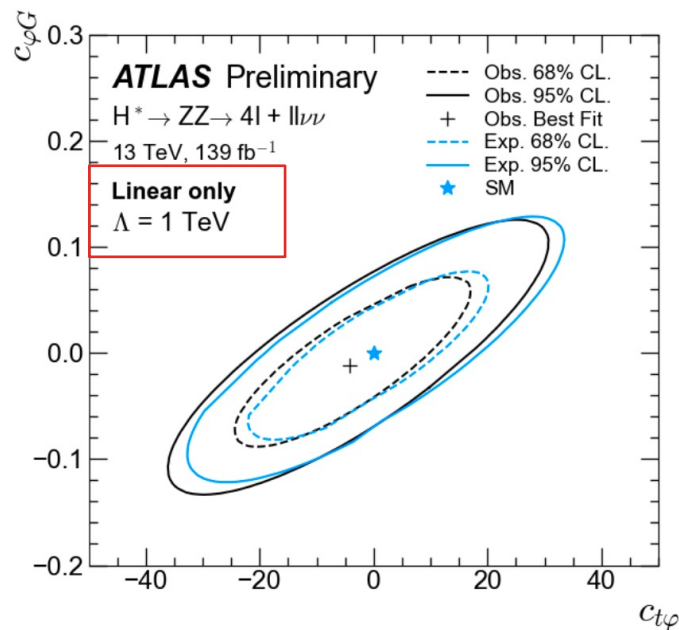
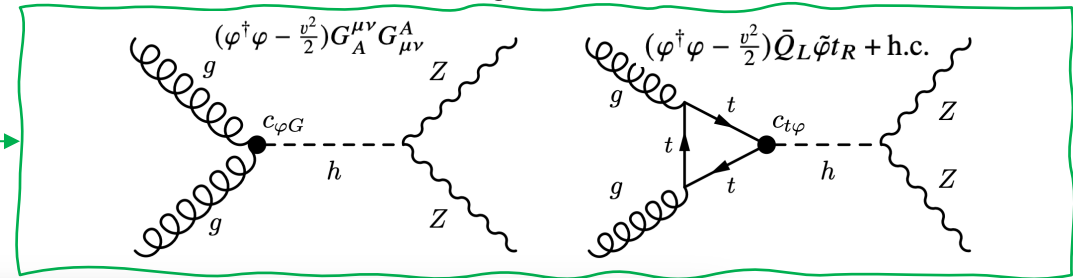
OFFSHELL $H \rightarrow ZZ$ IN SMEFT ATL-PHYS-PUB-2023-012/

- Breaks $c_g - c_t$ degeneracy present in inclusive on-shell measurements
- High invariant mass (TeV level), $ZZ \rightarrow 4l$ and $ZZ \rightarrow 2l2\nu$ final states, with $l = e$ or μ

k-framework



SMEFT

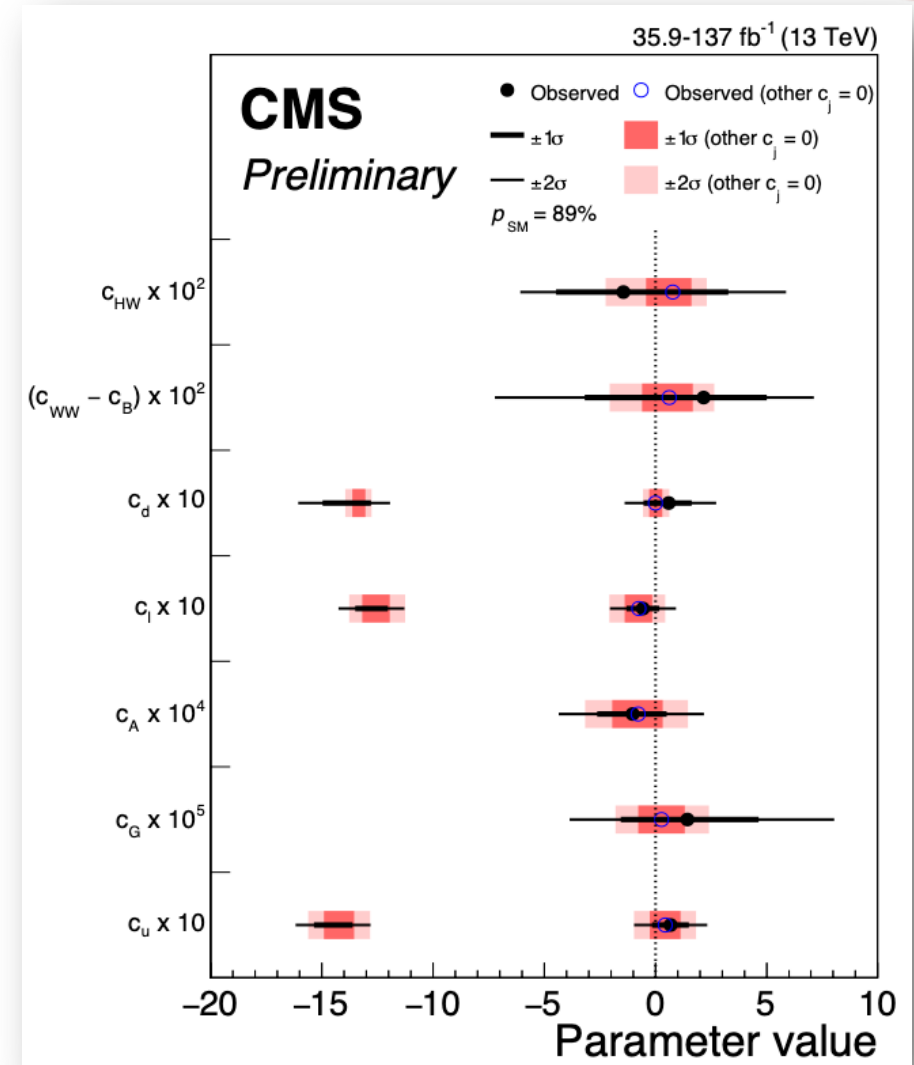


See also CMS's Higgs width analysis [s41567-022-01682-0](https://arxiv.org/abs/1507.04084) setting constraints on anomalous HVV couplings

CMS HIGGS COMBINATION

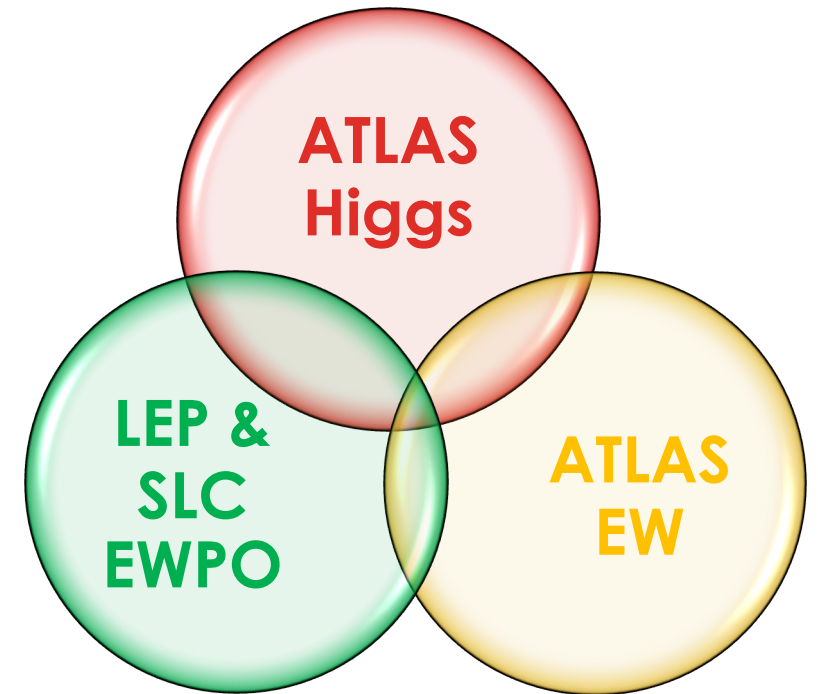
[HIG-19-005-pas](#)

- Interpretation of **Higgs boson production and decay rates** in terms of simultaneous constraints on EFT couplings in the **Higgs Effective Lagrangian (HEL) model**
 - Paper provides mapping into WCs
- Included Higgs boson decays to $\gamma\gamma, ZZ, WW, \tau\tau, bb$ (*non boosted*) @ 13 TeV, 35.9–137 fb^{-1} depending on the analysis

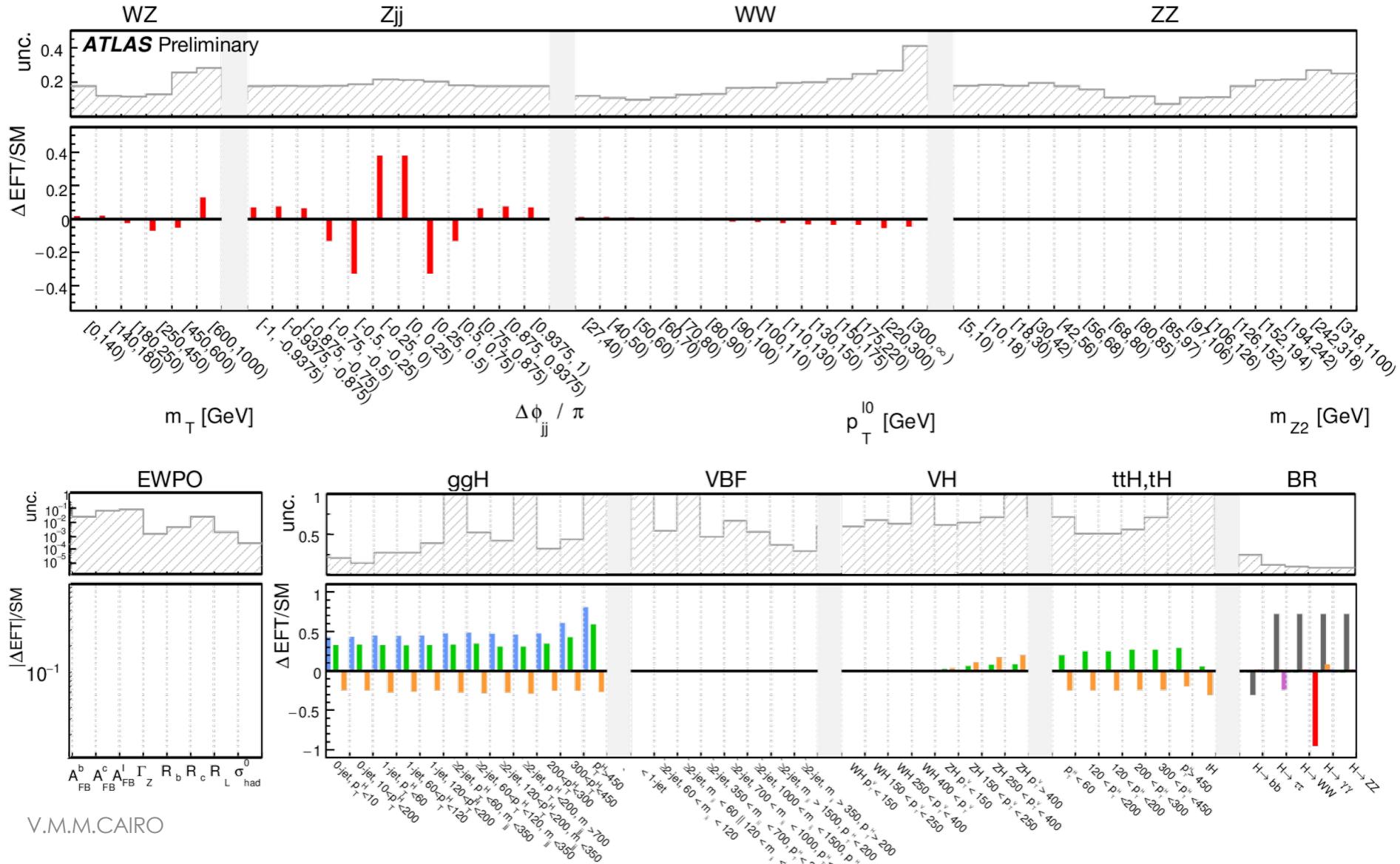


ATLAS GLOBAL COMBINATION ATL-PHYS-PUB-2022-037

- Constraints on **28 SMEFT Wilson coefficients** for **dim.6 operators**
- **Insufficient information to constraint simultaneously all coefficients**
 - Basis modified: **linear combination of WCs**
 - **First combine inputs from ATLAS**, constraining 7 individual and 17 linear combinations of WCs
 - **Higgs production and decay in STXS bins**
 - **EW differential cross-section measurements**
 - Then **add EW Precision Observables (EWPO)**

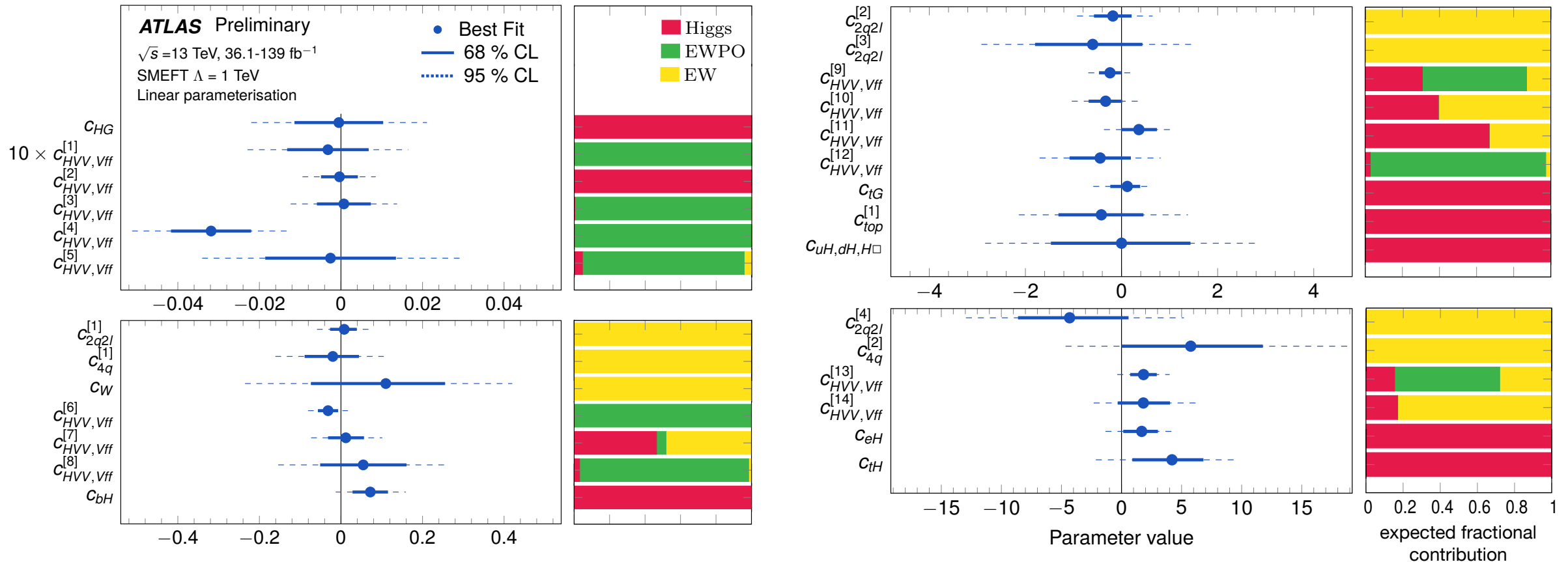


ATLAS GLOBAL COMBINATION ATL-PHYS-PUB-2022-037



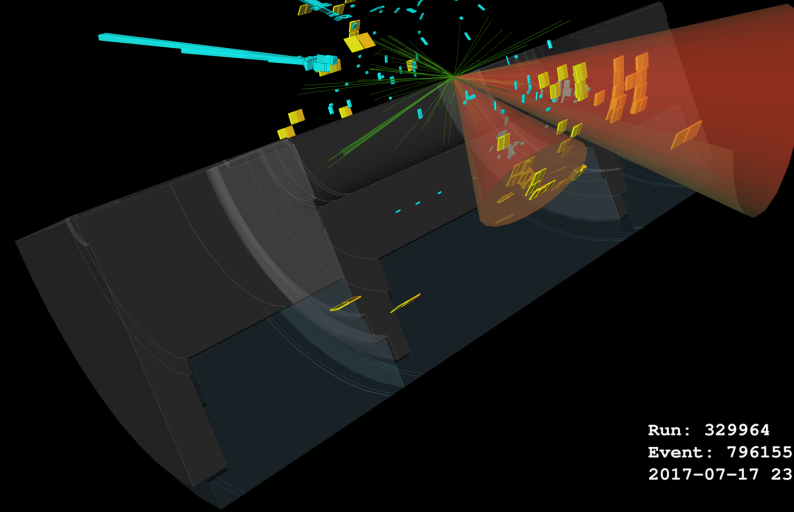
- $C_{HG} = 0.01$
- $C_W = 1.0$
- $C_{tG} = 0.2$
- $C_{bH} = 2.0$
- $C_{tH} = 2.0$
- C_{eH}

ATLAS GLOBAL COMBINATION ATL-PHYS-PUB-2022-037



- Some WCs tightly constrained by single sector, but contributions from ATLAS expected to become more important with larger datasets. **Results largely consistent with SM.**

Double the Higgs, Double the Challenge!

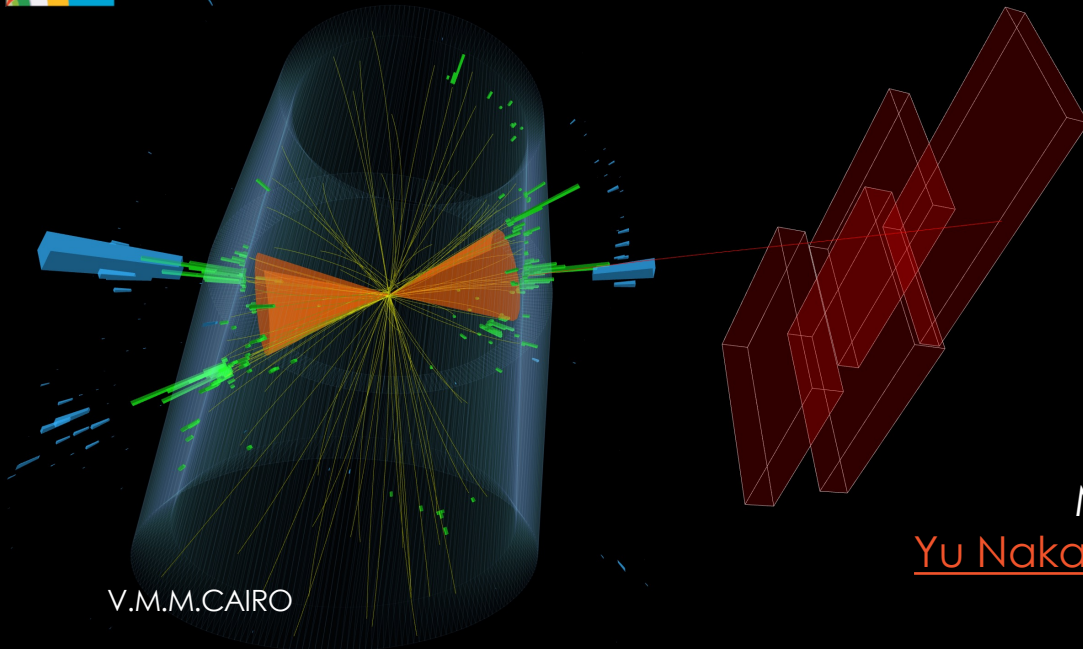


Run: 329964
Event: 796155578
2017-07-17 23:58:15 CEST

$HH \rightarrow b\bar{b}b\bar{b}$



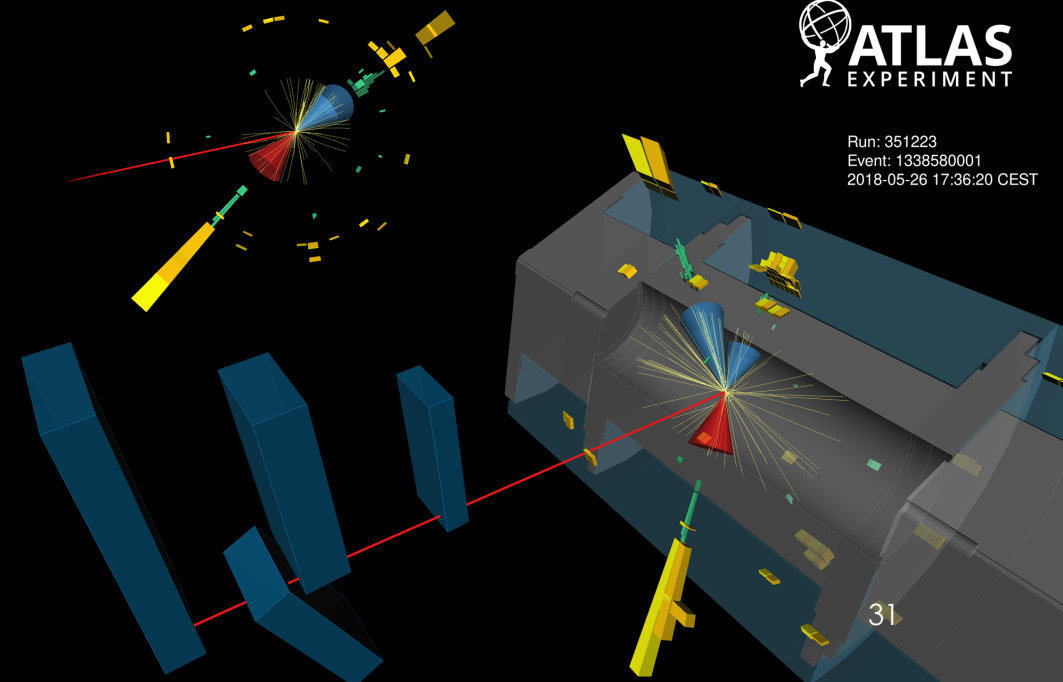
CMS Experiment at the LHC, CERN
Data recorded: 2016-Aug-13 16:51:13.749568 C
Run / Event / LS: 278803 / 465417690 / 259



V.M.M.CAIRO

$HH \rightarrow b\bar{b}\tau\tau$

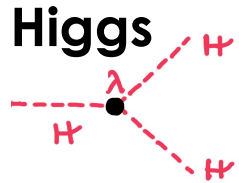
Run: 351223
Event: 1338580001
2018-05-26 17:36:20 CEST



More in
[Yu Nakahama Higuchi](#)

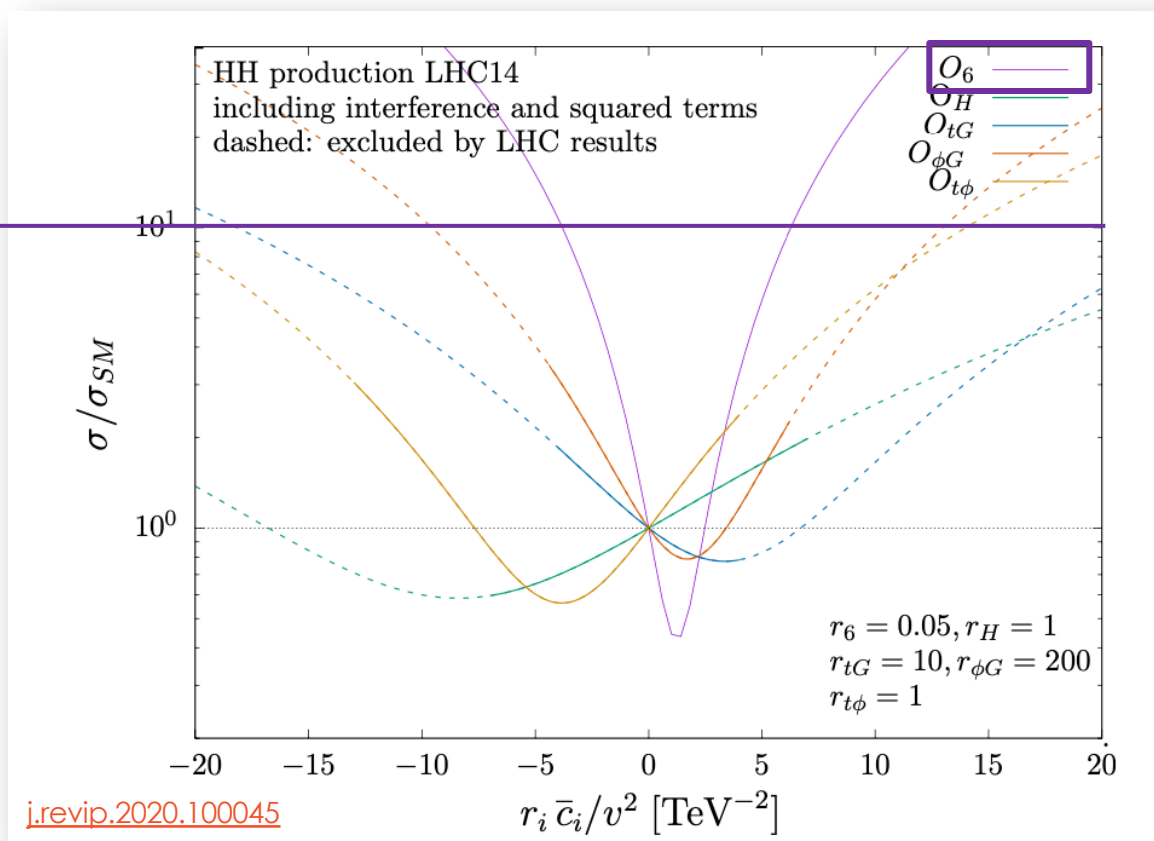
WHY HH? AND WHY IN EFT?

Higgs pairs produced by means of various interactions at the LHC, including the **self-coupling**, λ , giving us *direct* access to its measurement when searching for HH



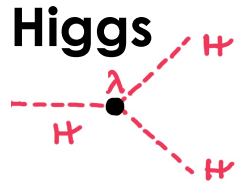
LHC early Run 2
constraints ≈ 10

No sensitivity to
parameters other
than O_6 ($\sim k_\lambda$)



WHY HH? AND WHY IN EFT?

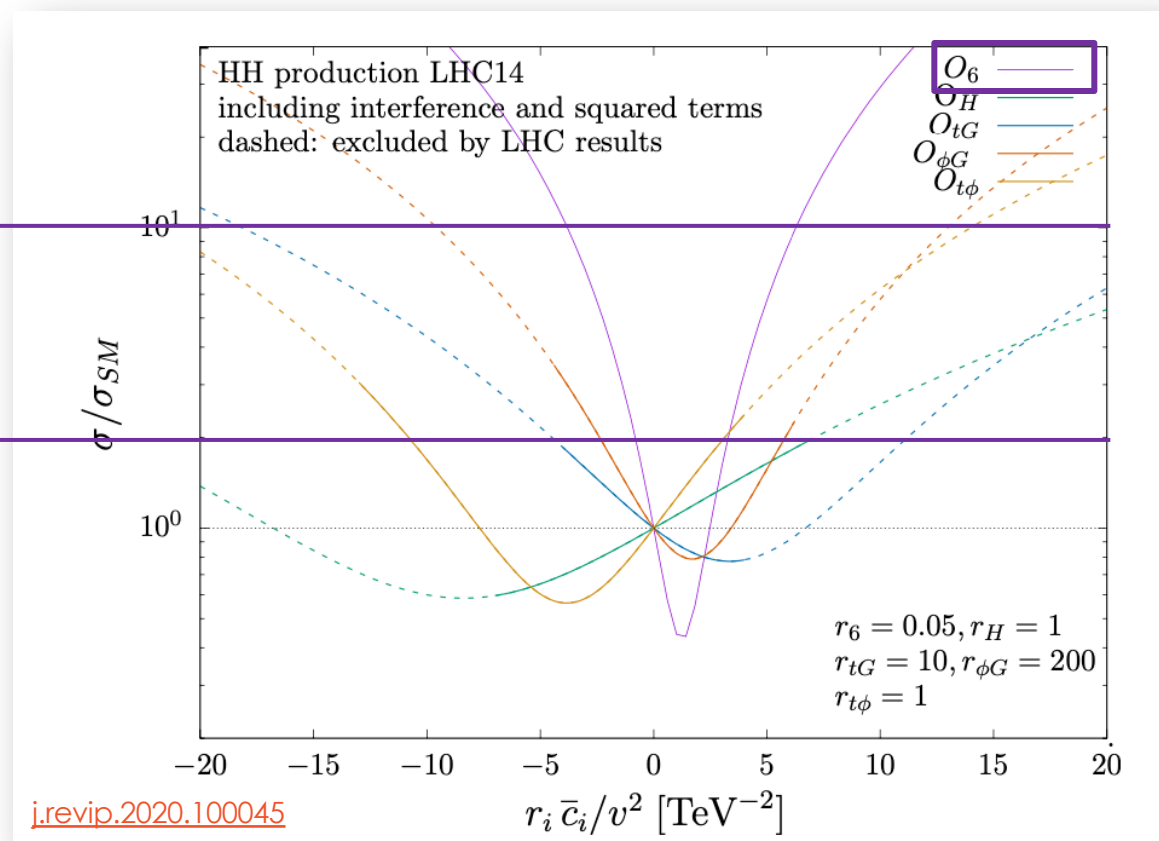
Higgs pairs produced by means of various interactions at the LHC, including the **self-coupling**, λ , giving us *direct* access to its measurement when searching for HH



LHC early Run 2
constraints ≈ 10

LHC full Run 2
constraints ≈ 3

Relevant to
consider general
coupling
variations



HIGGS PAIRS IN SMEFT

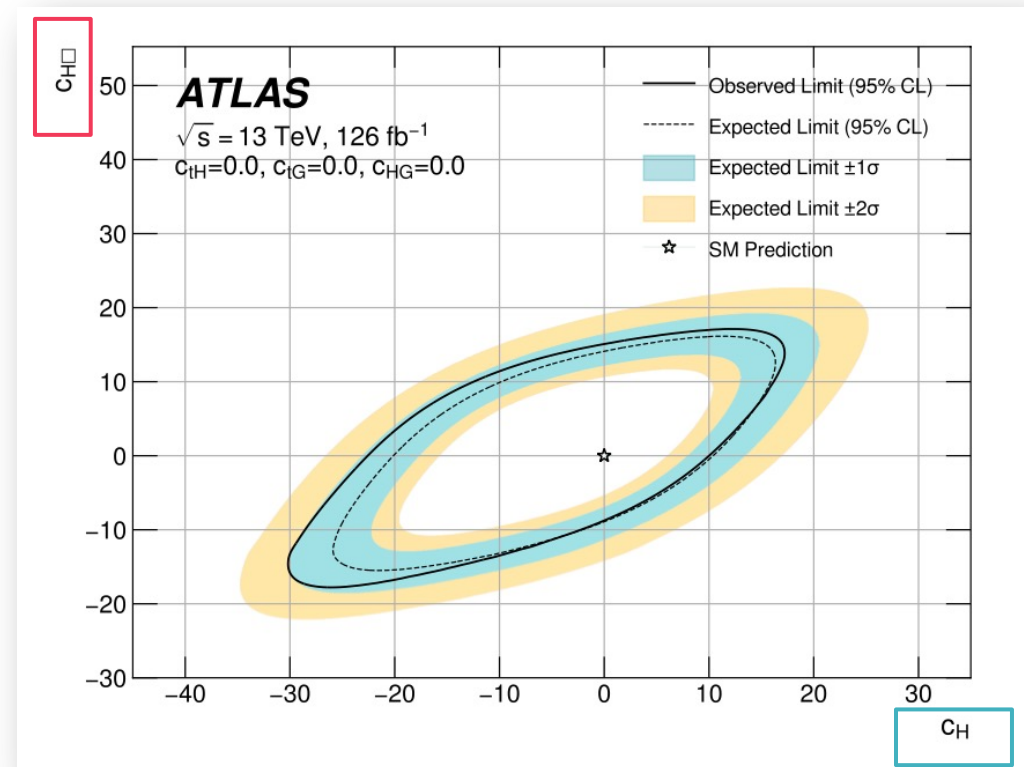
[2301.03212](#)

Wilson Coefficient	Operator
c_H	$(H^\dagger H)^3$
$c_{H\Box}$	$(H^\dagger H)\Box(H^\dagger H)$
c_{tH}	$(H^\dagger H)(\bar{Q}\tilde{H}t)$
c_{HG}	$H^\dagger H G_{\mu\nu}^A G_A^{\mu\nu}$
c_{tG}	$(\bar{Q}\sigma^{\mu\nu}T^A t)\tilde{H}G_{\mu\nu}^A$

In Single Higgs, only included in linear combination with other WCs

Probed uniquely by HH

ATLAS $HH \rightarrow 4b$



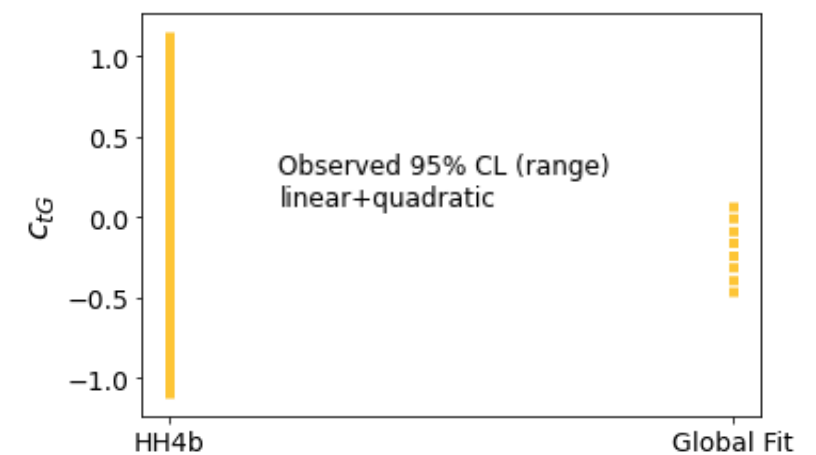
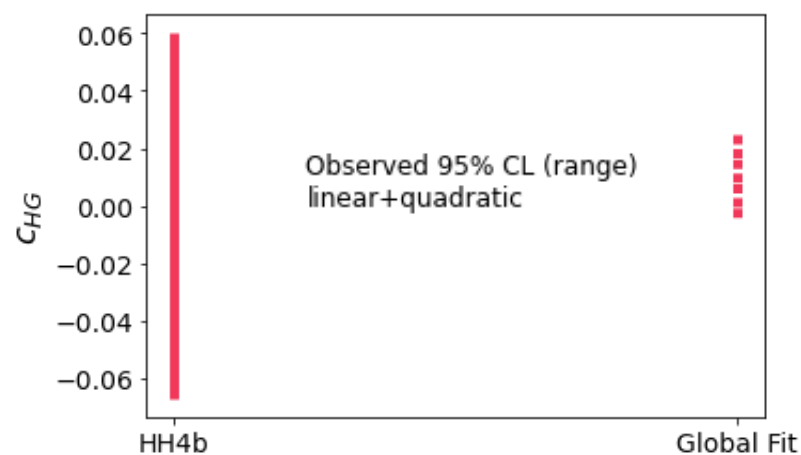
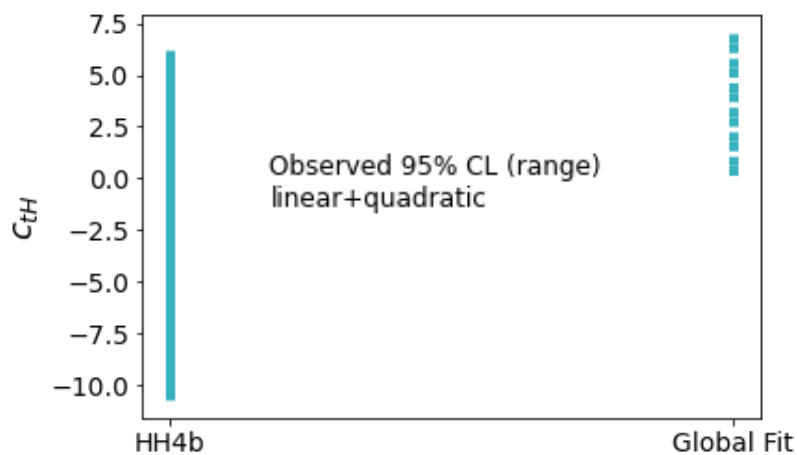
More 2D scans in the extra slides

HIGGS PAIRS IN SMEFT [2301.03212](#)

Wilson Coefficient	Operator
c_H	$(H^\dagger H)^3$
$c_{H\Box}$	$(H^\dagger H)\Box(H^\dagger H)$
c_{tH}	$(H^\dagger H)(\bar{Q}\tilde{H}t)$
c_{HG}	$H^\dagger H G_{\mu\nu}^A G_A^{\mu\nu}$
c_{tG}	$(Q\sigma^{\mu\nu}T^A t)\tilde{H}G_{\mu\nu}^A$

Limits are ~ comparable with global combination (dominated by single Higgs)

Order-of-magnitude **hand-made** comparison between [2301.03212](#) (Global Fit) and [ATL-PHYS-PUB-2022-037](#) (HH4b)

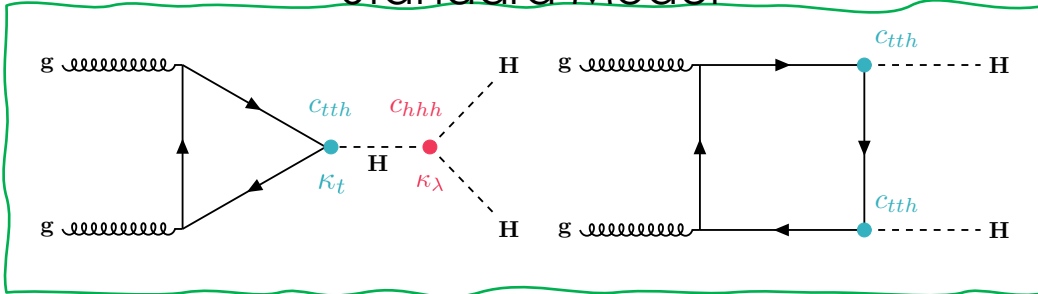


HIGGS PAIRS IN HEFT

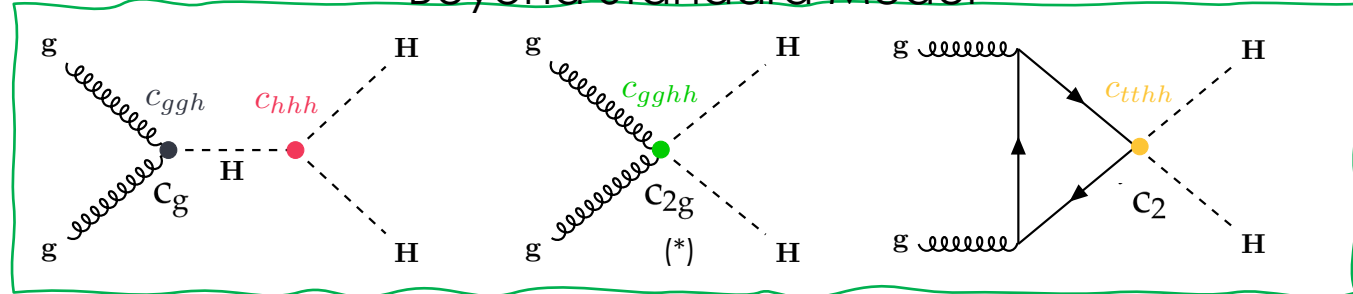
[2301.03212](#), [ATL-PHYS-PUB-2022-019](#), [JHEP 03 \(2021\) 257](#)

In **HEFT**, anomalous **single-Higgs couplings** \neq **HH couplings** ($c_{ggHH} \neq c_{ggH}, c_{ttHH} \neq c_{ttH}$)

Standard Model



Beyond Standard Model



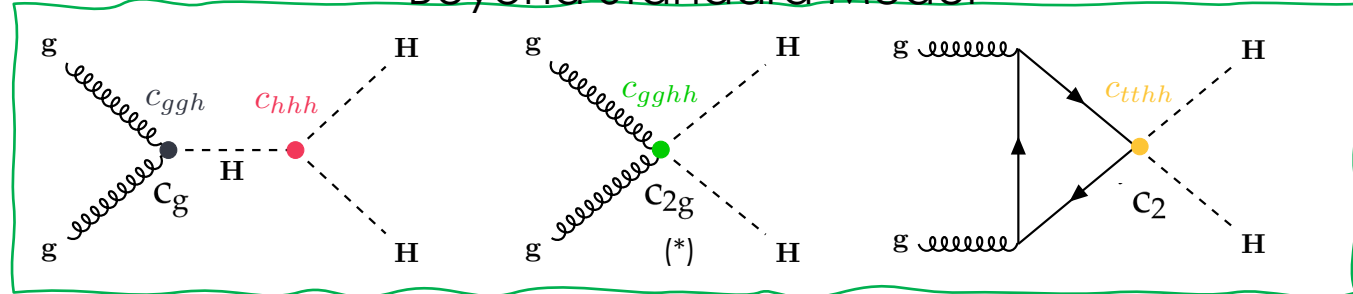
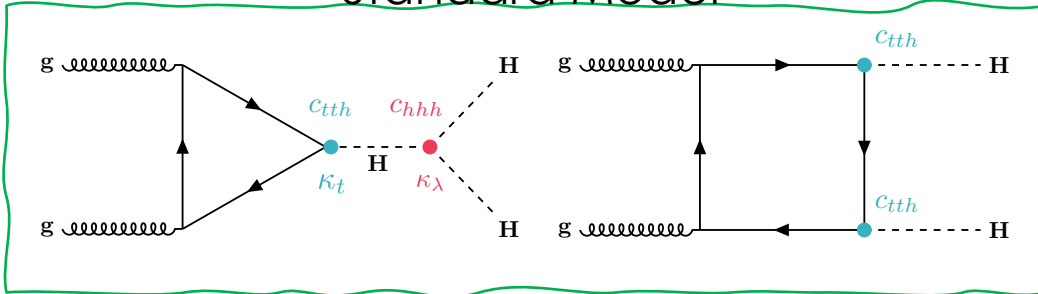
HIGGS PAIRS IN HEFT

[2301.03212](#), [ATL-PHYS-PUB-2022-019](#), [JHEP 03 \(2021\) 257](#)

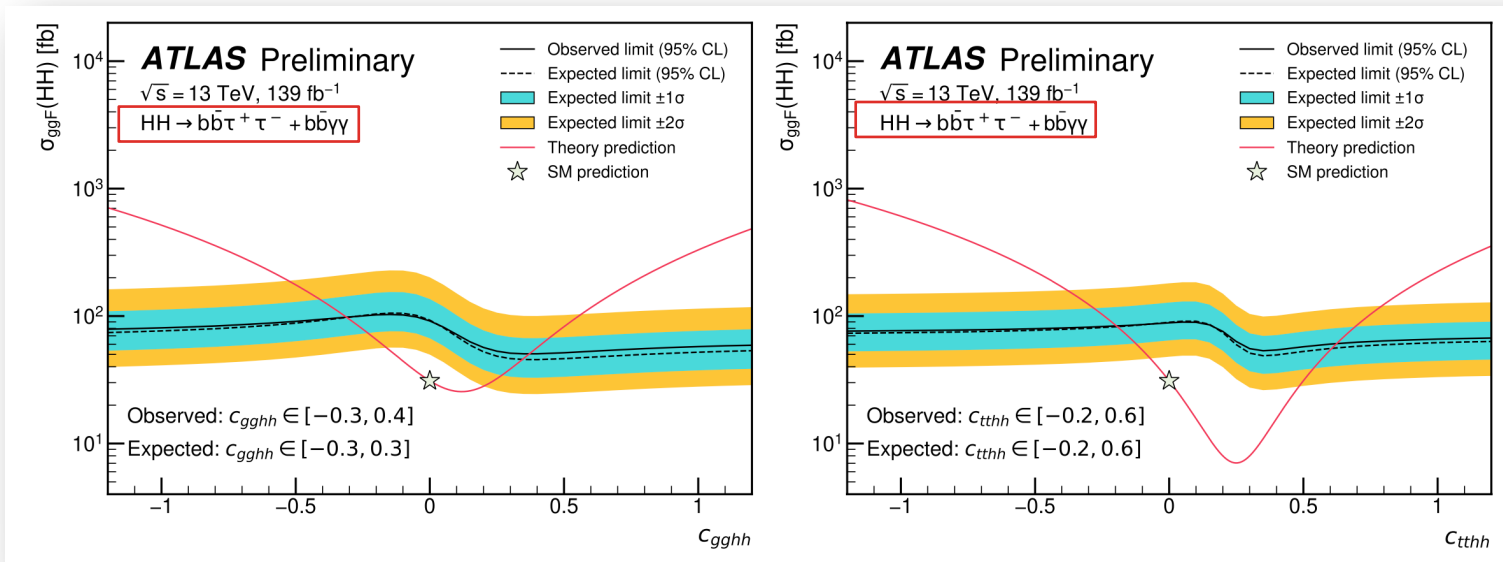
In HEFT, anomalous **single-Higgs couplings** \neq **HH couplings** ($c_{ggHH} \neq c_{ggH}, c_{ttHH} \neq c_{tth}$)

Standard Model

Beyond Standard Model



HEFT results for ATLAS $HH \rightarrow \gamma\gamma bb + HH \rightarrow bb\tau\tau$ ($\sigma/\sigma_{SM} < 0(3)$), ATLAS $HH \rightarrow 4b$ and CMS $HH \rightarrow \gamma\gamma bb$

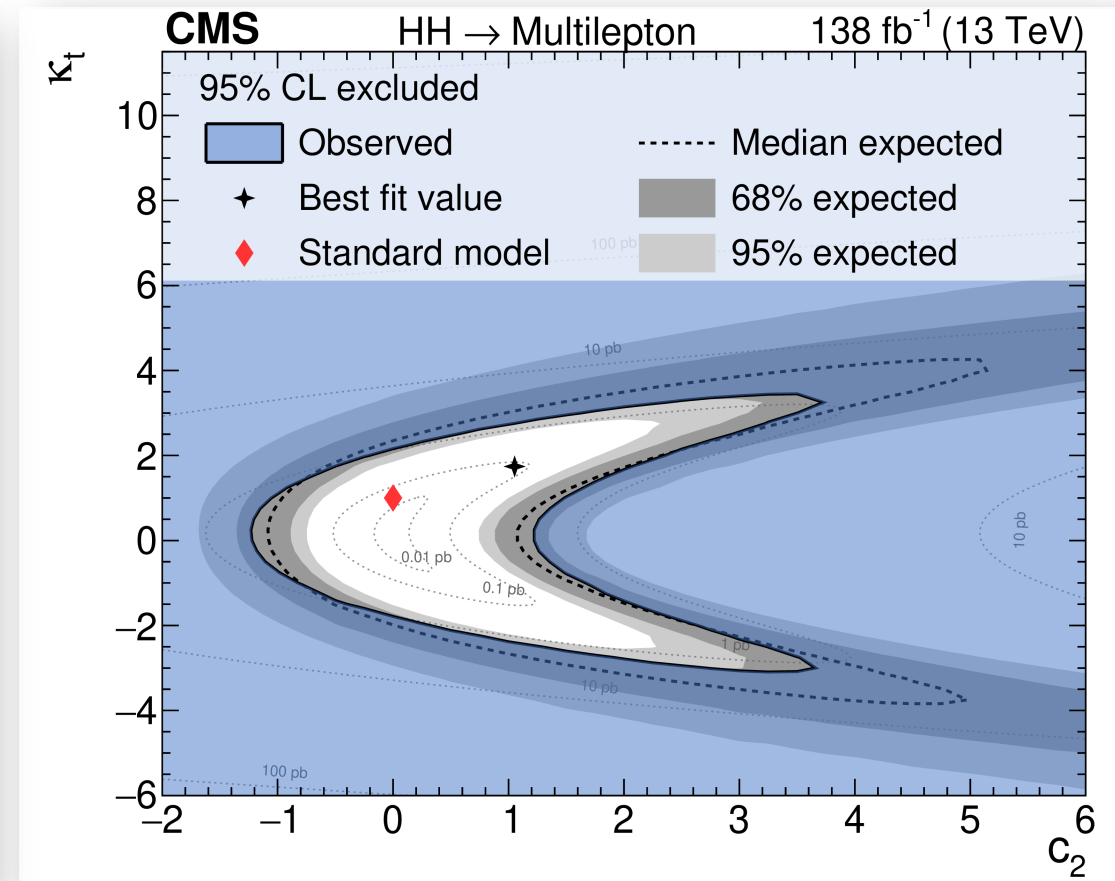
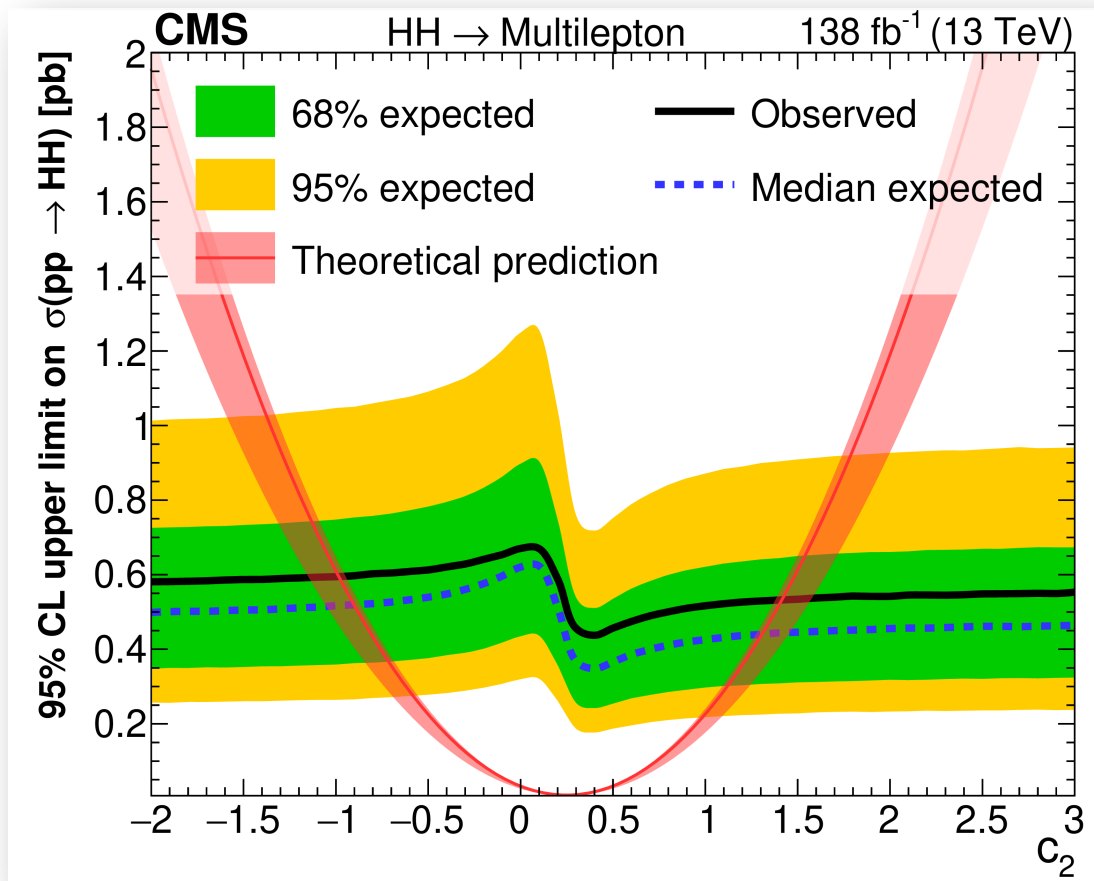


See extra slides for constraints on “benchmarks”, i.e. xs limits on recommended combinations of WCs values

(*) In black the CMS WCs convention, in colors the ATLAS one

HIGGS PAIRS IN HEFT 2206.10268

- CMS full Run 2 search for $HH \rightarrow WWWW, WW\tau\tau, \text{ and } \tau\tau\tau$
- Require multi-leptons (e, μ, τ_{had}) in the final state
- $\sigma/\sigma_{SM} < 0(20)$



CONCLUSIONS

SM

- The success of the Standard Model is extensively confirmed by the current ATLAS and CMS results

BSM

- This motivates searching for hints of physics BSM which could manifest at a higher energy scale

EFT

- Effective Field Theory frameworks are powerful ways to map our current understanding and look for anomalies

LHC

- LHC results include more and more EFT direct and indirect searches
 - SM, top, Higgs and more recently also Higgs pairs
 - Global combinations can unveil mysteries that are potentially still hidden

Thanks for your attention!



F. Cairo, From *Conn(II)ecting the dots*



EXTRA SLIDES

EFFECTIVE FIELD THEORIES AT THE LHC

<https://arxiv.org/pdf/2204.01763.pdf>

SMEFT $SU(2)$ doublet $H = \frac{1}{\sqrt{2}} \begin{pmatrix} \phi_1 + i\phi_2 \\ \phi_4 + i\phi_3 \end{pmatrix}$

HEFT $\phi = (1 + h/v)\mathbf{n}$

SMEFT

JHEP04(2021)279

X^3		H^6 and $H^4 D^2$		$\psi^2 H^3$	
\mathcal{O}_G	$f^{ABC} G_\mu^{A\nu} G_\nu^{B\rho} G_\rho^{C\mu}$	\mathcal{O}_H	$(H^\dagger H)^3$	\mathcal{O}_{eH}	$(H^\dagger H)(\bar{l}_p e_r H)$
$\mathcal{O}_{\tilde{G}}$	$f^{ABC} \tilde{G}_\mu^{A\nu} G_\nu^{B\rho} G_\rho^{C\mu}$	$\mathcal{O}_{H\Box}$	$(H^\dagger H)\Box(H^\dagger H)$	\mathcal{O}_{uH}	$(H^\dagger H)(\bar{q}_p u_r \tilde{H})$
\mathcal{O}_W	$\varepsilon^{IJK} W_\mu^{I\nu} W_\nu^{J\rho} W_\rho^{K\mu}$	\mathcal{O}_{HD}	$(H^\dagger D^\mu H)^* (H^\dagger D_\mu H)$	\mathcal{O}_{dH}	$(H^\dagger H)(\bar{q}_p d_r H)$
$\mathcal{O}_{\tilde{W}}$	$\varepsilon^{IJK} \tilde{W}_\mu^{I\nu} W_\nu^{J\rho} W_\rho^{K\mu}$				
$X^2 H^2$		$\psi^2 XH$		$\psi^2 H^2 D$	
\mathcal{O}_{HG}	$H^\dagger H G_{\mu\nu}^A G^{A\mu\nu}$	\mathcal{O}_{eW}	$(\bar{l}_p \sigma^{\mu\nu} e_r) \tau^I H W_{\mu\nu}^I$	$\mathcal{O}_{Hl}^{(1)}$	$(H^\dagger i \overleftrightarrow{D}_\mu H)(\bar{l}_p \gamma^\mu l_r)$
$\mathcal{O}_{H\tilde{G}}$	$H^\dagger H \tilde{G}_{\mu\nu}^A G^{A\mu\nu}$	\mathcal{O}_{eB}	$(\bar{l}_p \sigma^{\mu\nu} e_r) H B_{\mu\nu}$	$\mathcal{O}_{Hl}^{(3)}$	$(H^\dagger i \overleftrightarrow{D}_\mu^I H)(\bar{l}_p \tau^I \gamma^\mu l_r)$
\mathcal{O}_{HW}	$H^\dagger H W_{\mu\nu}^I W^{I\mu\nu}$	\mathcal{O}_{uG}	$(\bar{q}_p \sigma^{\mu\nu} T^A u_r) \tilde{H} G_{\mu\nu}^A$	\mathcal{O}_{He}	$(H^\dagger i \overleftrightarrow{D}_\mu H)(\bar{e}_p \gamma^\mu e_r)$
$\mathcal{O}_{H\tilde{W}}$	$H^\dagger H \tilde{W}_{\mu\nu}^I W^{I\mu\nu}$	\mathcal{O}_{uW}	$(\bar{q}_p \sigma^{\mu\nu} u_r) \tau^I \tilde{H} W_{\mu\nu}^I$	$\mathcal{O}_{Hq}^{(1)}$	$(H^\dagger i \overleftrightarrow{D}_\mu H)(\bar{q}_p \gamma^\mu q_r)$
\mathcal{O}_{HB}	$H^\dagger H B_{\mu\nu} B^{\mu\nu}$	\mathcal{O}_{uB}	$(\bar{q}_p \sigma^{\mu\nu} u_r) \tilde{H} B_{\mu\nu}$	$\mathcal{O}_{Hq}^{(3)}$	$(H^\dagger i \overleftrightarrow{D}_\mu^I H)(\bar{q}_p \tau^I \gamma^\mu q_r)$
$\mathcal{O}_{H\tilde{B}}$	$H^\dagger H \tilde{B}_{\mu\nu} B^{\mu\nu}$	\mathcal{O}_{dG}	$(\bar{q}_p \sigma^{\mu\nu} T^A d_r) H G_{\mu\nu}^A$	\mathcal{O}_{Hu}	$(H^\dagger i \overleftrightarrow{D}_\mu H)(\bar{u}_p \gamma^\mu u_r)$
\mathcal{O}_{HWB}	$H^\dagger \tau^I H W_{\mu\nu}^I B^{\mu\nu}$	\mathcal{O}_{dW}	$(\bar{q}_p \sigma^{\mu\nu} d_r) \tau^I H W_{\mu\nu}^I$	\mathcal{O}_{Hd}	$(H^\dagger i \overleftrightarrow{D}_\mu H)(\bar{d}_p \gamma^\mu d_r)$
$\mathcal{O}_{H\tilde{W}B}$	$H^\dagger \tau^I H \tilde{W}_{\mu\nu}^I B^{\mu\nu}$	\mathcal{O}_{dB}	$(\bar{q}_p \sigma^{\mu\nu} d_r) H B_{\mu\nu}$	\mathcal{O}_{Hud}	$i(\tilde{H}^\dagger D_\mu H)(\bar{u}_p \gamma^\mu d_r)$
$(\bar{L}L)(\bar{L}L)$		$(\bar{R}R)(\bar{R}R)$		$(\bar{L}L)(\bar{R}R)$	
\mathcal{O}_{ll}	$(\bar{l}_p \gamma_\mu l_r)(\bar{l}_s \gamma^\mu l_t)$	\mathcal{O}_{ee}	$(\bar{e}_p \gamma_\mu e_r)(\bar{e}_s \gamma^\mu e_t)$	\mathcal{O}_{le}	$(\bar{l}_p \gamma_\mu l_r)(\bar{e}_s \gamma^\mu e_t)$
$\mathcal{O}_{qq}^{(1)}$	$(\bar{q}_p \gamma_\mu q_r)(\bar{q}_s \gamma^\mu q_t)$	\mathcal{O}_{uu}	$(\bar{u}_p \gamma_\mu u_r)(\bar{u}_s \gamma^\mu u_t)$	\mathcal{O}_{lu}	$(\bar{l}_p \gamma_\mu l_r)(\bar{u}_s \gamma^\mu u_t)$
$\mathcal{O}_{qq}^{(3)}$	$(\bar{q}_p \gamma_\mu \tau^I q_r)(\bar{q}_s \gamma^\mu \tau^I q_t)$	\mathcal{O}_{dd}	$(\bar{d}_p \gamma_\mu d_r)(\bar{d}_s \gamma^\mu d_t)$	\mathcal{O}_{ld}	$(\bar{l}_p \gamma_\mu l_r)(\bar{d}_s \gamma^\mu d_t)$
$\mathcal{O}_{lq}^{(1)}$	$(\bar{l}_p \gamma_\mu l_r)(\bar{q}_s \gamma^\mu q_t)$	\mathcal{O}_{cu}	$(\bar{e}_p \gamma_\mu e_r)(\bar{u}_s \gamma^\mu u_t)$	\mathcal{O}_{qe}	$(\bar{q}_p \gamma_\mu q_r)(\bar{e}_s \gamma^\mu e_t)$
$\mathcal{O}_{lq}^{(3)}$	$(\bar{l}_p \gamma_\mu \tau^I l_r)(\bar{q}_s \gamma^\mu \tau^I q_t)$	\mathcal{O}_{cd}	$(\bar{e}_p \gamma_\mu e_r)(\bar{d}_s \gamma^\mu d_t)$	$\mathcal{O}_{qu}^{(1)}$	$(\bar{q}_p \gamma_\mu q_r)(\bar{u}_s \gamma^\mu u_t)$
		$\mathcal{O}_{ud}^{(1)}$	$(\bar{u}_p \gamma_\mu u_r)(\bar{d}_s \gamma^\mu d_t)$	$\mathcal{O}_{qu}^{(8)}$	$(\bar{q}_p \gamma_\mu T^A q_r)(\bar{u}_s \gamma^\mu T^A u_t)$
		$\mathcal{O}_{ud}^{(8)}$	$(\bar{u}_p \gamma_\mu T^A u_r)(\bar{d}_s \gamma^\mu T^A d_t)$	$\mathcal{O}_{qd}^{(1)}$	$(\bar{q}_p \gamma_\mu q_r)(\bar{d}_s \gamma^\mu d_t)$
				$\mathcal{O}_{qd}^{(8)}$	$(\bar{q}_p \gamma_\mu T^A q_r)(\bar{d}_s \gamma^\mu T^A d_t)$
$(\bar{L}R)(\bar{R}L)$ and $(\bar{L}R)(\bar{L}R)$		B -violating			
\mathcal{O}_{ledq}	$(\bar{l}_p^j e_r)(\bar{d}_s^k q_t^j)$	\mathcal{O}_{duq}	$\varepsilon^{\alpha\beta\gamma} \varepsilon_{jk} [(d_p^\alpha)^T C u_r^\beta] [(q_s^{\gamma j})^T C l_t^k]$		
$\mathcal{O}_{quqd}^{(1)}$	$(\bar{q}_p^j u_r) \varepsilon_{jk} (\bar{q}_s^k d_t)$	\mathcal{O}_{quu}	$\varepsilon^{\alpha\beta\gamma} \varepsilon_{jk} [(q_p^{\alpha j})^T C q_r^{\beta k}] [(u_s^\gamma)^T C e_t]$		
$\mathcal{O}_{quqd}^{(8)}$	$(\bar{q}_p^j T^A u_r) \varepsilon_{jk} (\bar{q}_s^k T^A d_t)$	\mathcal{O}_{quq}	$\varepsilon^{\alpha\beta\gamma} \varepsilon_{jn} \varepsilon_{km} [(q_p^{\alpha j})^T C q_r^{\beta k}] [(q_s^{\gamma m})^T C l_t^n]$		
$\mathcal{O}_{lequ}^{(1)}$	$(\bar{l}_p^j e_r) \varepsilon_{jk} (\bar{q}_s^k u_t)$	\mathcal{O}_{duu}	$\varepsilon^{\alpha\beta\gamma} [(d_p^\alpha)^T C u_r^\beta] [(u_s^\gamma)^T C e_t]$		
$\mathcal{O}_{lequ}^{(3)}$	$(\bar{l}_p^j \sigma_{\mu\nu} e_r) \varepsilon_{jk} (\bar{q}_s^k \sigma^{\mu\nu} u_t)$				

Table 1. Dimension-6 operators in the Warsaw basis, adapted from Ref. [81]. The grey cells indicate operators that break flavour $SU(3)^5$ explicitly.

OBLIQUE PARAMETER AND UNIVERSAL BASIS

<https://arxiv.org/pdf/1903.07725.pdf>

‘Higgs-only’

$$\begin{array}{lll} \mathcal{O}_\square = \frac{c_\square}{M^2} |\square H|^2 & \mathcal{O}_H = \frac{c_H}{2M^2} (\partial^\mu |H|^2)^2 & \mathcal{O}_6 = \frac{c_6}{M^2} |H|^6 \\ & \mathcal{O}_T = \frac{c_T}{2M^2} (H^\dagger \overleftrightarrow{D}^\mu H)^2 & \\ & \mathcal{O}_R = \frac{c_R}{M^2} |H|^2 |D^\mu H|^2 & \end{array}$$

‘Gauge-only’

$$\mathcal{O}_{2G} = -\frac{c_{2G}}{4M^2} (D_\rho G_{\mu\nu}^a)^2 \quad \mathcal{O}_{2W} = -\frac{c_{2W}}{4M^2} (D_\rho W_{\mu\nu}^a)^2 \quad \mathcal{O}_{2B} = -\frac{c_{2B}}{4M^2} (\partial_\rho B_{\mu\nu})^2$$

‘Mixed gauge-Higgs’

$$\begin{array}{ll} \mathcal{O}_B = \frac{ig' c_B}{2M^2} (H^\dagger \overleftrightarrow{D}^\mu H) \partial^\nu B_{\mu\nu} & \mathcal{O}_{GG} = \frac{g_s^2 c_{GG}}{M^2} |H|^2 G^{a,\mu\nu} G_{\mu\nu}^a \\ \mathcal{O}_W = \frac{ig c_W}{2M^2} (H^\dagger \sigma^a \overleftrightarrow{D}^\mu H) D^\nu W_{\mu\nu}^a & \mathcal{O}_{WB} = \frac{gg' c_{WB}}{M^2} H^\dagger \sigma^a H B^{\mu\nu} W_{\mu\nu}^a \\ & \mathcal{O}_{WW} = \frac{g^2 c_{WW}}{M^2} |H|^2 W^{a,\mu\nu} W_{\mu\nu}^a \\ & \mathcal{O}_{BB} = \frac{g'^2 c_{BB}}{M^2} |H|^2 B^{\mu\nu} B_{\mu\nu} \end{array}$$

Relations between oblique parameters and Wilson coefficients

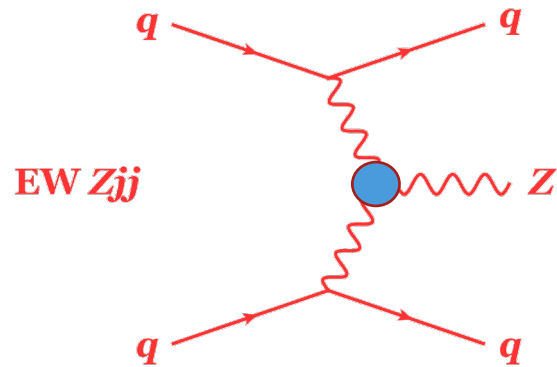
$$\begin{array}{ll} \hat{S} = 4 \left(c_{WB} + \frac{c_W + c_B}{4} \right) \frac{m_W^2}{M^2} & \hat{T} = c_T \frac{v^2}{M^2} \\ \hat{W} = c_{2W} \frac{m_W^2}{M^2} & \hat{Y} = c_{2B} \frac{m_W^2}{M^2} \\ \hat{Z} = c_{2G} \frac{m_W^2}{M^2} & \hat{H} = c_\square \frac{m_h^2}{M^2} \end{array}$$

Standard Model

CP TESTS WITH V-BOSONS

Eur. Phys. J. C 81 (2021) 163

- Additional sources of **CP-violation** required to explain the matter-antimatter asymmetry in the Universe → can manifest as anomalous Higgs/multiboson interactions



Wilson coefficient	Includes $ \mathcal{M}_{d6} ^2$	95% confidence interval [TeV^{-2}]		p -value (SM)
		Expected	Observed	
c_W/Λ^2	no	$[-0.30, 0.30]$	$[-0.19, 0.41]$	45.9%
	yes	$[-0.31, 0.29]$	$[-0.19, 0.41]$	43.2%
\bar{c}_W/Λ^2	no	$[-0.12, 0.12]$	$[-0.11, 0.14]$	82.0%
	yes	$[-0.12, 0.12]$	$[-0.11, 0.14]$	81.8%
c_{HWB}/Λ^2	no	$[-2.45, 2.45]$	$[-3.78, 1.13]$	29.0%
	yes	$[-3.11, 2.10]$	$[-6.31, 1.01]$	25.0%
\bar{c}_{HWB}/Λ^2	no	$[-1.06, 1.06]$	$[0.23, 2.34]$	1.7%
	yes	$[-1.06, 1.06]$	$[0.23, 2.35]$	1.6%

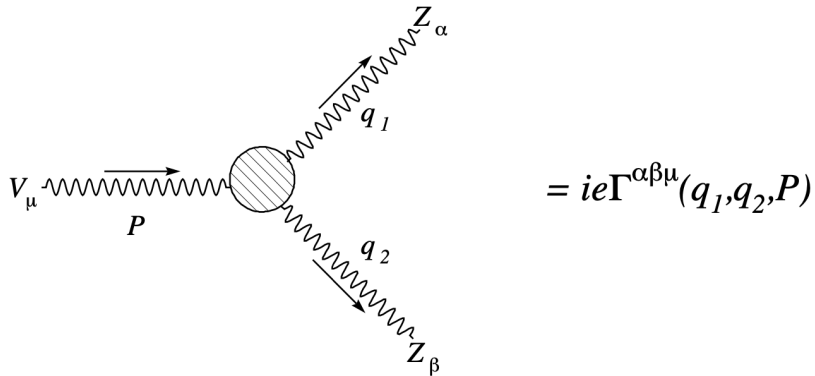
Strongest limits when pure dimension-six contributions are excluded from the theoretical prediction

DI-BOSONS AS TESTS OF α TGC

neutral

<https://arxiv.org/pdf/hep-ph/0008063.pdf>

f_4^γ and f_4^Z (CP violating),
 f_5^γ and f_5^Z (CP conserving)



II. ZZZ AND ZZ γ ANOMALOUS COUPLINGS

In the SM, at the parton level, the reaction $p\bar{p} \rightarrow ZZ$ proceeds by the Feynman diagrams of Fig. 1. Including the anomalous couplings under discussion requires the addition of the graphs of Fig. 2. In the massless fermion limit, a reasonable approximation for hadron collider processes, the most general form of the $Z^\alpha(q_1)Z^\beta(q_2)V^\mu(P)$ ($V = Z, \gamma$) vertex function (see Fig. 3 for notation) for on-shell Z 's which respects Lorentz invariance and electromagnetic gauge invariance may be written as [12]

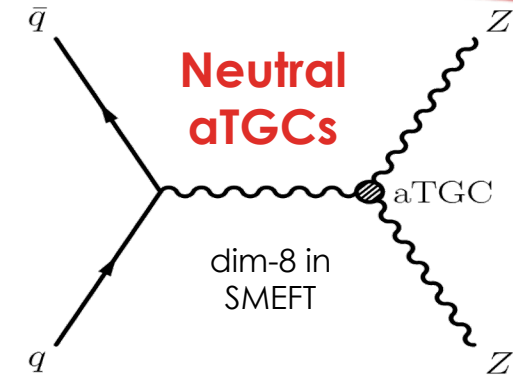
$$g_{ZZV}\Gamma_{ZZV}^{\alpha\beta\mu} = e \frac{P^2 - M_V^2}{M_Z^2} \left[i f_4^V (P^\alpha g^{\mu\beta} + P^\beta g^{\mu\alpha}) + i f_5^V \epsilon^{\mu\alpha\beta\rho} (q_1 - q_2)_\rho \right], \quad (1)$$

where M_Z is the Z -boson mass and e is the proton charge. The overall factor $(P^2 - M_V^2)$ in Eq. (1) is a consequence of Bose symmetry for ZZZ couplings, while it is due to electromagnetic gauge invariance for the $ZZ\gamma$ couplings. The couplings f_i^V ($i = 4, 5$) are dimensionless complex functions of q_1^2 , q_2^2 and P^2 . All couplings are C odd; CP invariance forbids f_4^V and parity conservation requires that f_5^V vanishes. Because f_4^Z and f_4^γ are CP -odd, contributions to the helicity amplitudes proportional to these couplings will not interfere with the SM terms. In the static limit, f_5^γ corresponds to the anapole moment of the Z boson [13]. In the SM, at tree level, $f_4^V = f_5^V = 0$. At the one-loop level, only the CP conserving couplings f_5^V receive contributions. Numerically, these contributions are of $\mathcal{O}(10^{-4})$ [14]. Loop contributions from supersymmetric particles and additional heavy fermions produce ZZV couplings of a similar magnitude [14]. If the Z bosons are allowed to be off-shell, five additional ZZZ couplings, and five additional $ZZ\gamma$ couplings contribute [15]. For these couplings, the factor $(P^2 - M_V^2)$ in the vertex function is replaced by $(q_1^2 - q_2^2)$. The effect of these couplings thus is strongly suppressed and we shall ignore them in our discussion.

DI-BOSONS AS TESTS OF α TGC

[JHEP 10 \(2019\) 127](#)

- $V\gamma$ and VV production sensitive to **anomalous triple gauge couplings (α TGCs)**
- **ATLAS Run 2 analysis examines high-energy tails of $p_T^{\ell\ell}$ in $ZZ(\ell\nu\nu)$ events** (Z boosted against the other in the transv. plane) to test α TGCs in an *effective vertex function* approach
 - f_4^γ and f_4^Z (CP violating), f_5^γ and f_5^Z (CP conserving)



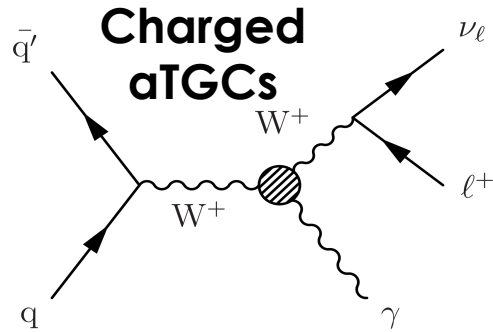
Step	Selection criteria
Two leptons	Two opposite-sign leptons, leading (subleading) $p_T > 30$ (20) GeV
Jets	$p_T > 20$ GeV, $ \eta < 4.5$, and $\Delta R > 0.4$ relative to the leptons
Third-lepton veto	No additional lepton with $p_T > 7$ GeV
$m_{\ell\ell}$	$76 < m_{\ell\ell} < 106$ GeV
Hard jets	$p_T > 25$ GeV for $ \eta < 2.4$, $p_T > 40$ GeV for $2.4 < \eta < 4.5$
E_T^{miss} and V_T/S_T	$E_T^{\text{miss}} > 110$ GeV and $V_T/S_T > 0.65$
$\Delta R_{\ell\ell}$	$\Delta R_{\ell\ell} < 1.9$
$\Delta\phi(\vec{p}_T^{\ell\ell}, \vec{E}_T^{\text{miss}})$	$\Delta\phi(\vec{p}_T^{\ell\ell}, \vec{E}_T^{\text{miss}}) > 2.2$ radians
b -jet veto	$N(b\text{-jets}) = 0$ with b -jet $p_T > 20$ GeV and $ \eta < 2.5$

Table 2: Event selection criteria for the $\ell\ell\nu\nu$ signature.

DI-BOSONS AS TESTS OF α TGC

[JHEP 07 \(2022\) 032](#), [JHEP 07 \(2022\) 032](#), [JHEP 10 \(2019\) 127](#)

- WV production sensitive to anomalous triple gauge couplings (α TGCs)



Use p_T^γ and ϕ_l to enhance sensitivity to interference between SM and \mathcal{O}_{3W} $\mathcal{O}_{3W} = \epsilon^{ijk} W_\mu^{iv} W_\nu^{jp} W_\rho^{k\mu}$

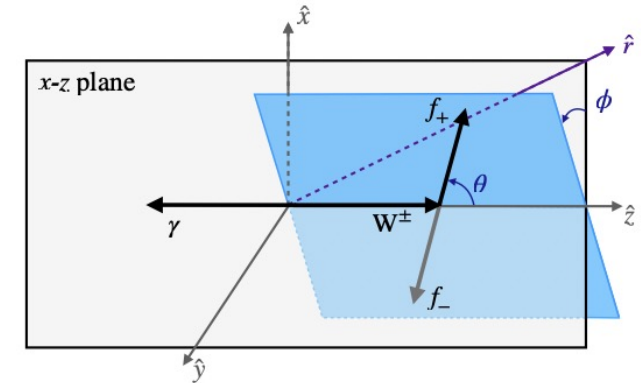
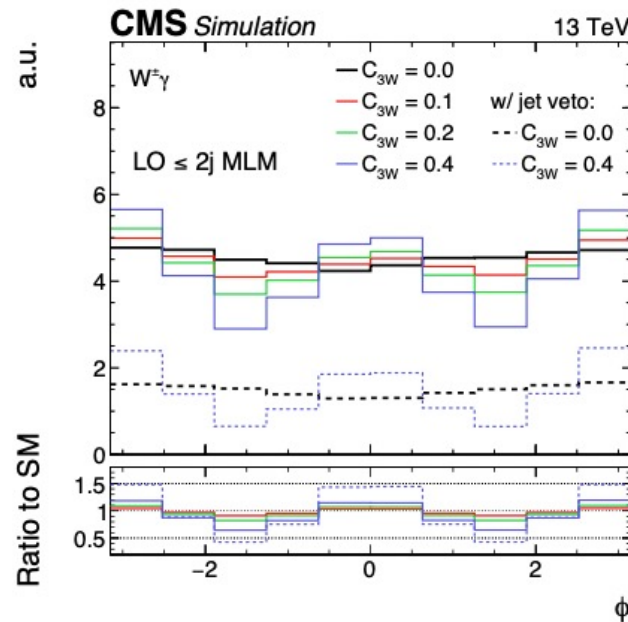
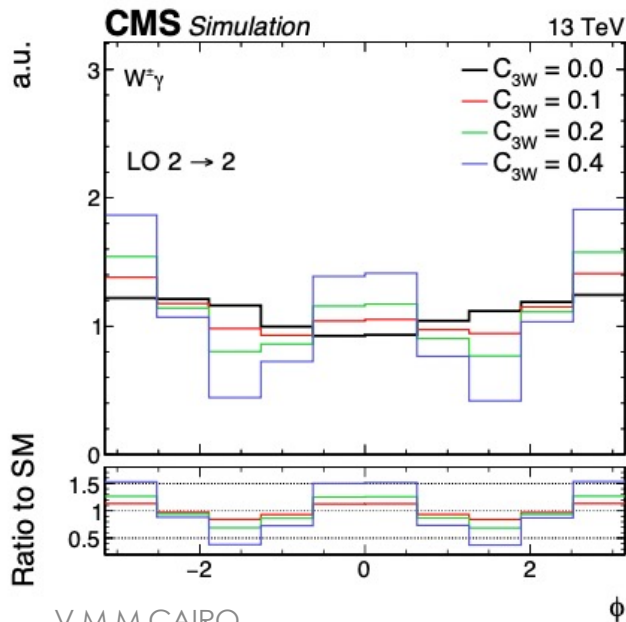


Figure 2: Scheme of the special coordinate system for $W^\pm\gamma$ production, defined by a Lorentz boost to the center-of-mass frame along the direction \hat{r} . The z axis is chosen as the W^\pm boson direction in this frame, and y is given by $\hat{z} \times \hat{r}$. The W^\pm boson decay plane is indicated in blue, where the labels f_+ and f_- refer to positive and negative helicity final-state fermions. The angles ϕ and θ are the azimuthal and polar angles of f_+ .

DI-BOSONS AS TESTS OF α TGC

[JHEP 07 \(2022\) 032](#), [JHEP 07 \(2022\) 032](#), [JHEP 10 \(2019\) 127](#)

- VV production sensitive to anomalous triple gauge couplings (α TGCs)

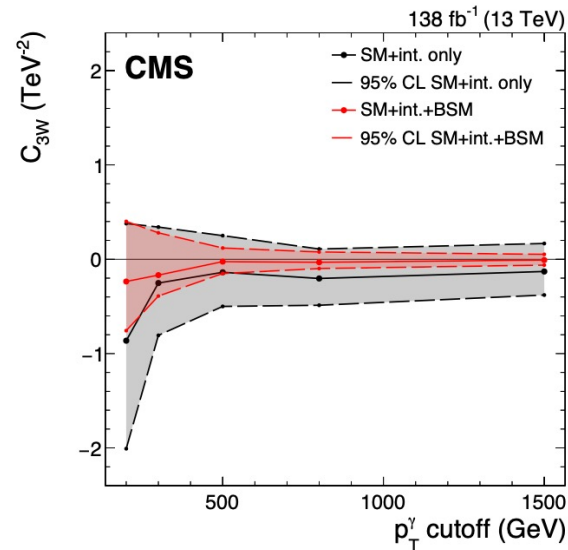
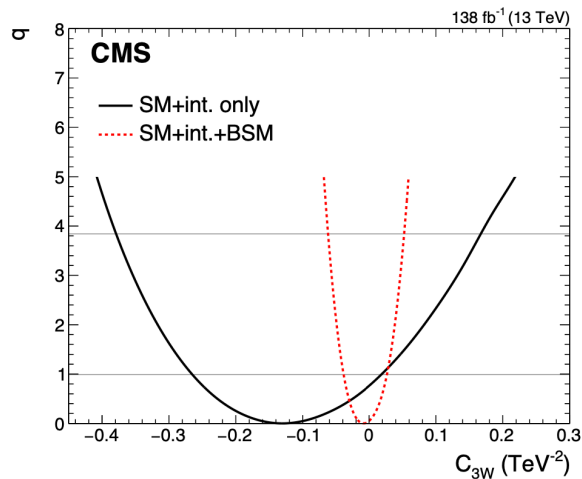


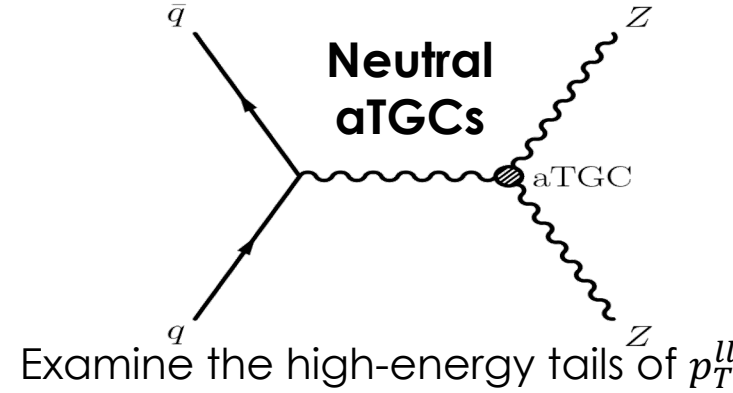
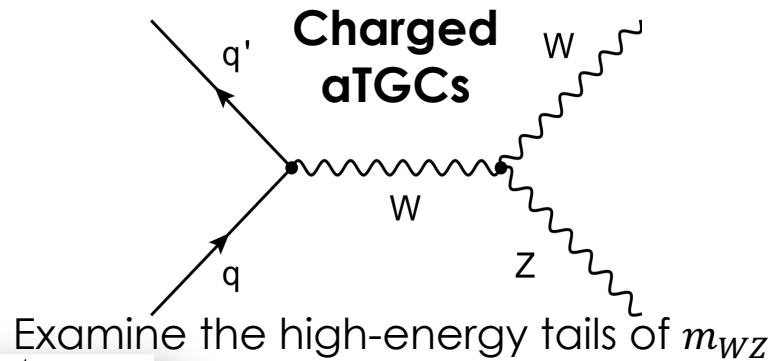
Table 4: Best fit values of C_{3W} and corresponding 95% CL confidence intervals as a function of the maximum p_T^γ bin included in the fit.

p_T^γ cutoff (GeV)	Best fit C_{3W} (TeV ⁻²)		Observed 95% CL (TeV ⁻²)		Expected 95% CL (TeV ⁻²)	
	SM+int. only	SM+int.+BSM	SM+int. only	SM+int.+BSM	SM+int. only	SM+int.+BSM
200	-0.86	-0.24	[-2.01, 0.38]	[-0.76, 0.40]	[-1.16, 1.27]	[-0.81, 0.71]
300	-0.25	-0.17	[-0.81, 0.34]	[-0.39, 0.28]	[-0.56, 0.60]	[-0.33, 0.33]
500	-0.13	-0.025	[-0.50, 0.25]	[-0.15, 0.12]	[-0.35, 0.38]	[-0.17, 0.16]
800	-0.20	-0.033	[-0.49, 0.11]	[-0.10, 0.08]	[-0.29, 0.31]	[-0.097, 0.095]
1500	-0.13	-0.009	[-0.38, 0.17]	[-0.062, 0.052]	[-0.27, 0.29]	[-0.066, 0.065]

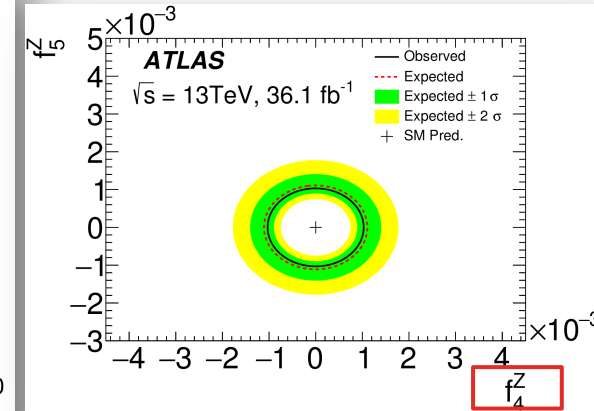
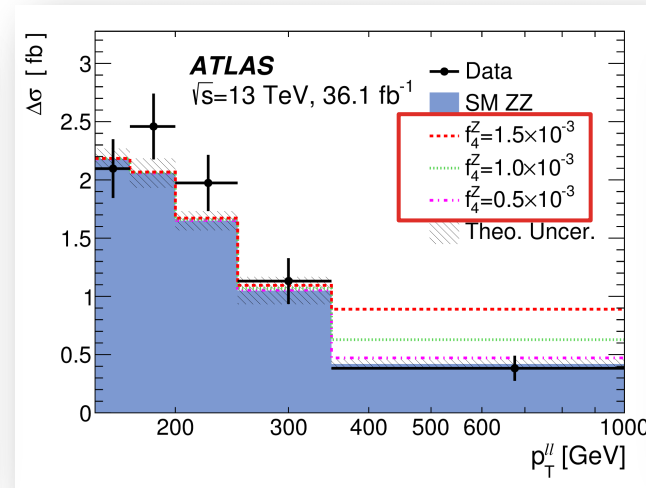
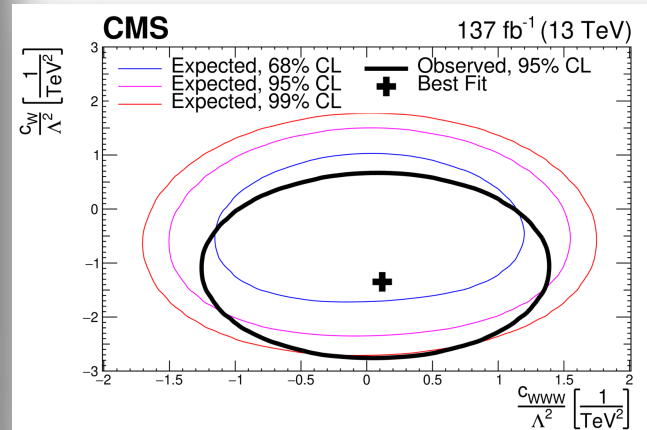
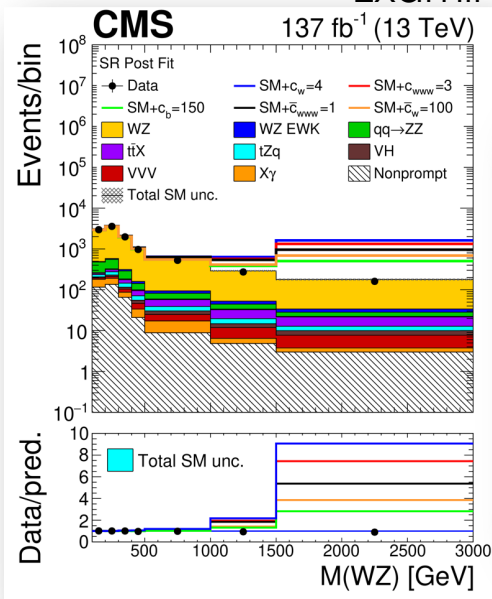
DI-BOSONS AS TESTS OF $aTGC$

[JHEP 07 \(2022\) 032](#), [JHEP 07 \(2022\) 032](#), [JHEP 10 \(2019\) 127](#)

- VV production sensitive to anomalous triple gauge couplings ($aTGCs$)



f_4^Y and f_4^Z CP violating
 f_5^Y and f_5^Z CP conserving



DI-BOSONS AS TESTS OF α TGC

[JHEP 07 \(2022\) 032](#), [JHEP 07 \(2022\) 032](#), [JHEP 10 \(2019\) 127](#)

- VV production sensitive to anomalous triple gauge couplings (α TGCs)

Figure 1 shows representative Feynman diagrams for ZZ production at the LHC. The dominant process is t -channel production with a quark and anti-quark initial state, hereafter denoted by the $qqZZ$ process. Higher-order QCD corrections to the $qqZZ$ process are found to be sizeable [4], and two tree-level diagrams concerning production of two Z bosons and one outgoing parton are shown. The gluon fusion process ($ggZZ$) includes two sub-processes, one with a fermion loop and the other involving a virtual Higgs boson. Although the $ggZZ$ process only appears at $O(\alpha_S^2)$, it nevertheless has a non-negligible contribution of $O(10\%)$ to the total ZZ production rate due to the large gluon flux at the LHC. The s -channel production is forbidden at the lowest order; however, the neutral TGCs can still acquire small values of $O(10^{-4})$ in the SM, due to the correction with a fermion loop [5]. The observation of α TGCs with larger values would hint at the existence of new physics.

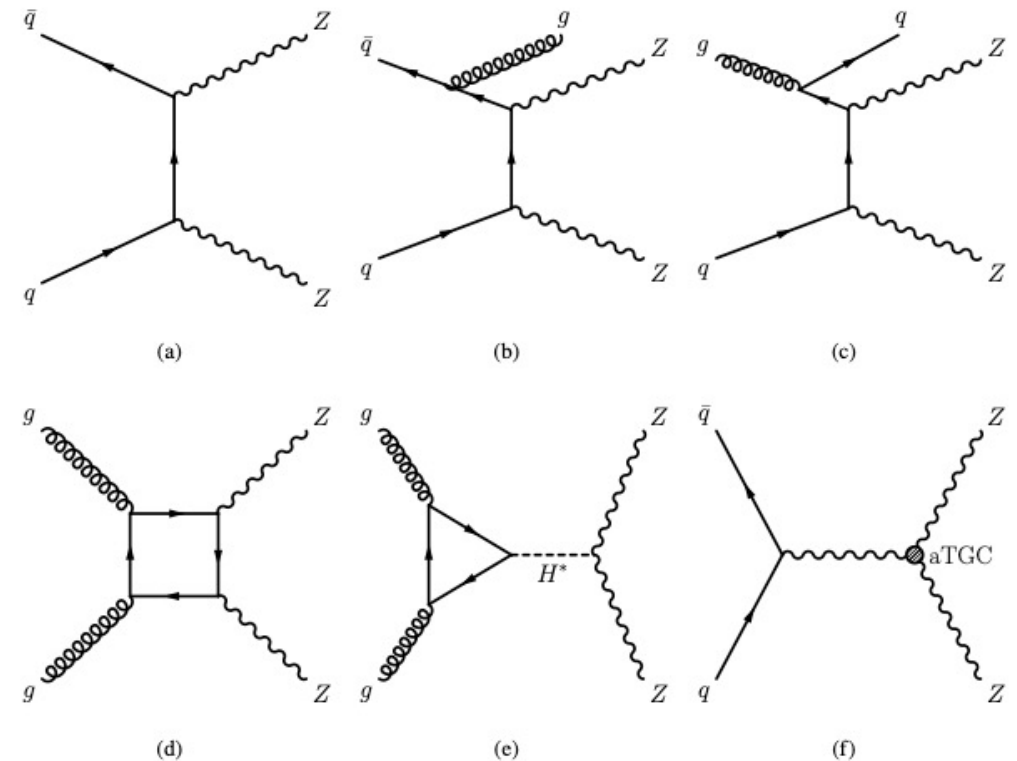


Figure 1: Representative Feynman diagrams for ZZ production at the LHC: (a) lowest-order t -channel $qqZZ$ production; (b) production of ZZ plus one parton through the $q\bar{q}$ initial state; (c) production of ZZ plus one parton through the qg initial state; (d) $ggZZ$ production with a fermion loop; (e) $ggZZ$ production involving an exchange of a virtual Higgs boson; (f) s -channel production with α TGCs.

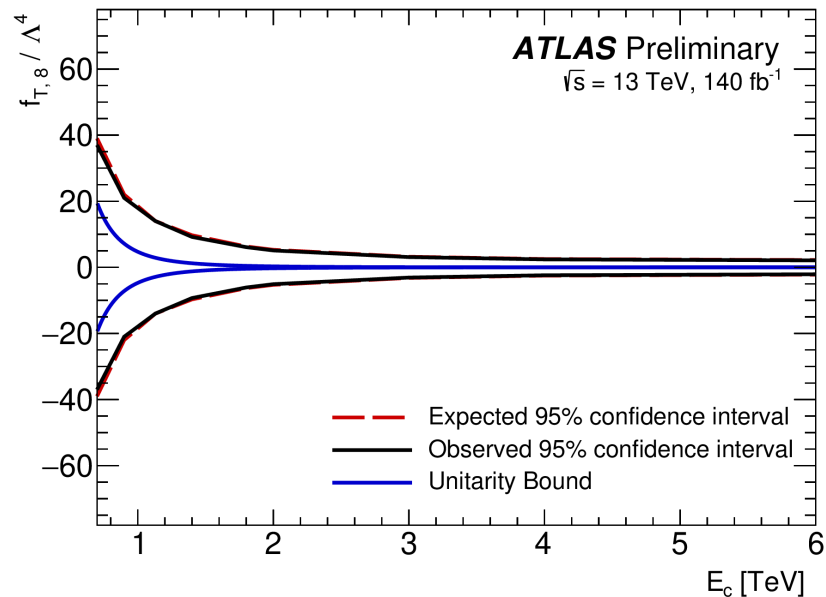
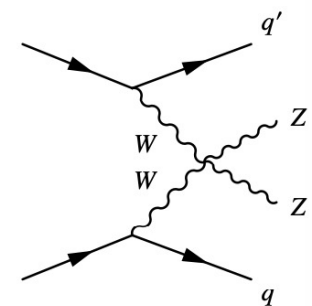
DI-BOSONS AS TESTS OF a QGC

[2212.12592](#), [ATLAS-CONF-2023-023](#), [JHEP 06 \(2023\) 082](#), [ATLAS-CONF-2023-024](#)

- $V\gamma$ or VV plus jets used by CMS and ATLAS to test **anomalous quartic gauge couplings (aQGCs)** in terms of dimension-8 EFT operators
 - 4 covariant derivatives of the Higgs field ($O_{S0,1,2}$, scalar type)
 - 2 Higgs covariant derivatives and 2 field strength tensors ($O_{M0,1,2,3,4,5,7}$ of mixed – scalar and tensor – type)
 - 4 field strength tensors ($O_{T0,1,2,5,6,7,8,9}$ of tensor type).

$$\mathcal{L}_{\text{eff}} = \mathcal{L}_{\text{SM}} + \sum_i \frac{f_i^{(6)}}{\Lambda^2} O_i^{(6)} + \sum_j \frac{f_j^{(8)}}{\Lambda^4} O_j^{(8)} + \dots$$

$ZZ \rightarrow 4l$



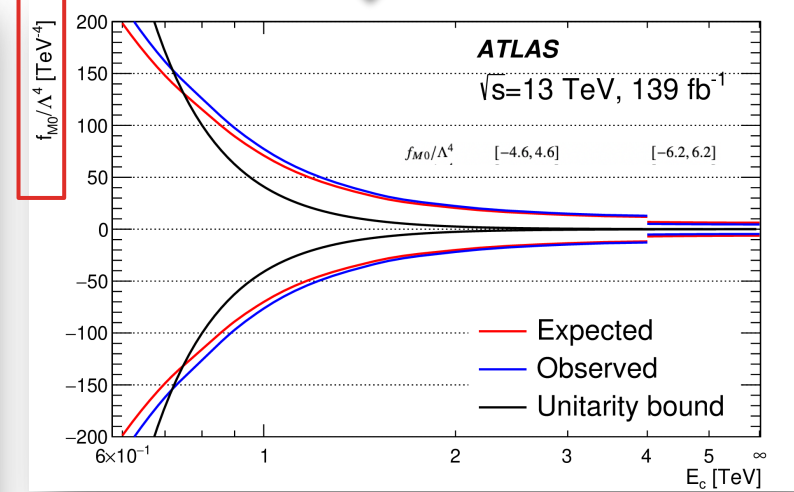
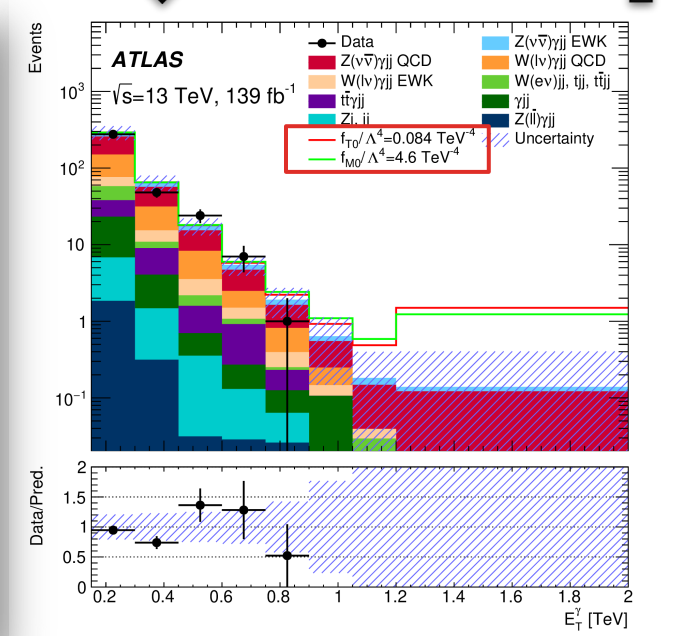
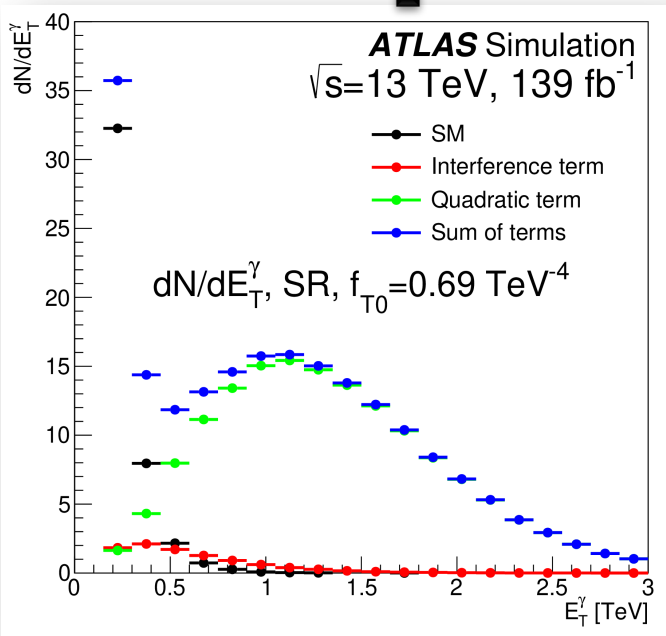
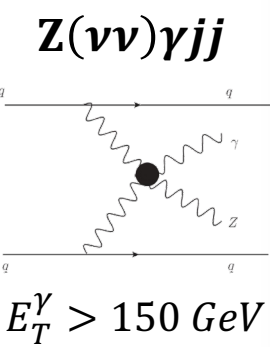
Wilson coefficient	$ \mathcal{M}_{d6} ^2$ Included	95% confidence interval [TeV ⁻²] Expected	Observed
c_W/Λ^2	yes	[-1.3, 1.3]	[-1.2, 1.2]
	no	[-32, 32]	[-37, 28]
$c_{\bar{W}}/\Lambda^2$	yes	[-1.3, 1.3]	[-1.2, 1.2]
	no	[-17, 17]*	[0, 30]*
c_{HWB}/Λ^2	yes	[-16, 7]	[-16, 6]
	no	[-12, 12]	[-15, 10]
$c_{H\bar{W}B}/\Lambda^2$	yes	[-1.3, 1.3]	[-1.2, 1.2]
	no	[-67, 67]*	[-25, 130]*
c_{HB}/Λ^2	yes	[-13, 13]	[-12, 12]
	no	[-38, 38]	[-38, 38]
$c_{H\bar{B}}/\Lambda^2$	yes	[-13, 13]	[-12, 12]
	no	[-420, 420]*	[-200, 790]*

The analysis sets also limits on dim6 operators, obtained using a 2D fit to the $4lj$ differential cross-sections as a function of m_{4l} and m_{jj} , except for the constraints on CP-odd operators when the pure dimension-six contribution to the EFT is excluded. Those constraints, denoted with a (*), are obtained in a fit to the differential cross section as a function of $\Delta\phi_{jj}$.

DI-BOSONS AS TESTS OF a QGC

[CMS: 2212.12592](#),
[ATLAS: ATLAS-CONF-2023-023](#), [JHEP 06 \(2023\) 082](#), [ATLAS-CONF-2023-024](#)

- $V\gamma$ or VV plus jets used by CMS and ATLAS to test **anomalous quartic gauge couplings (aQGCs)** in terms of dimension-8 EFT operators
 - 4 covariant derivatives of the Higgs field ($O_{S0,1,2}$, scalar type)
 - 2 Higgs covariant derivatives and 2 field strength tensors ($O_{M0,1,2,3,4,5,7}$ of mixed – scalar and tensor – type)
 - 4 field strength tensors ($O_{T0,1,2,5,6,7,8,9}$ of tensor type).



In addition, on $T_{5,8,9}$ tighter limits than previous results by ATLAS and CMS ($T_{8,9}$ uniquely probed via neutral quartic vertices)

DI-BOSONS AS TESTS OF α QGC

[CMS: 2212.12592](#),

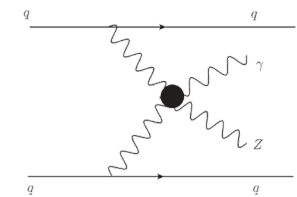
[ATLAS: ATLAS-CONF-2023-023](#), [JHEP 06 \(2023\) 082](#), [ATLAS-CONF-2023-024](#)

- $V\gamma$ or VV plus jets used by CMS and ATLAS to test **anomalous quartic gauge couplings (aQGCs)** in terms of dimension-8 EFT operators
 - 4 covariant derivatives of the Higgs field ($O_{S0,1,2}$, scalar type)
 - 2 Higgs covariant derivatives and 2 field strength tensors ($O_{M0,1,2,3,4,5,7}$ of mixed – scalar and tensor – type)
 - 4 field strength tensors ($O_{T0,1,2,5,6,7,8,9}$ of tensor type).

Table 2: Fiducial region definition.

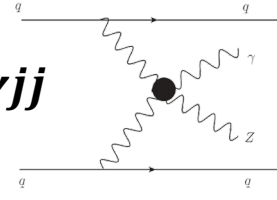
Selections	Cut value
E_T^{miss}	$> 120 \text{ GeV}$
E_T^γ	$> 150 \text{ GeV}$
Number of isolated photons	$N_\gamma = 1$
Photon isolation	$E_T^{\text{cone40}} < 0.022p_T + 2.45 \text{ GeV}$, $p_T^{\text{cone20}}/p_T < 0.05$
Number of jets	$N_{\text{jets}} \geq 2$ with $p_T > 50 \text{ GeV}$
Overlap removal	$\Delta R(\gamma, \text{jet}) > 0.3$
Lepton veto	$N_e = 0, N_\mu = 0$
$ \Delta\phi(\gamma, \vec{p}_T^{\text{miss}}) $	> 0.4
$ \Delta\phi(j_1, \vec{p}_T^{\text{miss}}) $	> 0.3
$ \Delta\phi(j_2, \vec{p}_T^{\text{miss}}) $	> 0.3
m_{jj}	$> 300 \text{ GeV}$
γ -centrality	< 0.6

$Z(\nu\nu)\gamma jj$



$E_T^\gamma > 150 \text{ GeV}$

EW DIBOSONS AS TESTS OF a QGC

 $Z(\nu\nu)\gamma jj$


$$\mathcal{L}_{\text{eff}} = \mathcal{L}_{\text{SM}} + \sum_i \frac{f_i^{(6)}}{\Lambda^2} O_i^{(6)} + \sum_j \frac{f_j^{(8)}}{\Lambda^4} O_j^{(8)} + \dots$$

[JHEP 06 \(2023\) 082](#)

Table 6: Observed and expected one-dimensional limits on dimension-8 aQGC coefficients. Limits are obtained by setting all aQGC coefficients except one to zero. Unitarity is not preserved.

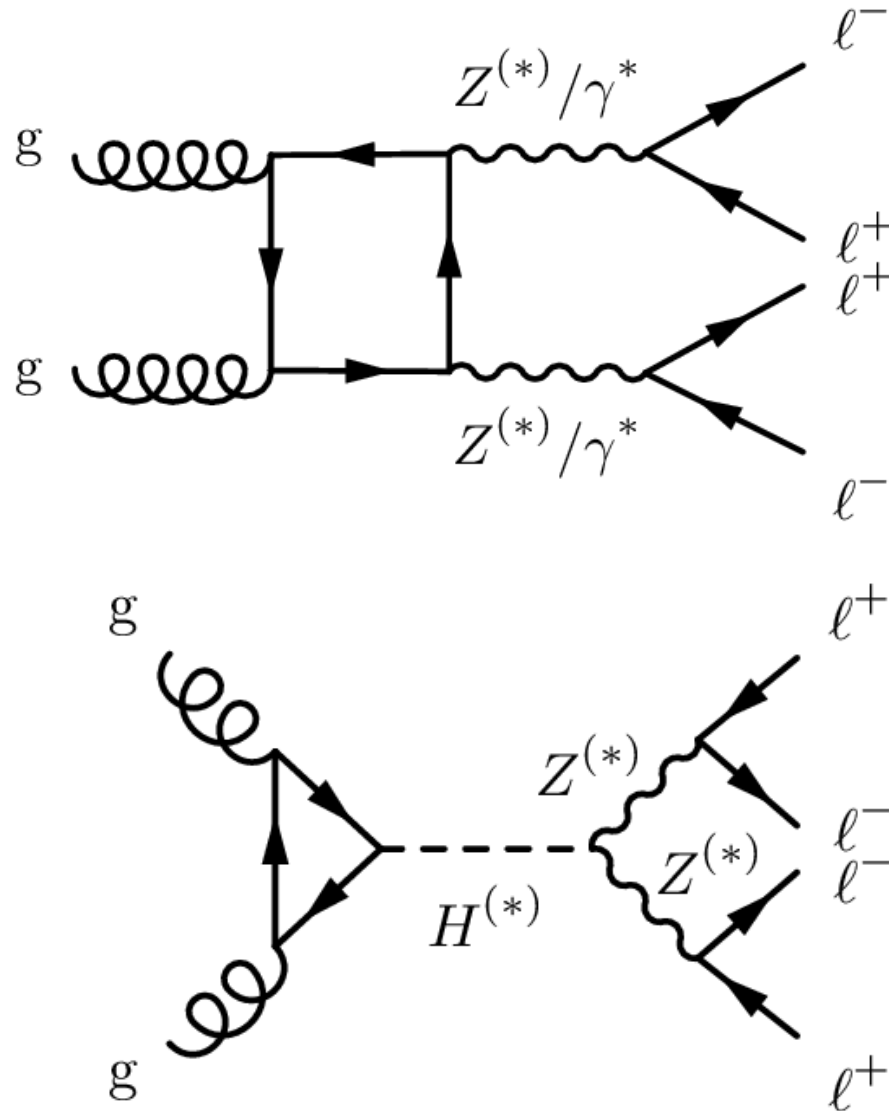
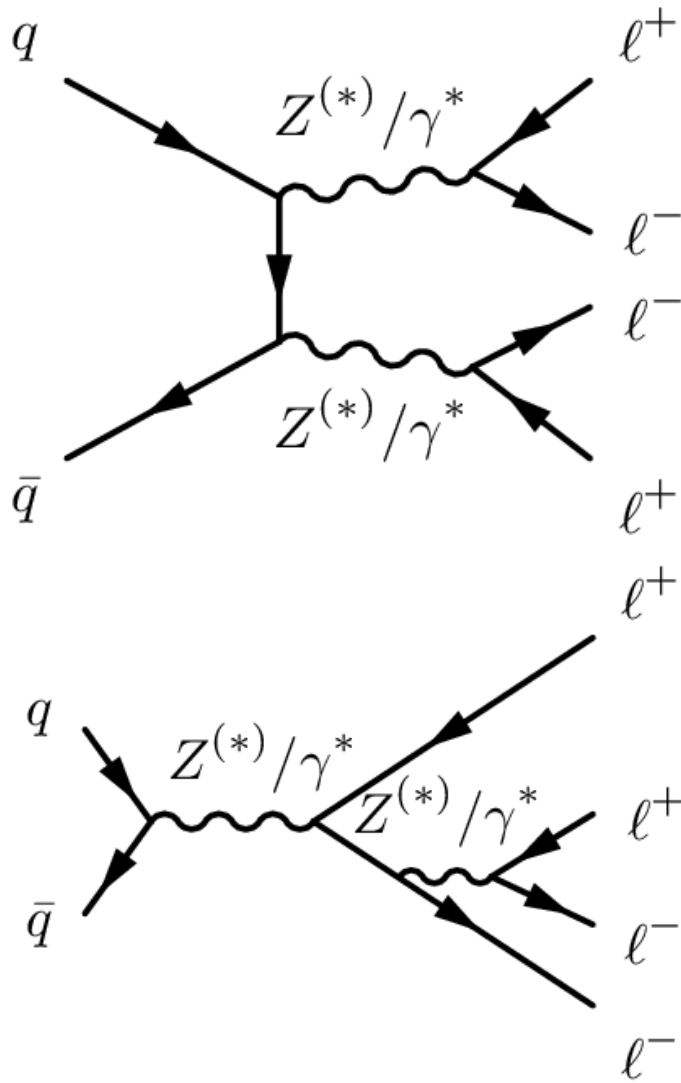
Coefficient	Observed limit [TeV ⁻⁴]	Expected limit [TeV ⁻⁴]
f_{T0}/Λ^4	$[-9.4, 8.4] \times 10^{-2}$	$[-1.3, 1.2] \times 10^{-1}$
f_{T5}/Λ^4	$[-8.8, 9.9] \times 10^{-2}$	$[-1.2, 1.3] \times 10^{-1}$
f_{T8}/Λ^4	$[-5.9, 5.9] \times 10^{-2}$	$[-8.1, 8.0] \times 10^{-2}$
f_{T9}/Λ^4	$[-1.3, 1.3] \times 10^{-1}$	$[-1.7, 1.7] \times 10^{-1}$
f_{M0}/Λ^4	$[-4.6, 4.6]$	$[-6.2, 6.2]$
f_{M1}/Λ^4	$[-7.7, 7.7]$	$[-1.0, 1.0] \times 10^1$
f_{M2}/Λ^4	$[-1.9, 1.9]$	$[-2.6, 2.6]$

Table 7: Observed and expected one-dimensional limits on dimension-8 aQGC coefficients in the region where unitarity is preserved. The cut-off scale E_c in the simulation is given for each parameter. Limits are obtained by setting all aQGC coefficients except one to zero.

Coefficient	E_c [TeV]	Observed limit [TeV ⁻⁴]	Expected limit [TeV ⁻⁴]
f_{T0}/Λ^4	1.7	$[-8.7, 7.1] \times 10^{-1}$	$[-8.9, 7.3] \times 10^{-1}$
f_{T5}/Λ^4	2.4	$[-3.4, 4.2] \times 10^{-1}$	$[-3.5, 4.3] \times 10^{-1}$
f_{T8}/Λ^4	1.7	$[-5.2, 5.2] \times 10^{-1}$	$[-5.3, 5.3] \times 10^{-1}$
f_{T9}/Λ^4	1.9	$[-7.9, 7.9] \times 10^{-1}$	$[-8.1, 8.1] \times 10^{-1}$
f_{M0}/Λ^4	0.7	$[-1.6, 1.6] \times 10^2$	$[-1.5, 1.5] \times 10^2$
f_{M1}/Λ^4	1.0	$[-1.6, 1.5] \times 10^2$	$[-1.4, 1.4] \times 10^2$
f_{M2}/Λ^4	1.0	$[-3.3, 3.2] \times 10^1$	$[-3.0, 3.0] \times 10^1$

4LEPTON EVENTS

[JHEP 07 \(2021\) 005](#)



4LEPTON EVENTS

JHEP 07 (2021) 005

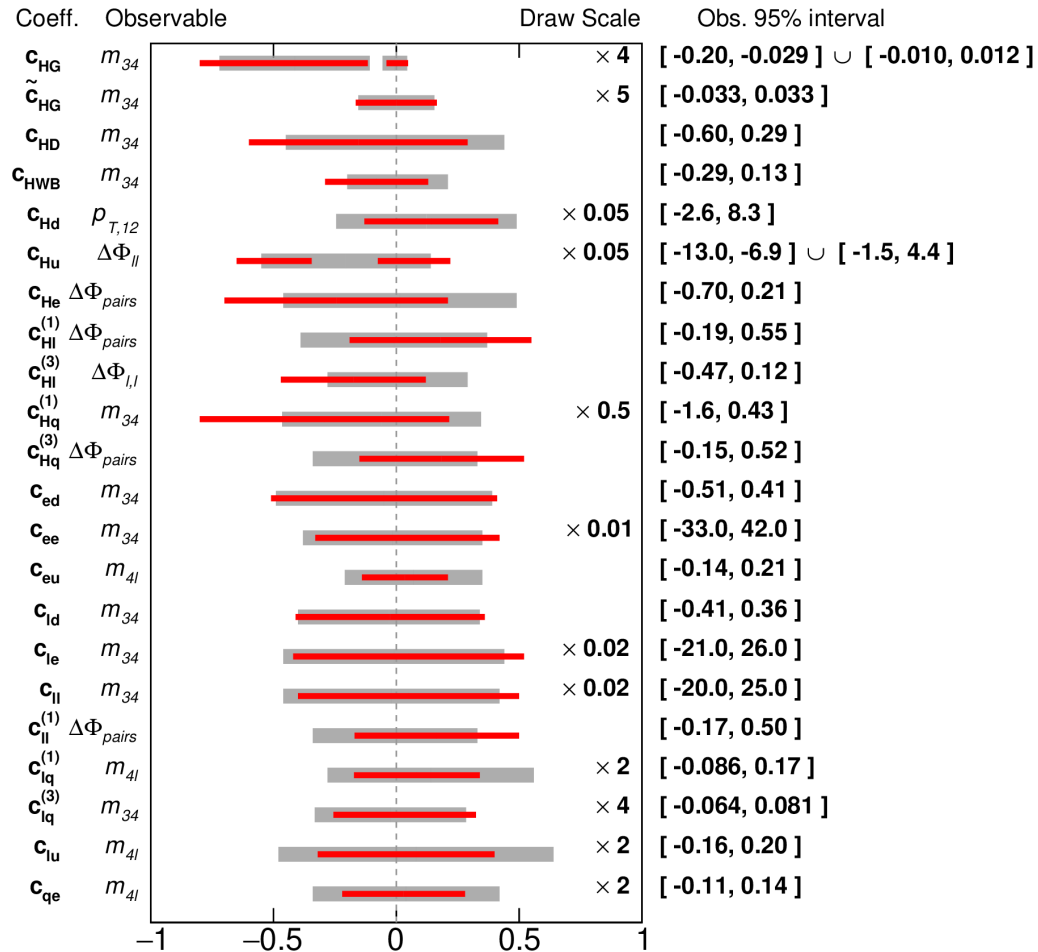
ATLAS

$\sqrt{s}=13$ TeV, 139 fb⁻¹

full model

Expected 95% CL

Observed 95% CL



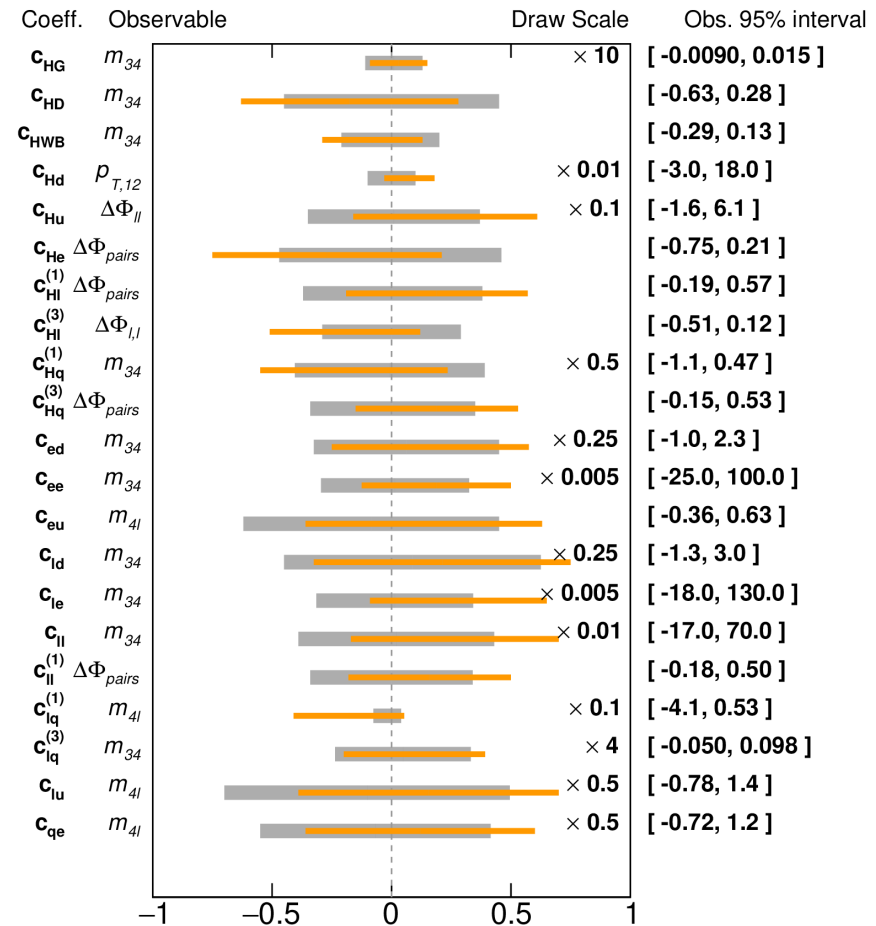
ATLAS

$\sqrt{s}=13$ TeV, 139 fb⁻¹

only linear term

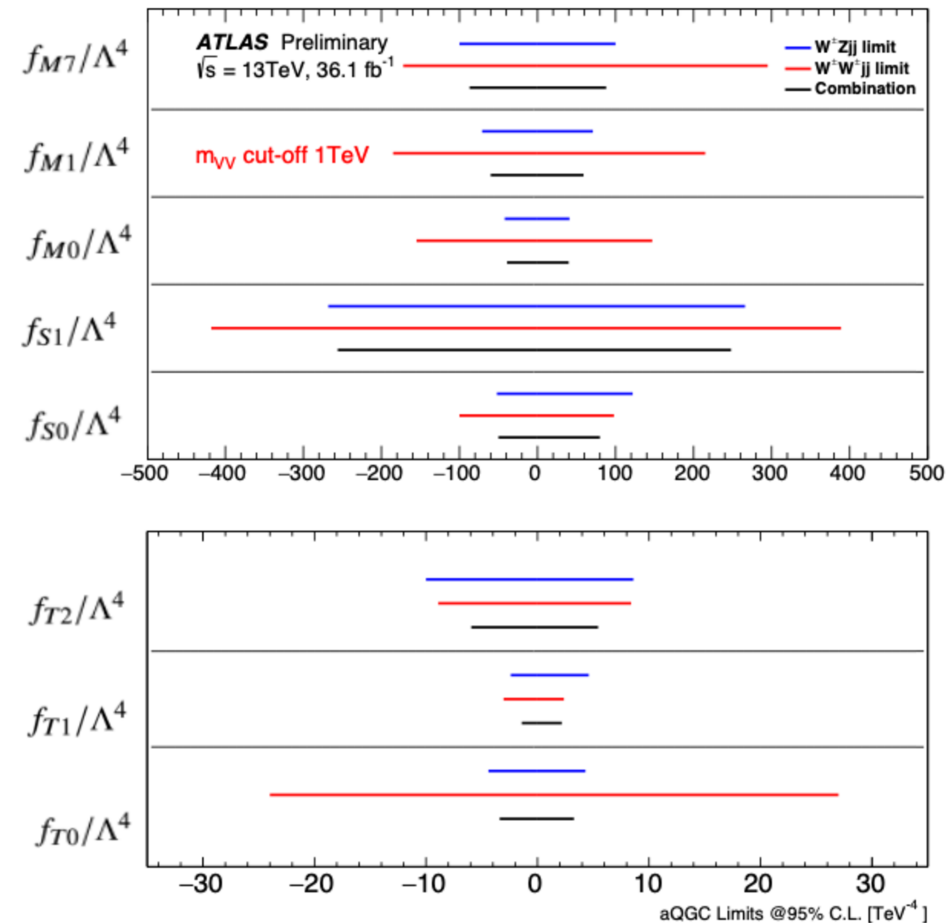
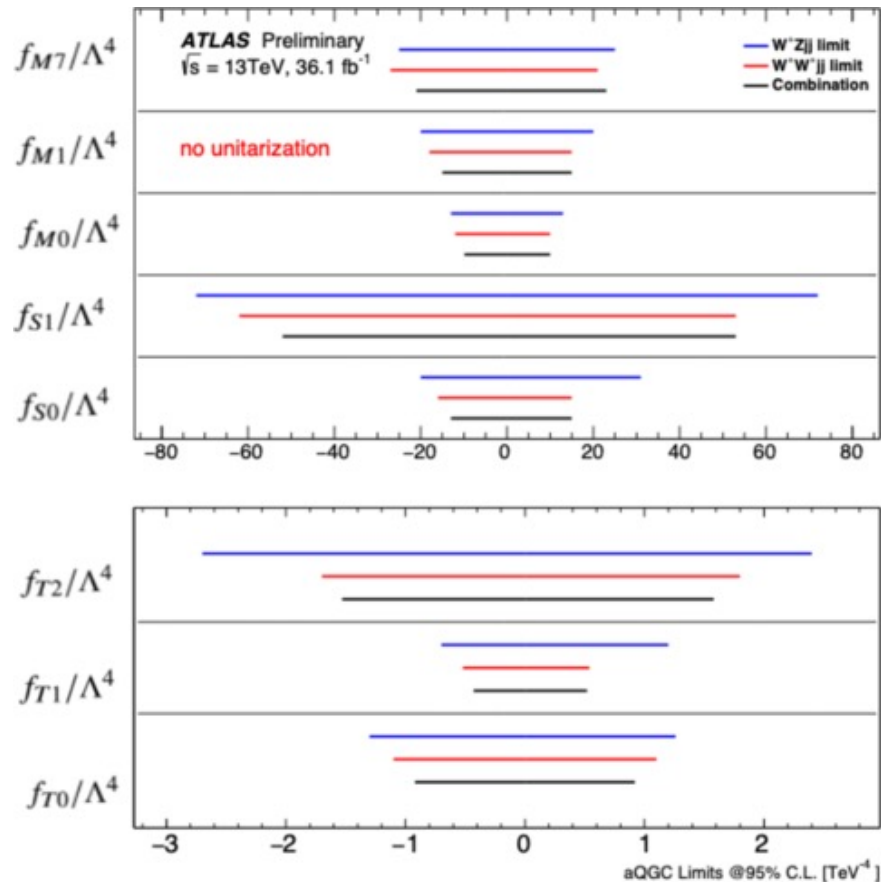
Expected 95% CL

Observed 95% CL



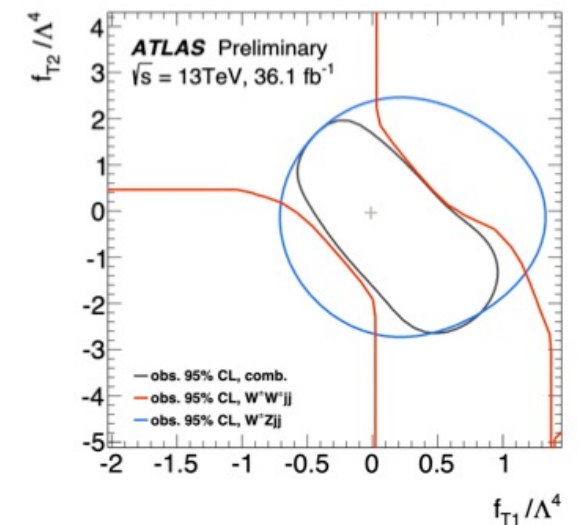
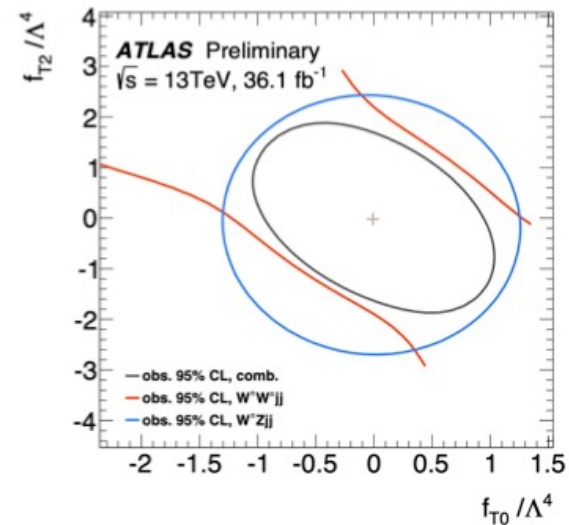
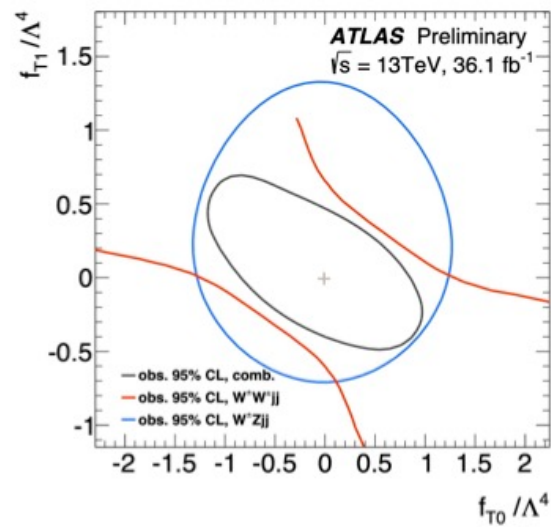
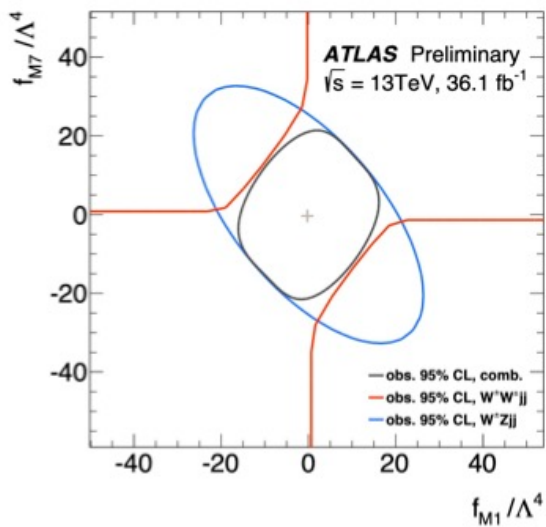
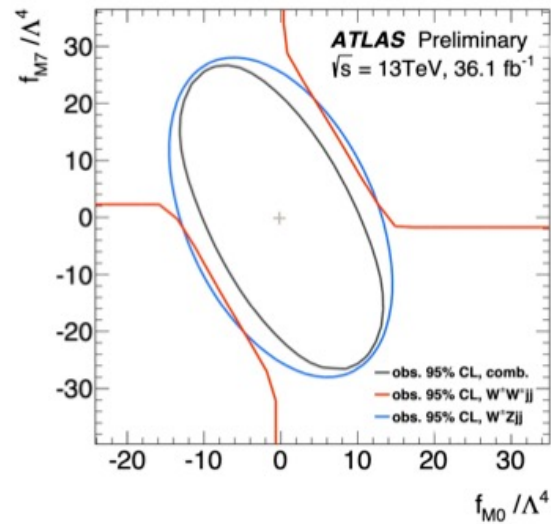
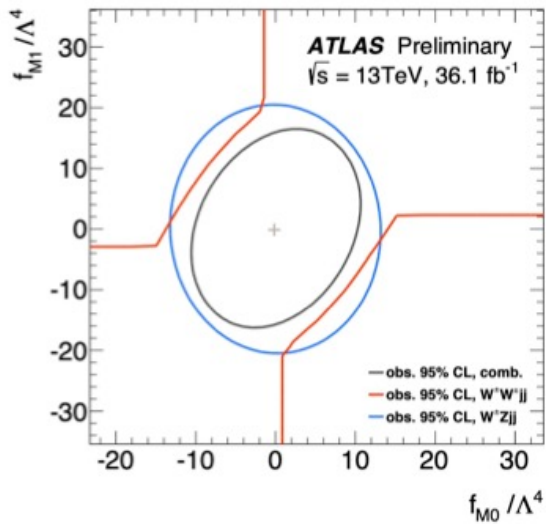
aQGC COMBINATION ATL-PHYS-PUB-2023-002/

These limits represent the first limits at 13 TeV on aQGC parameters in the electroweak $W_{\pm}Zjj$ and $W_{\pm}W_{\pm}jj$ processes, as well as the first combination of D-8 EFT operators, performed using unfolded and reconstruction-level results.



a QGC COMBINATION

[ATL-PHYS-PUB-2023-002/](#)



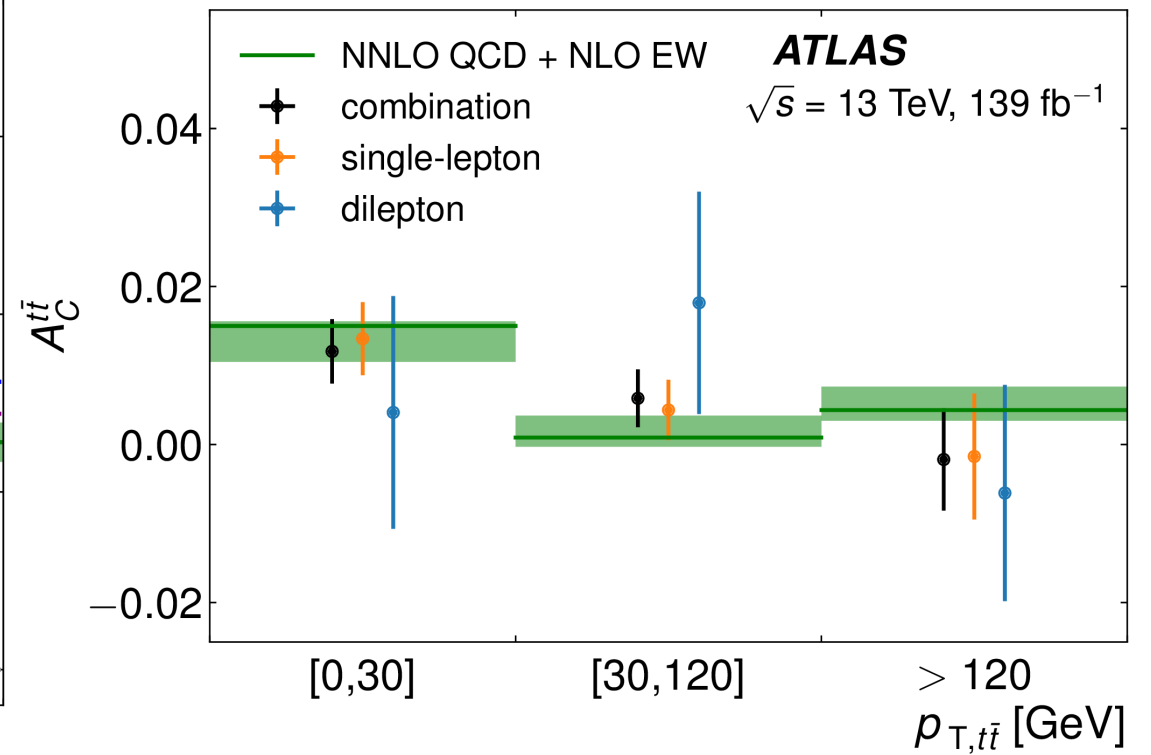
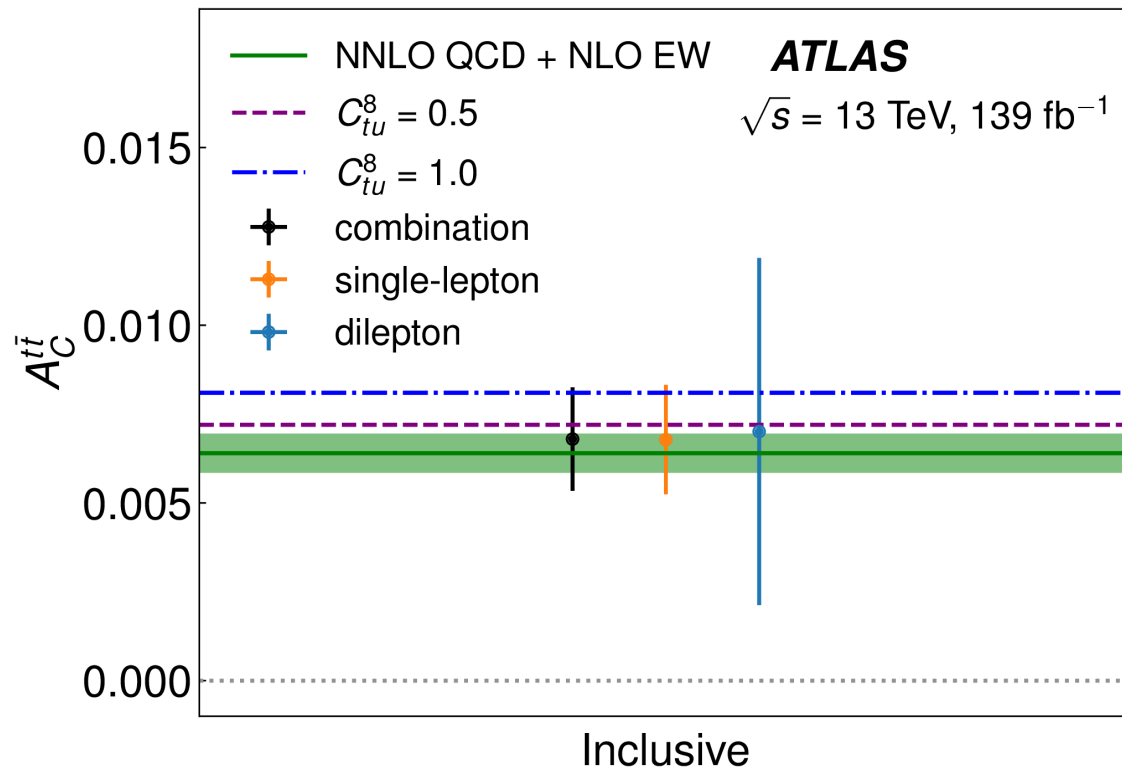
*a*QGC COMBINATION [ATL-PHYS-PUB-2023-002/](#)

Comparing the nominal unclipped exclusion intervals with the current best limits, obtained by the CMS collaboration using the $W_{\pm}V jj$ fully leptonic [10] and semileptonic [17] channels, it can be seen that the limits are not competitive. However, no optimization was done regarding the binning or the phase space used for this study. The individual limits can be improved by using the Full Run 2 dataset and the combination can be improved, for example, by including more channels as well as a more extensive correlation of the experimental systematic uncertainties. The analysis flow developed for this result makes it straightforward to include additional measurements in the combination in the future.

TOP

$t\bar{t}$ CHARGE ASYMMETRY

TOPQ-2020-06



$t\bar{t}$ CHARGE ASYMMETRY TOPQ-2020-06

$$A_C^{\ell\bar{\ell}} = \frac{N(\Delta|\eta_{\ell\bar{\ell}}| > 0) - N(\Delta|\eta_{\ell\bar{\ell}}| < 0)}{N(\Delta|\eta_{\ell\bar{\ell}}| > 0) + N(\Delta|\eta_{\ell\bar{\ell}}| < 0)}$$

The leptonic asymmetry is slightly diluted relative to the underlying top-quark asymmetry, but has the advantage that reconstruction of the top-quark pair is not required; only the directions and charges of the leptons are needed.

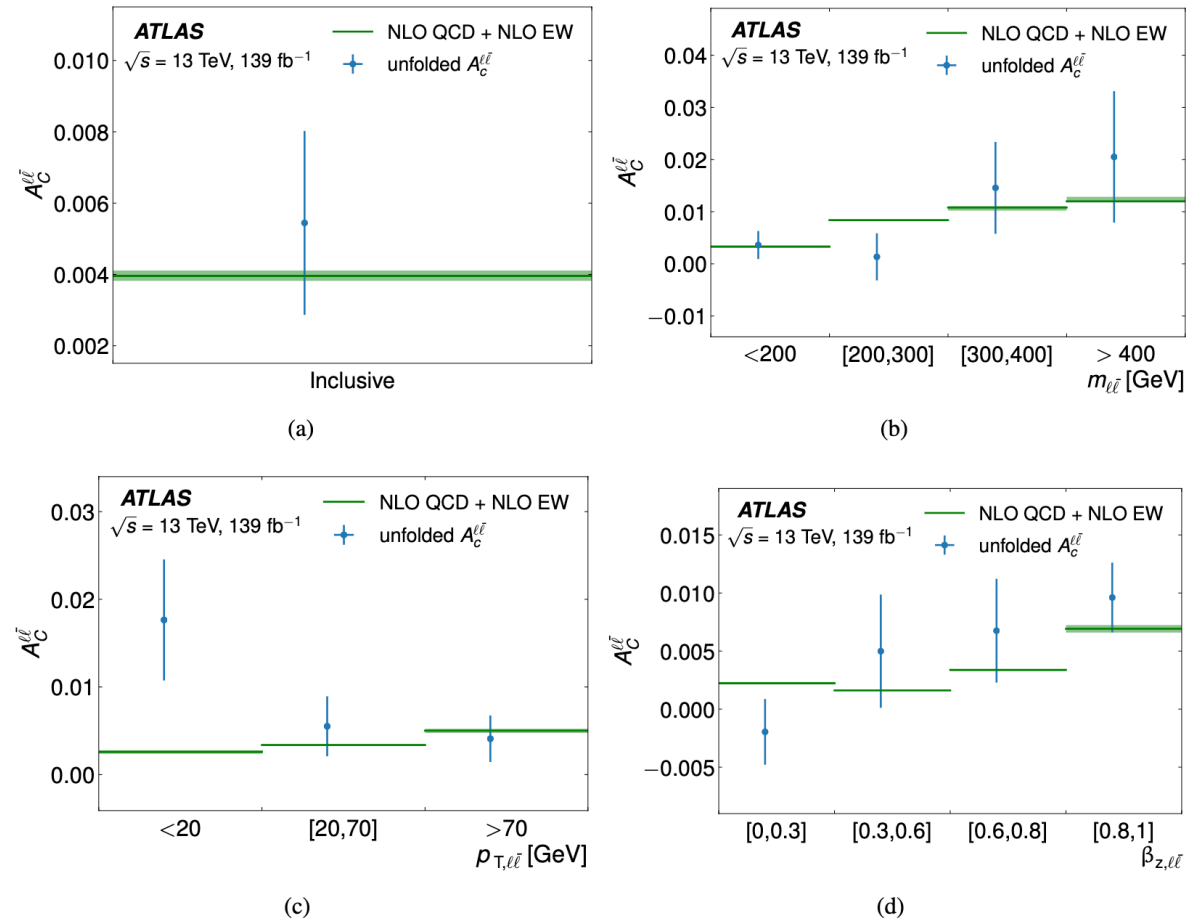
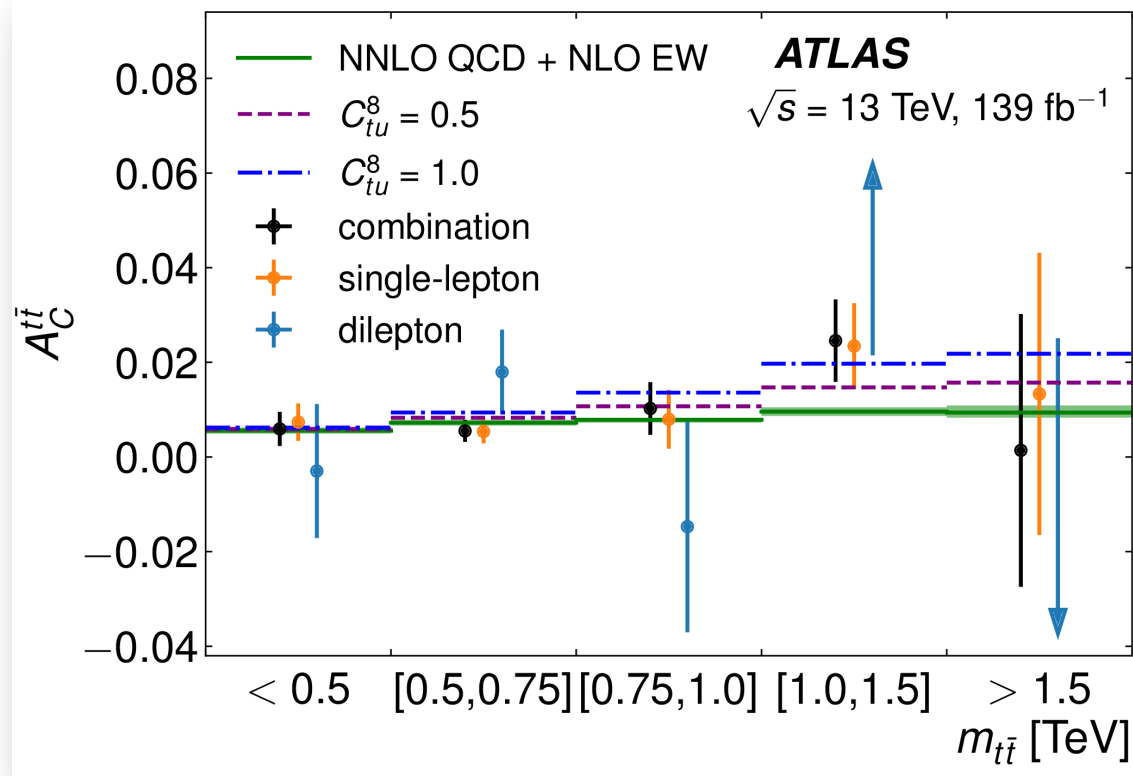


Figure 6: The unfolded inclusive (a) and differential leptonic asymmetries as a function of the invariant mass (b), transverse momentum (c), and the longitudinal boost (d) of the reconstructed lepton pair in dilepton channel data. Shaded regions show SM theory predictions calculated at NLO in QCD and NLO in EW theory. Vertical bars correspond to the total uncertainties.

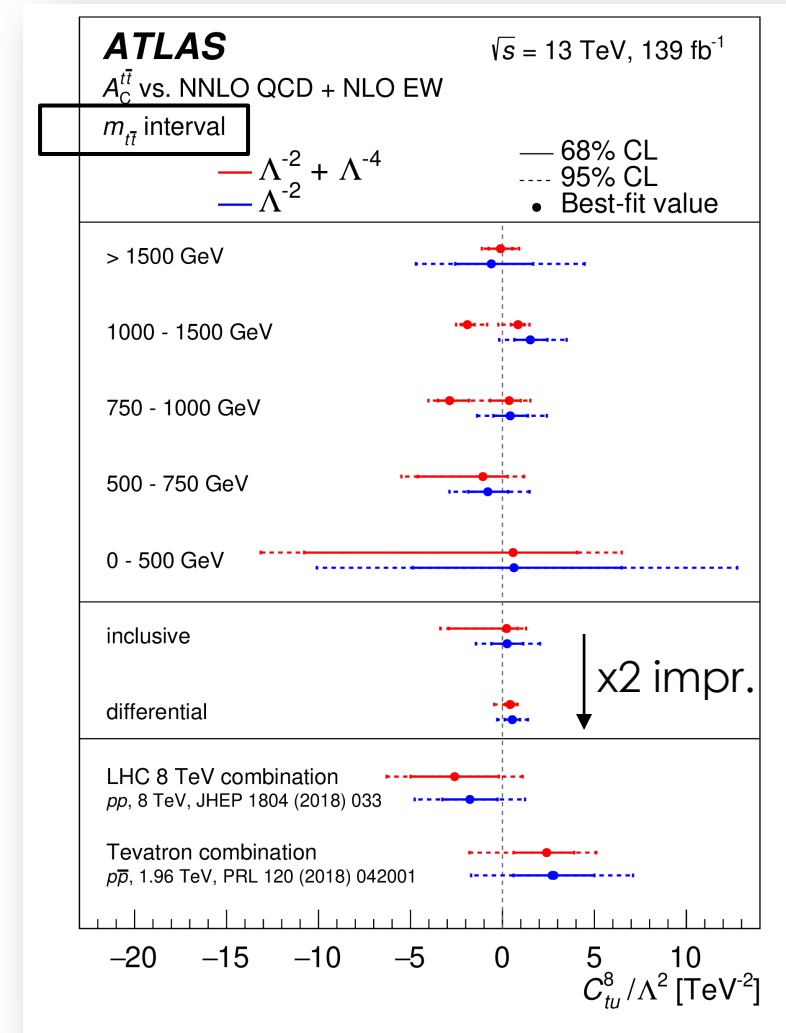
$t\bar{t}$ CHARGE ASYMMETRY 2208.12095

- Results are **interpreted in SMEFT** (14 four-fermion operators and 1 top-gluon operator, SMEFT@NLO)

$$O_{tu}^8 = (\bar{t}\gamma_\mu T^A t)(\bar{u}_i\gamma^\mu T^A u_i)$$



Complementary info to charge asymmetry (see extra slides)

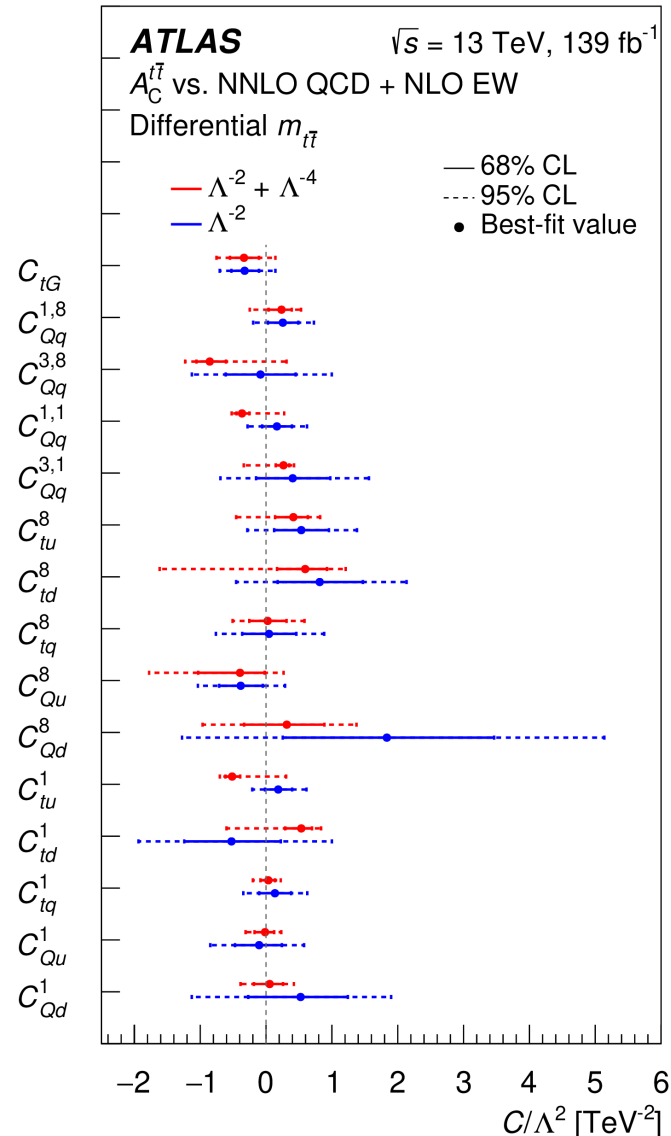


$t\bar{t}$ CHARGE ASYMMETRY

TOPQ-2020-06

Compared to global fits of the top-quark sector and fits including top, Higgs and EW data the bounds found in this analysis are of the same order of magnitude.

Often, the bounds from the differential analysis are significantly tighter than the global bounds, indicating that inclusion of these results in future global fits can improve the global result, by disentangling some of the poorly constrained combinations of operator coefficients.



In the following, the left-handed (L) quark doublets of the first two generations are represented by $q_i = (u_L, d_i)$, (c_L, s_L) , and the doublet of the third generation is given by $Q = (t_L, b_L)$. Right-handed (R) quarks of the first two generations are denoted by u_i, d_i and the right-handed top quark by t .

Using this notation, our interpretation considers 15 dimension-six operators in the Warsaw basis [44, 45]:

- There are eight $q\bar{q}t\bar{t}$ operators with LL and RR chiral structures:

$$\begin{aligned}
 O_{Qq}^{1,8} &= (\bar{Q}\gamma_\mu T^A Q)(\bar{q}_i\gamma^\mu T^A q_i), & O_{Qq}^{1,1} &= (\bar{Q}\gamma_\mu Q)(\bar{q}_i\gamma^\mu q_i), \\
 O_{Qq}^{3,8} &= (\bar{Q}\gamma_\mu T^A \tau^I Q)(\bar{q}_i\gamma^\mu T^A \tau^I q_i), & O_{Qq}^{3,1} &= (\bar{Q}\gamma_\mu \tau^I Q)(\bar{q}_i\gamma^\mu \tau^I q_i), \\
 O_{tu}^8 &= (\bar{t}\gamma_\mu T^A t)(\bar{u}_i\gamma^\mu T^A u_i) & O_{tu}^1 &= (\bar{t}\gamma_\mu t)(\bar{u}_i\gamma^\mu u_i) \\
 O_{td}^8 &= (\bar{t}\gamma_\mu T^A t)(\bar{d}_i\gamma^\mu T^A d_i) & O_{td}^1 &= (\bar{t}\gamma_\mu t)(\bar{d}_i\gamma^\mu d_i).
 \end{aligned}$$

- There are six further $q\bar{q}t\bar{t}$ operators with LR structures:

$$\begin{aligned}
 O_{Qu}^8 &= (\bar{Q}\gamma_\mu T^A Q)(\bar{u}_i\gamma^\mu T^A u_i) & O_{Qu}^1 &= (\bar{Q}\gamma_\mu Q)(\bar{u}_i\gamma^\mu u_i) \\
 O_{Qd}^8 &= (\bar{Q}\gamma_\mu T^A Q)(\bar{d}_i\gamma^\mu T^A d_i) & O_{Qd}^1 &= (\bar{Q}\gamma_\mu Q)(\bar{d}_i\gamma^\mu d_i) \\
 O_{tq}^8 &= (\bar{t}\gamma_\mu T^A t)(\bar{q}_i\gamma^\mu T^A q_i) & O_{tq}^1 &= (\bar{t}\gamma_\mu t)(\bar{q}_i\gamma^\mu q_i).
 \end{aligned}$$

- There is one tensor operator that modifies the top-gluon interaction:

$$O_{tG} = (\bar{t}\sigma^{\mu\nu} T^A t)\tilde{\varphi}G_{\mu\nu}^A.$$

The indices indicate the strong and weak structures: colour-singlet operators are indicated with (1) and colour-octet operators with (8), weak-singlet operators with (1) and weak-triplet operators with (3). Also, $T^A \equiv \lambda^A/2$ where λ^A are Gell-Mann matrices; τ^I represents Pauli matrices, $\tilde{\varphi}$ represents the Higgs doublet φ with the antisymmetric SU(2) tensor by $\epsilon = i\tau^2$ and $\tilde{\varphi} = \epsilon\varphi^*$. The CP-violating imaginary parts of operator coefficients are not considered.

$t\bar{t}$ CHARGE ASYMMETRY AND ENERGY ASYMMETRY

[TOPQ-2020-06](#), [TOPQ-2019-28](#)

The energy asymmetry in $t\bar{t}j$ production is defined as

$$A_E(\theta_j) \equiv \frac{\sigma^{\text{opt}}(\theta_j|\Delta E > 0) - \sigma^{\text{opt}}(\theta_j|\Delta E < 0)}{\sigma^{\text{opt}}(\theta_j|\Delta E > 0) + \sigma^{\text{opt}}(\theta_j|\Delta E < 0)}, \quad (1)$$

with the *optimised cross section*

$$\sigma^{\text{opt}}(\theta_j) = \sigma(\theta_j|y_{t\bar{t}j} > 0) + \sigma(\pi - \theta_j|y_{t\bar{t}j} < 0), \quad \theta_j \in [0, \pi], \quad (2)$$

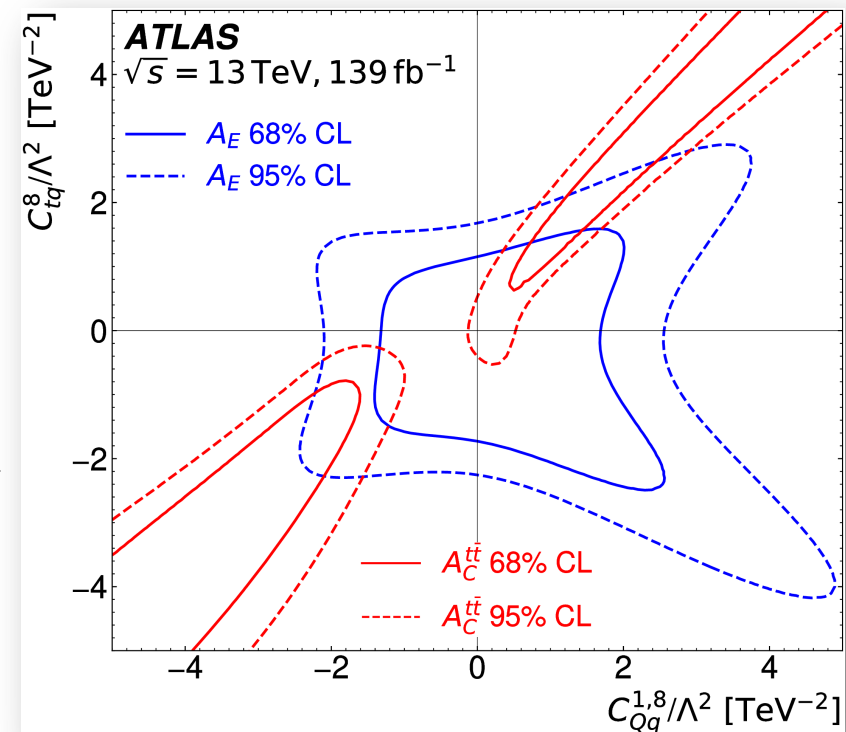
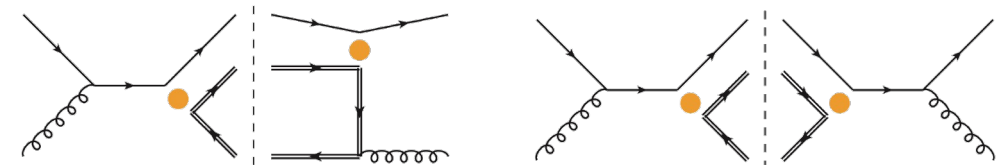
where $\sigma(\theta_j)$ is the differential cross section as a function of θ_j , and $y_{t\bar{t}j}$ is the rapidity of the $t\bar{t}j$ system.

$t\bar{t}$ CHARGE ASYMMETRY AND ENERGY ASYMMETRY

[2208.12095](#), [Eur. Phys. J. C 82 \(2022\) 374](#)

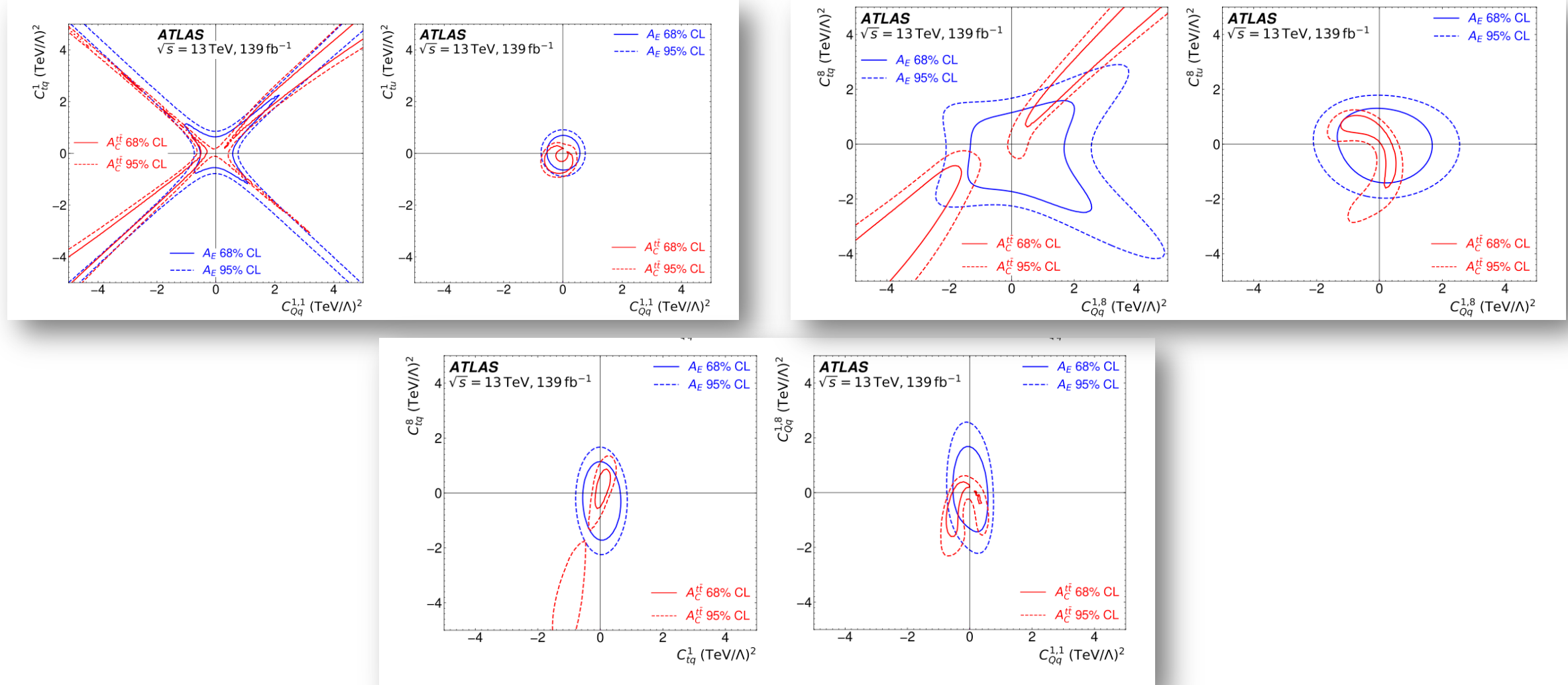
- The **energy asymmetry in boosted $t\bar{t}j$ production** provides complementary information that can eliminate a blind direction of the charge asymmetry measurement
- Asymmetries probe **different directions in chiral and colour space**
- For colour-octet operators with same chirality, shapes are different
- Charge asymmetry leaves a blind direction which is broken by the energy asymmetry due to operator interference with the QCD amplitude

$$A_E(\theta_j) \equiv \frac{\sigma^{\text{opt}}(\theta_j|\Delta E > 0) - \sigma^{\text{opt}}(\theta_j|\Delta E < 0)}{\sigma^{\text{opt}}(\theta_j|\Delta E > 0) + \sigma^{\text{opt}}(\theta_j|\Delta E < 0)}$$



$t\bar{t}$ CHARGE ASYMMETRY AND ENERGY ASYMMETRY

[TOPQ-2020-06](#), [TOPQ-2019-28](#)



$t\bar{t} + X$ TOP-22-006

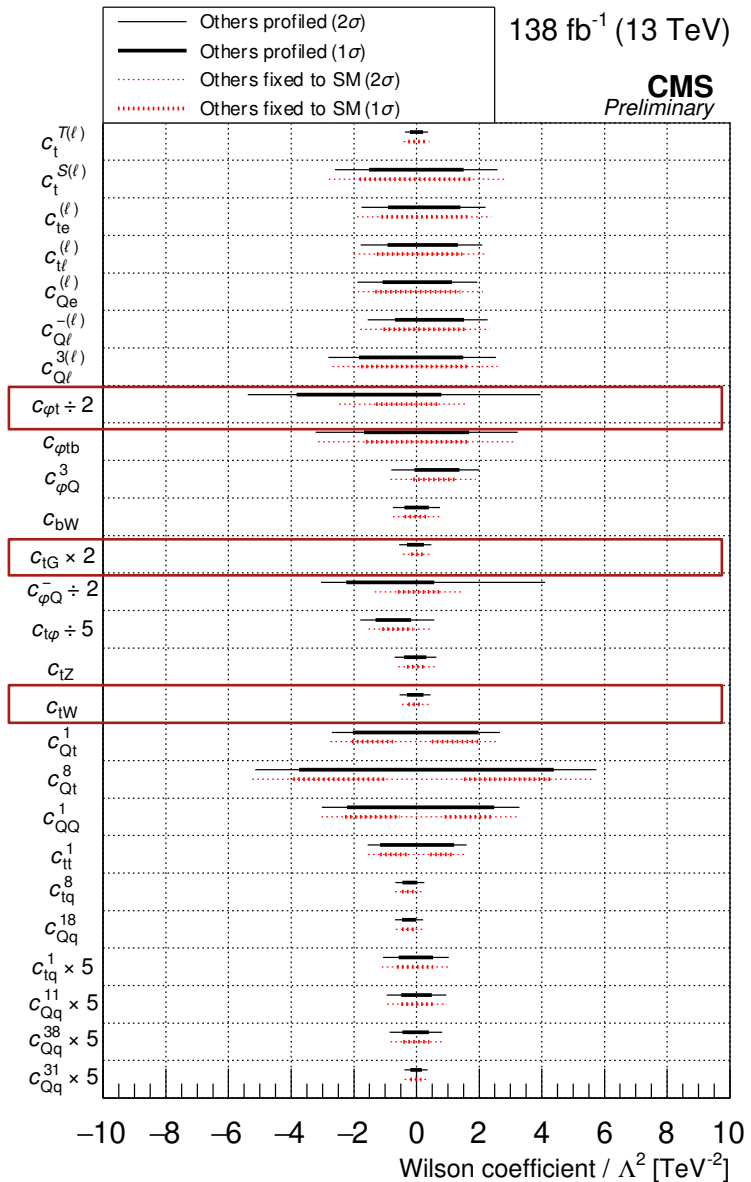
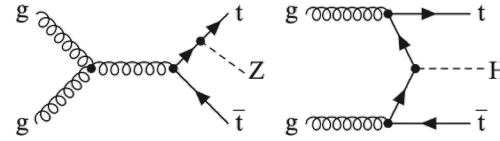


Table 6: Summary of categories that provide leading contributions to the sensitivity for subsets of the WCs.

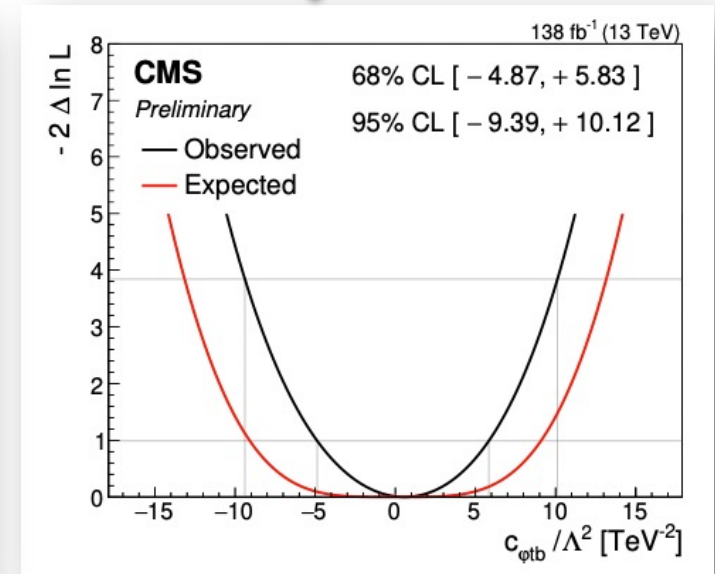
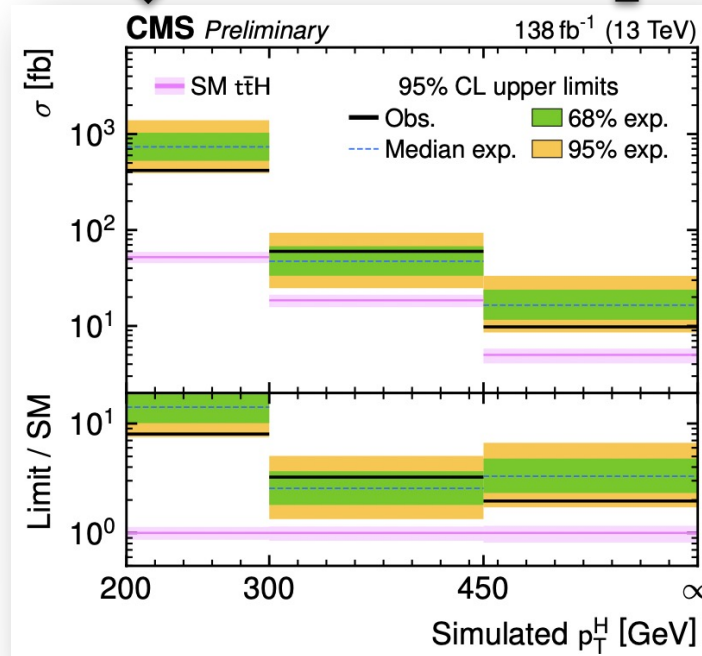
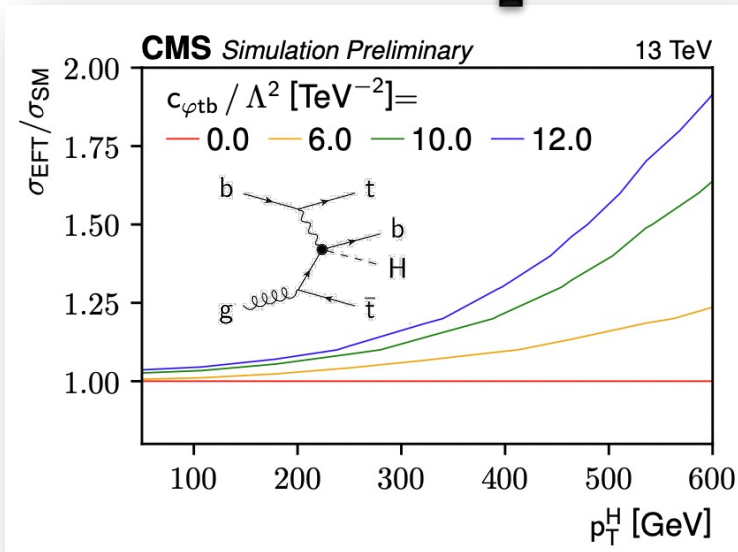
Grouping of WCs	WCs	Lead categories
Two heavy two leptons	$c_{Q\ell}^{3(\ell)}, c_{Q\ell}^{-(\ell)}, c_{Qe}^{(\ell)}, c_{t\ell}^{(\ell)}, c_{te}^{(\ell)}, c_t^{S(\ell)}, c_t^{T(\ell)}$	3l off-Z
Four heavy	$c_{QQ}^1, c_{Qt}^1, c_{Qt}^8, c_{tt}^1$	2lss
Two heavy two light “ $t\bar{t}l\nu$ -like”	$c_{Qq}^{11}, c_{Qq}^{18}, c_{tq}^1, c_{tq}^8$	2lss
Two heavy two light “ $t\bar{t}lq$ -like”	c_{Qq}^{31}, c_{Qq}^{38}	3l on-Z
Two heavy with bosons “ $t\bar{t}l\bar{l}$ -like”	$c_{tZ}, c_{\phi t}, c_{\phi Q}^-$	3l on-Z and 2lss
Two heavy with bosons “ tXq -like”	$c_{\phi Q}^3, c_{\phi tb}, c_{bW}$	3l on-Z
Two heavy with bosons with significant impacts on many processes	$c_{tG}, c_{t\varphi}, c_{tW}$	3l and 2lss

$t\bar{t}$ + BOOSTED H/Z

TOP-21-003

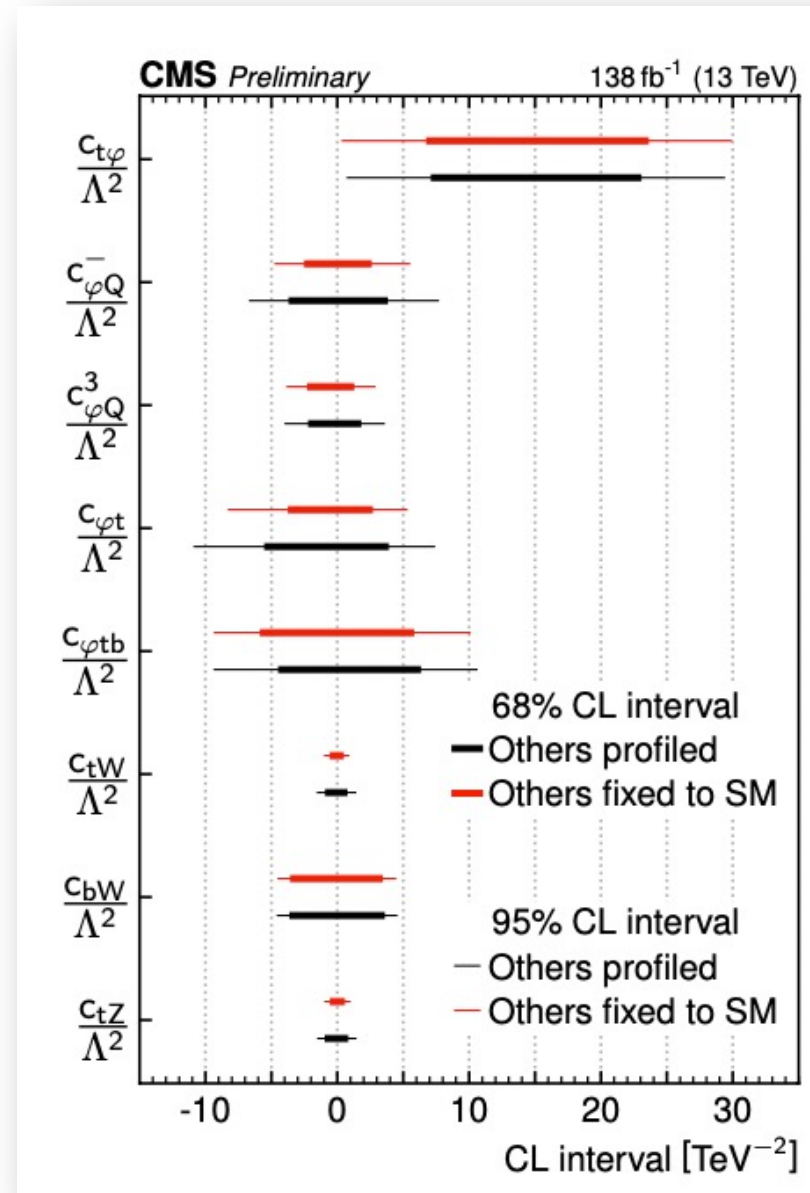
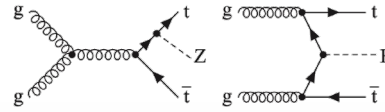


- CMS Run 2 analysis, **semi-leptonic $t\bar{t}$ and $H/Z \rightarrow b\bar{b}$** , 8 dimension-six operators added to the SM Lagrangian and their WCs constrained via a fit to the data
- Large $t\bar{t}$ +jets background



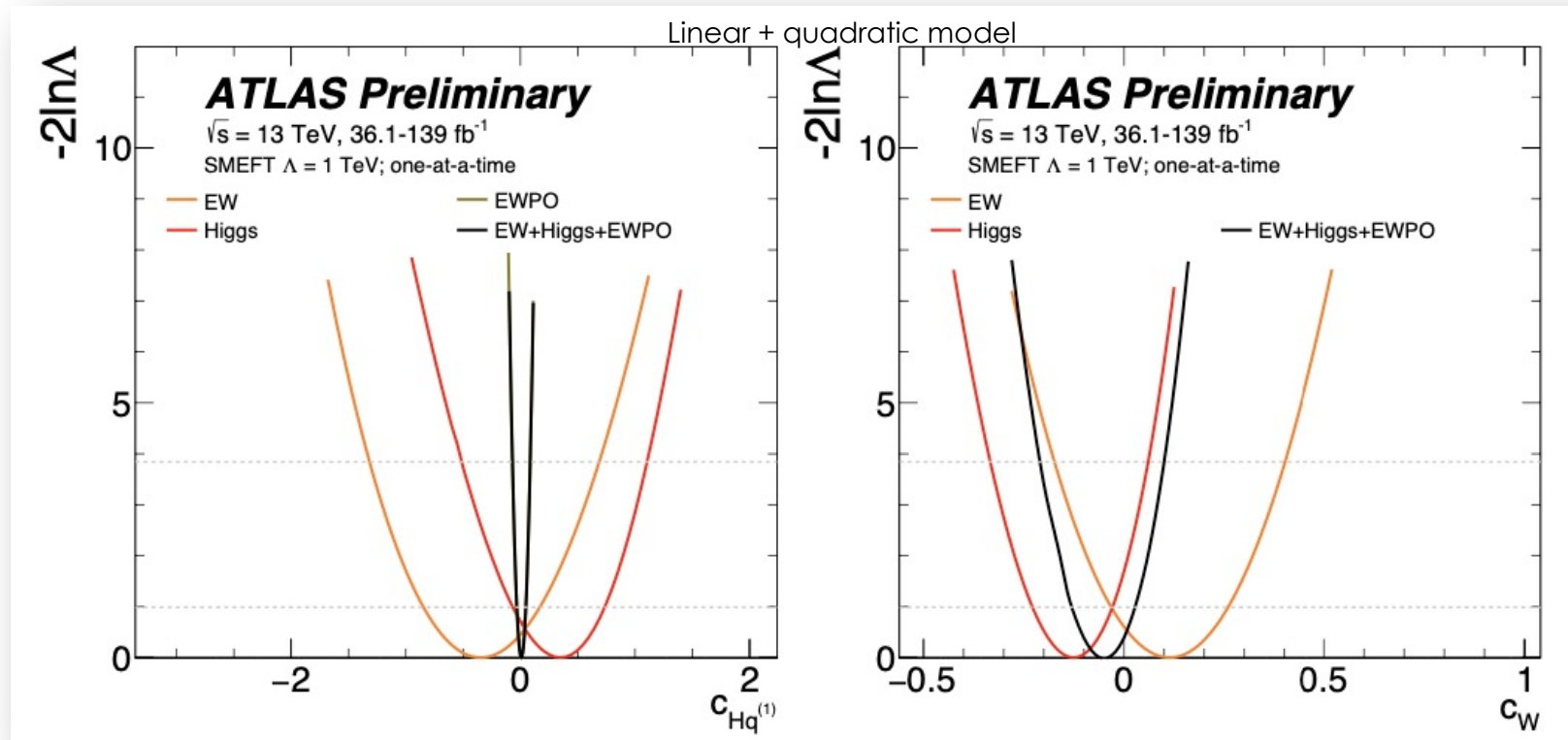
$t\bar{t}$ + BOOSTED H/Z

TOP-21-003



Global

GLOBAL COMBINATION [ATL-PHYS-PUB-2022-037](#)



$$c_{Hq}^{(1)} \quad (H^\dagger i \overleftrightarrow{D}_\mu H)(\bar{q}\gamma^\mu q)$$

Affects mainly EWPO and high energy tails for VH and diboson production

$$c_W \quad \epsilon^{IJK} W_\mu^{I\nu} W_\nu^{J\rho} W_\rho^{K\mu}$$

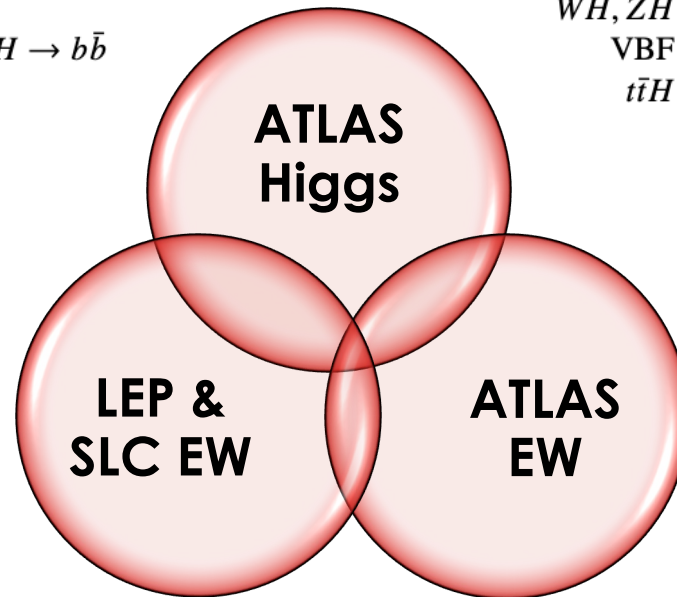
Triple-gauge-coupling parameter

ATLAS GLOBAL COMBINATION ATL-PHYS-PUB-2022-037

- Constraints on **28 SMEFT Wilson coefficients** (and mutually orthogonal linear combinations) for dim.6 operators

Decay channel	Target Production Modes
$H \rightarrow \gamma\gamma$	ggF, VBF, WH, ZH, $t\bar{t}H$, tH
$H \rightarrow ZZ^*$	ggF, VBF, WH, ZH, $t\bar{t}H(4\ell)$
$H \rightarrow WW^*$	ggF, VBF
$H \rightarrow \tau\tau$	ggF, VBF, WH, ZH, $t\bar{t}H(\tau_{\text{had}}\tau_{\text{had}})$
	WH, ZH
$H \rightarrow b\bar{b}$	VBF
	$t\bar{t}H$

Observable	Measurement	Prediction	Ratio
Γ_Z [MeV]	2495.2 ± 2.3	2495.7 ± 1	0.9998 ± 0.0010
R_ℓ^0	20.767 ± 0.025	20.758 ± 0.008	1.0004 ± 0.0013
R_c^0	0.1721 ± 0.0030	0.17223 ± 0.00003	0.999 ± 0.017
R_b^0	0.21629 ± 0.00066	0.21586 ± 0.00003	1.0020 ± 0.0031
$A_{\text{FB}}^{b,\ell}$	0.0171 ± 0.0010	0.01718 ± 0.00037	0.995 ± 0.062
$A_{\text{FB}}^{b,c}$	0.0707 ± 0.0035	0.0758 ± 0.0012	0.932 ± 0.048
$A_{\text{FB}}^{b,b}$	0.0992 ± 0.0016	0.1062 ± 0.0016	0.935 ± 0.021
σ_{had}^0 [pb]	41488 ± 6	41489 ± 5	0.99998 ± 0.00019

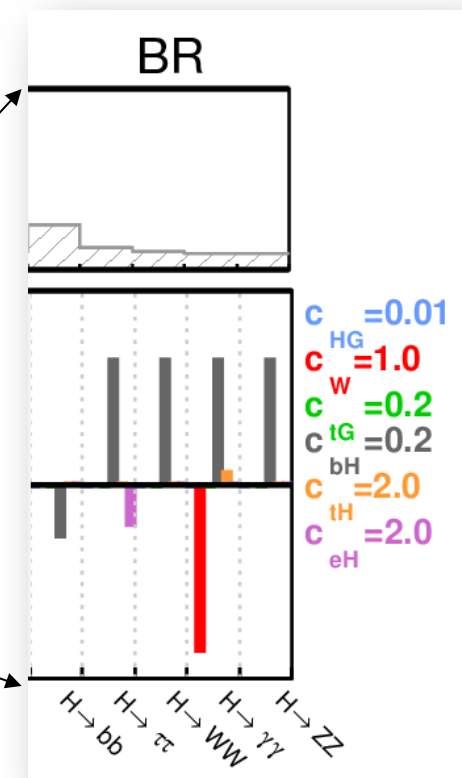
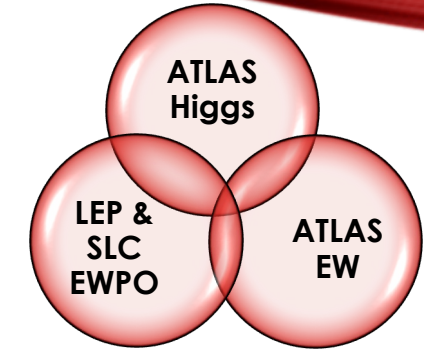
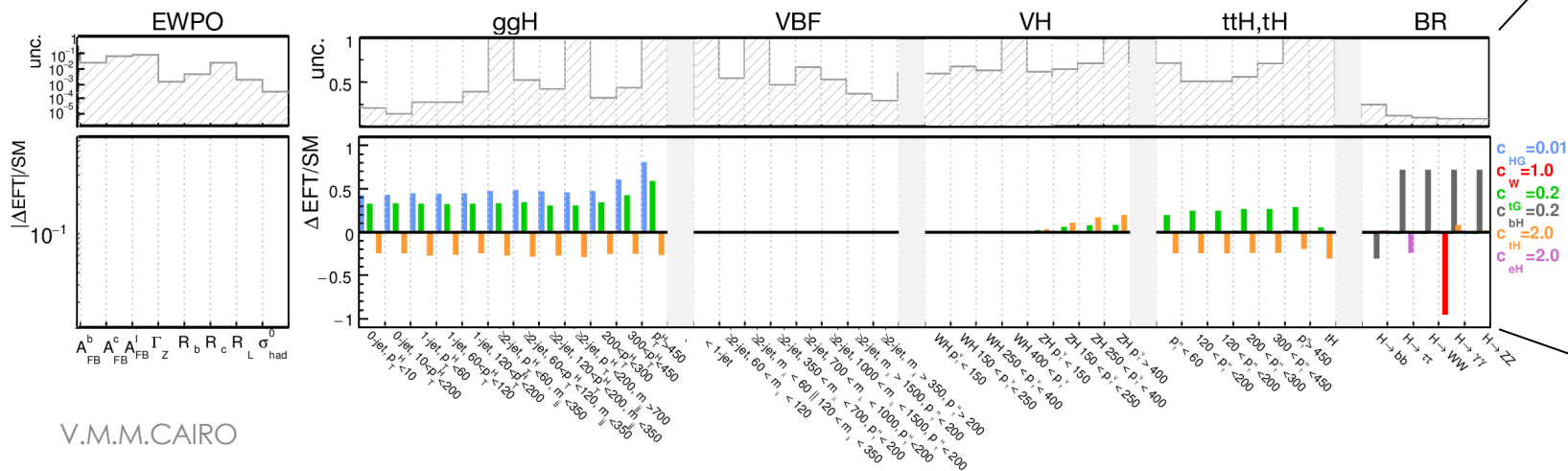
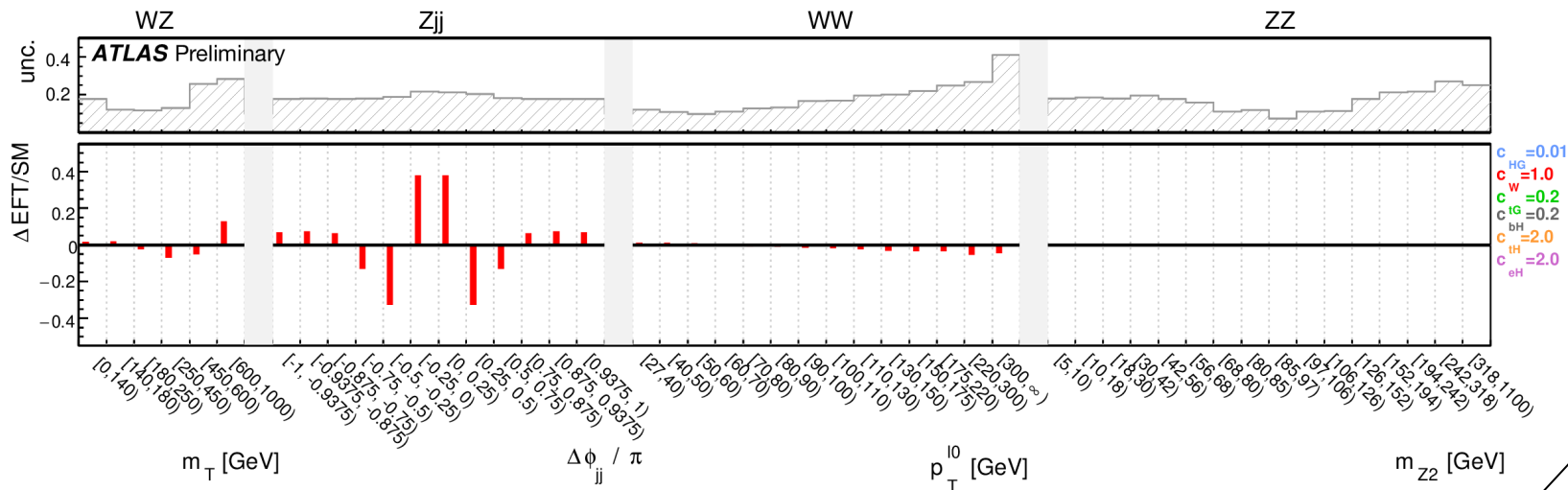


Process	Important phase space requirements	Observable
$pp \rightarrow e^\pm \nu \mu^\mp \nu$	$m_{\ell\ell} > 55 \text{ GeV}, p_T^{\text{jet}} < 35 \text{ GeV}$	$p_T^{\text{lead. lep.}}$
$pp \rightarrow \ell^\pm \nu \ell^+ \ell^-$	$m_{\ell\ell} \in (81, 101) \text{ GeV}$	m_T^{WZ}
$pp \rightarrow \ell^+ \ell^- \ell^+ \ell^-$	$m_{4\ell} > 180 \text{ GeV}$	m_{Z2}
$pp \rightarrow \ell^+ \ell^- jj$	$m_{jj} > 1000 \text{ GeV}, m_{\ell\ell} \in (81, 101) \text{ GeV}$	$\Delta\phi_{jj}$

- For processes in which kinematics are affected by different operators, parameterization done in a fiducial and not phase space. Overlap checked and dataset removed when relevant

ATLAS GLOBAL COMBINATION ATL-PHYS-PUB-2022-037

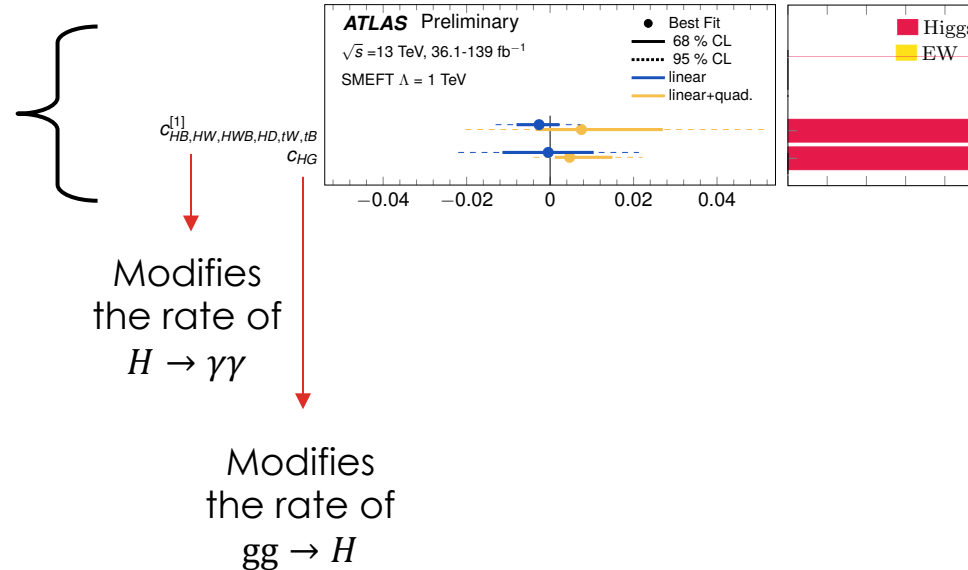
- Constraints on **28 SMEFT Wilson coefficients** (and mutually orthogonal linear combinations) for dim.6 operators



GLOBAL COMBINATION ATL-PHYS-PUB-2022-037

- Insufficient information to constraint simultaneously all coefficients
 - Basis modified: linear combination of WCs
 - First combine inputs from ATLAS, constraining 7 individual and 17 linear combinations of WCs

Best constrained WCs



GLOBAL COMBINATION ATL-PHYS-PUB-2022-037

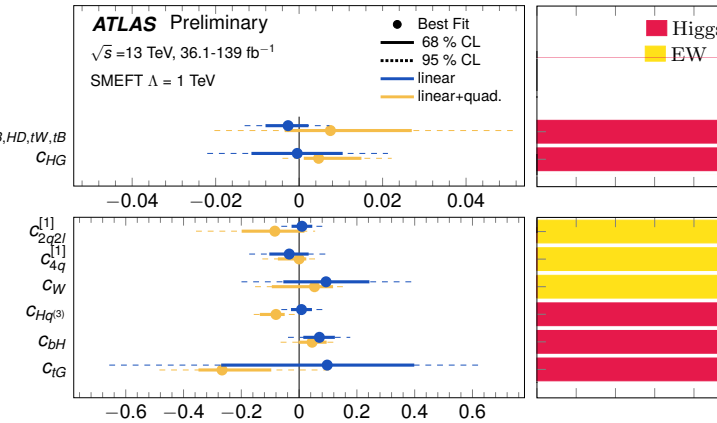
- Insufficient information to constraint simultaneously all coefficients
 - Basis modified: linear combination of WCs
 - First combine inputs from ATLAS, constraining 7 individual and 17 linear combinations of WCs

Weaker constraints from lin+quad e.g. $c_{2q2l}^{(1)}$

(introduction of quadratic terms leads to non-linear correlations between parameters)

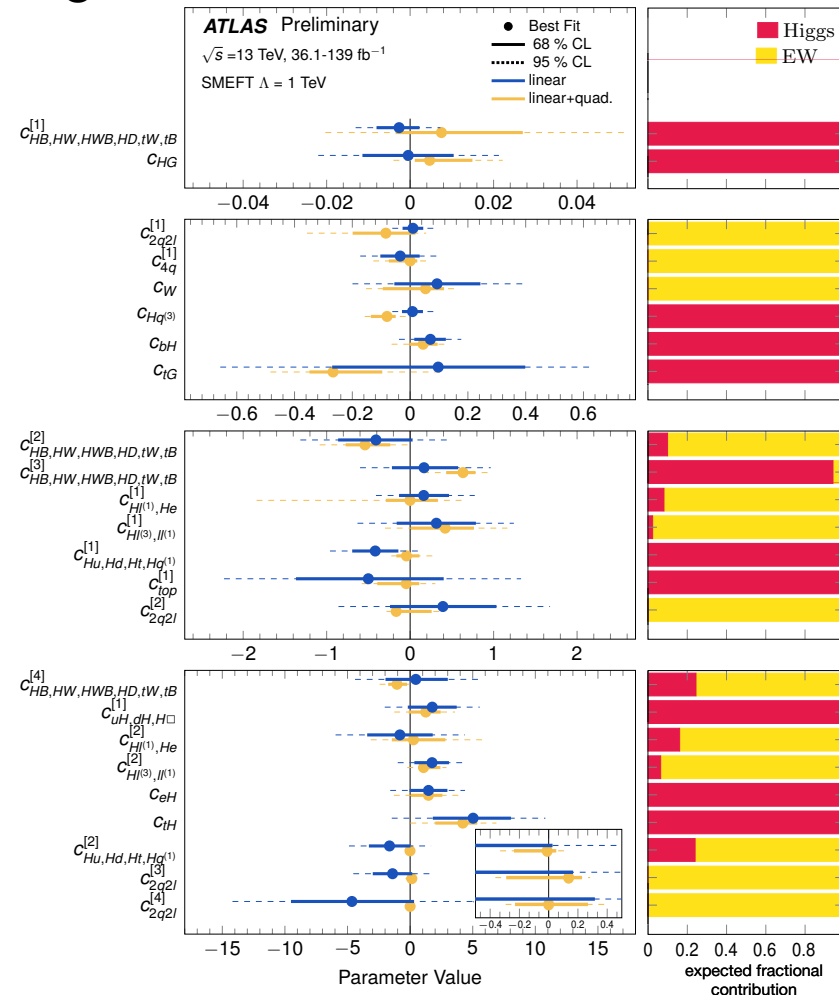
Stronger constraints from lin+quad e.g. c_W

(sizable quadratic contributions from VV)



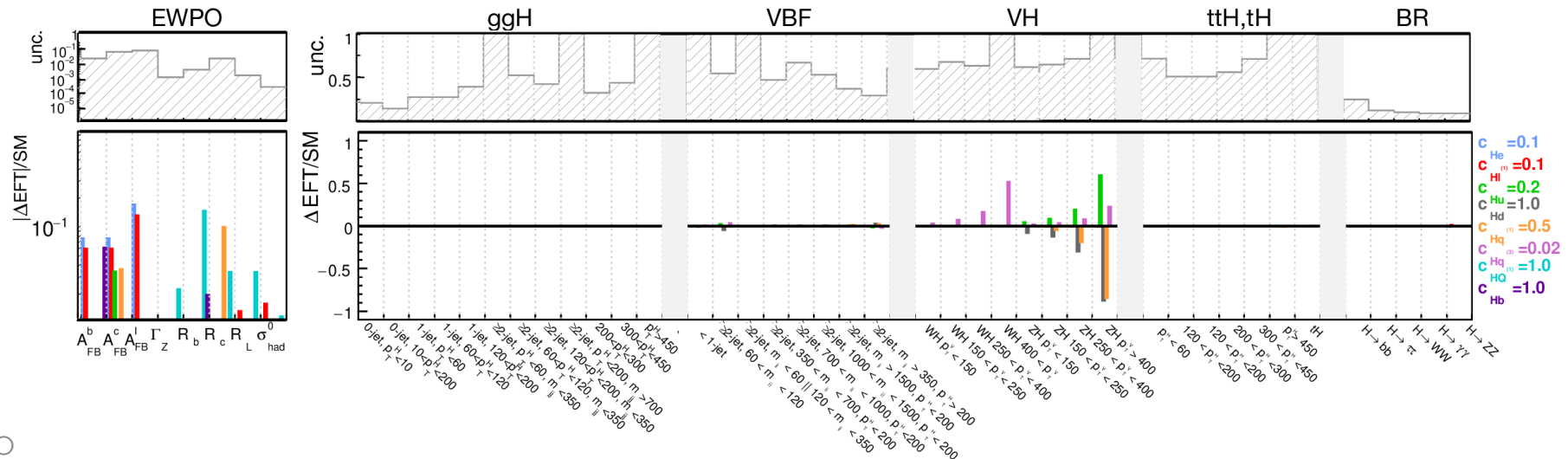
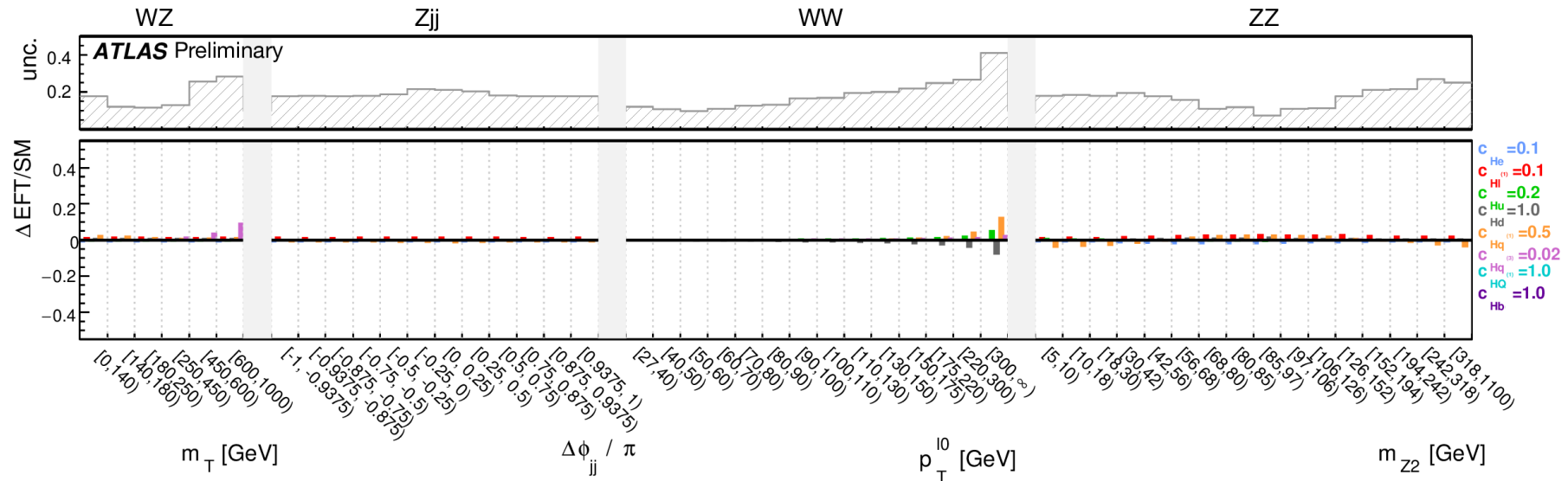
GLOBAL COMBINATION ATL-PHYS-PUB-2022-037

- Insufficient information to constraint simultaneously all coefficients
 - Basis modified: linear combination of WCs
 - First combine inputs from ATLAS, constraining 7 individual and 17 linear combinations of WCs

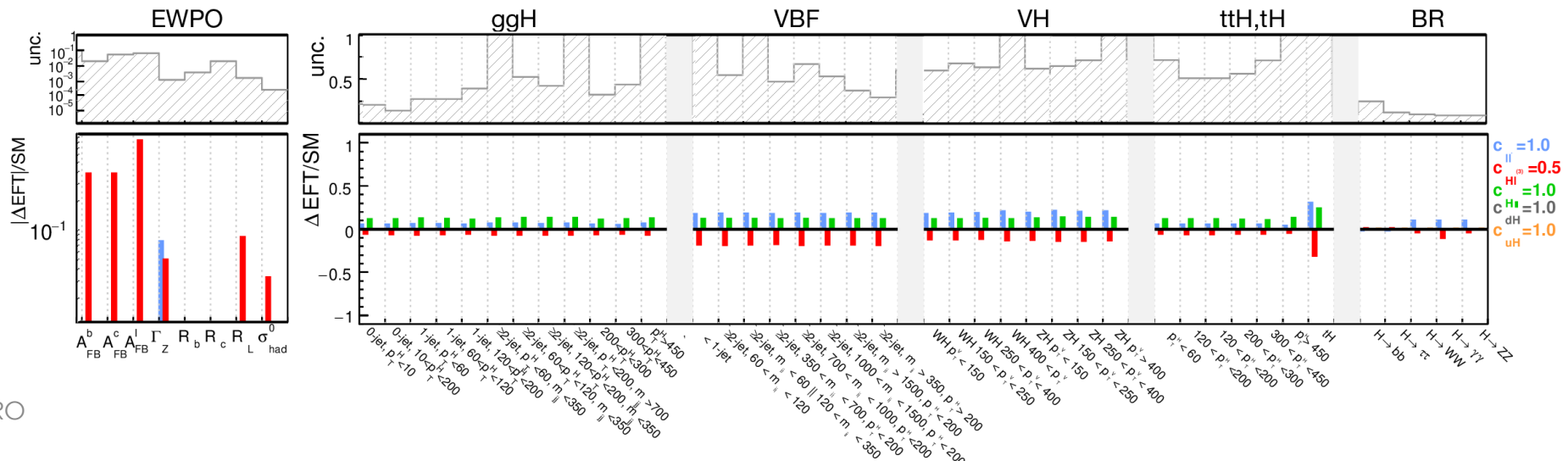
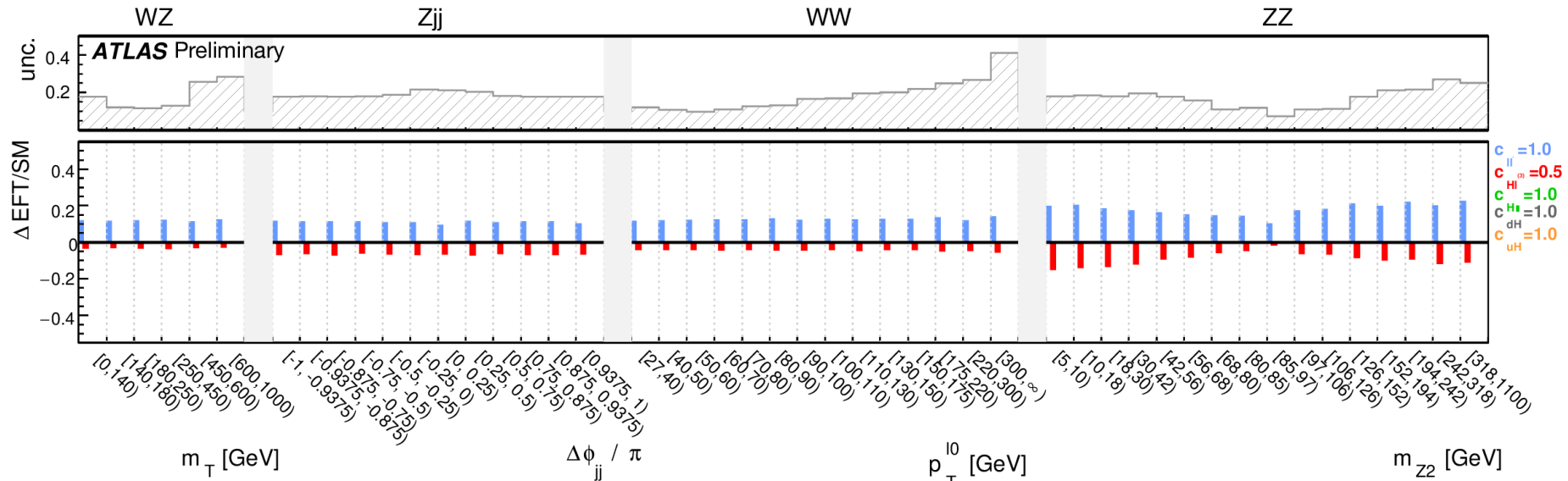


Least constrained WCs,
 quadratic contributions large due to
 quadratic dependence on WCs,
 questionable validity of obtained
 constraints

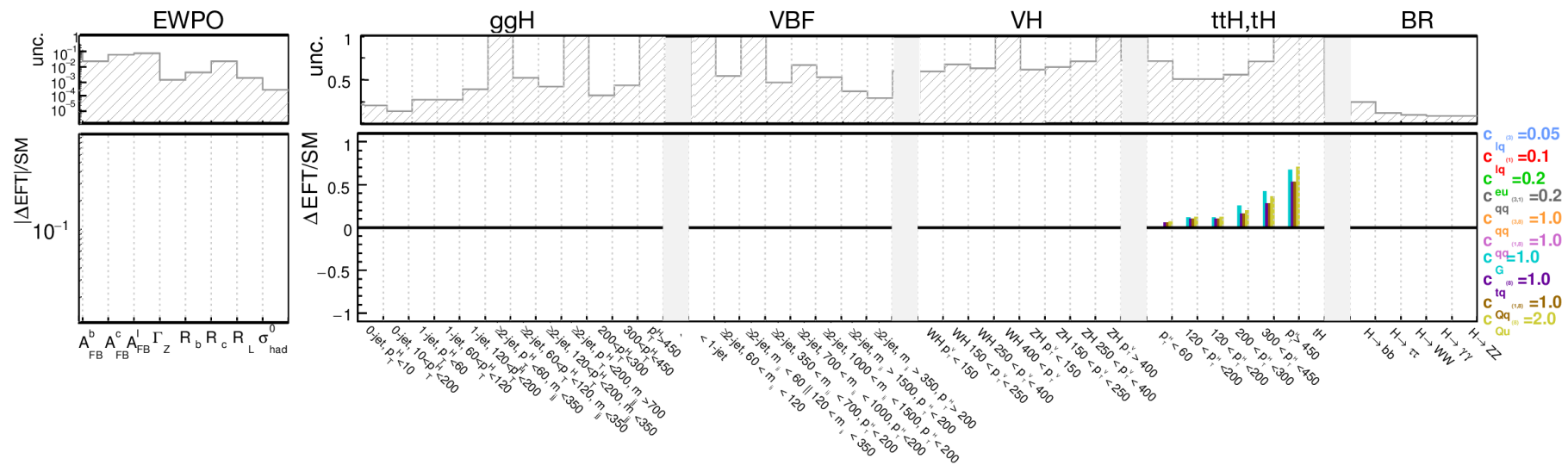
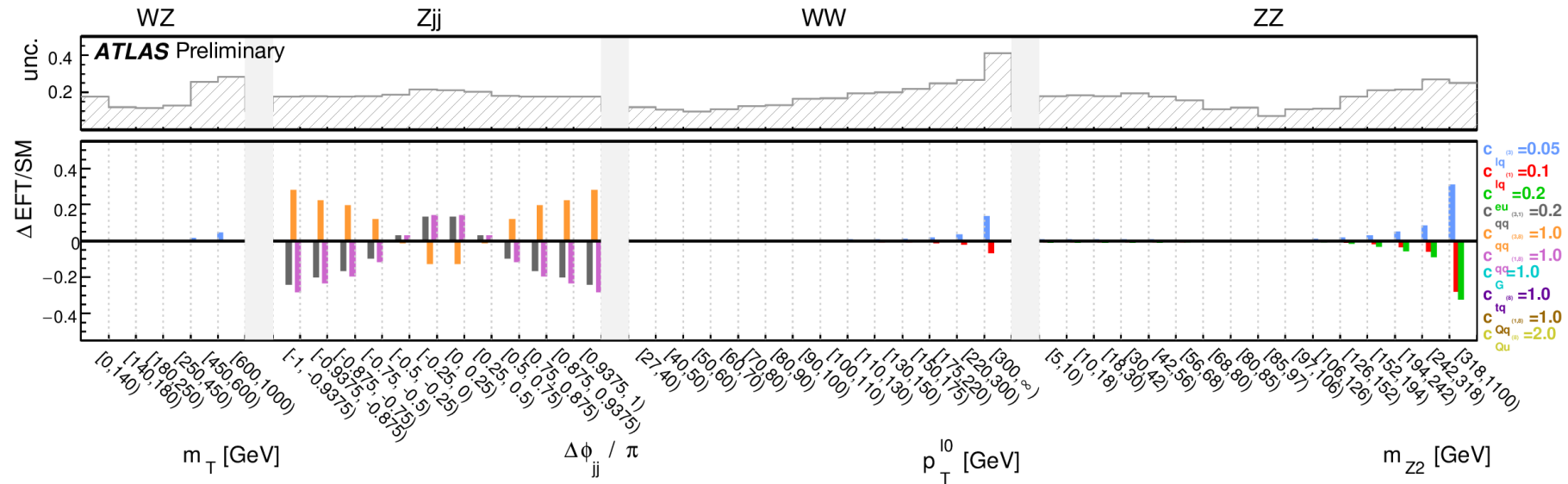
ATLAS GLOBAL COMBINATION ATL-PHYS-PUB-2022-037



ATLAS GLOBAL COMBINATION ATL-PHYS-PUB-2022-037



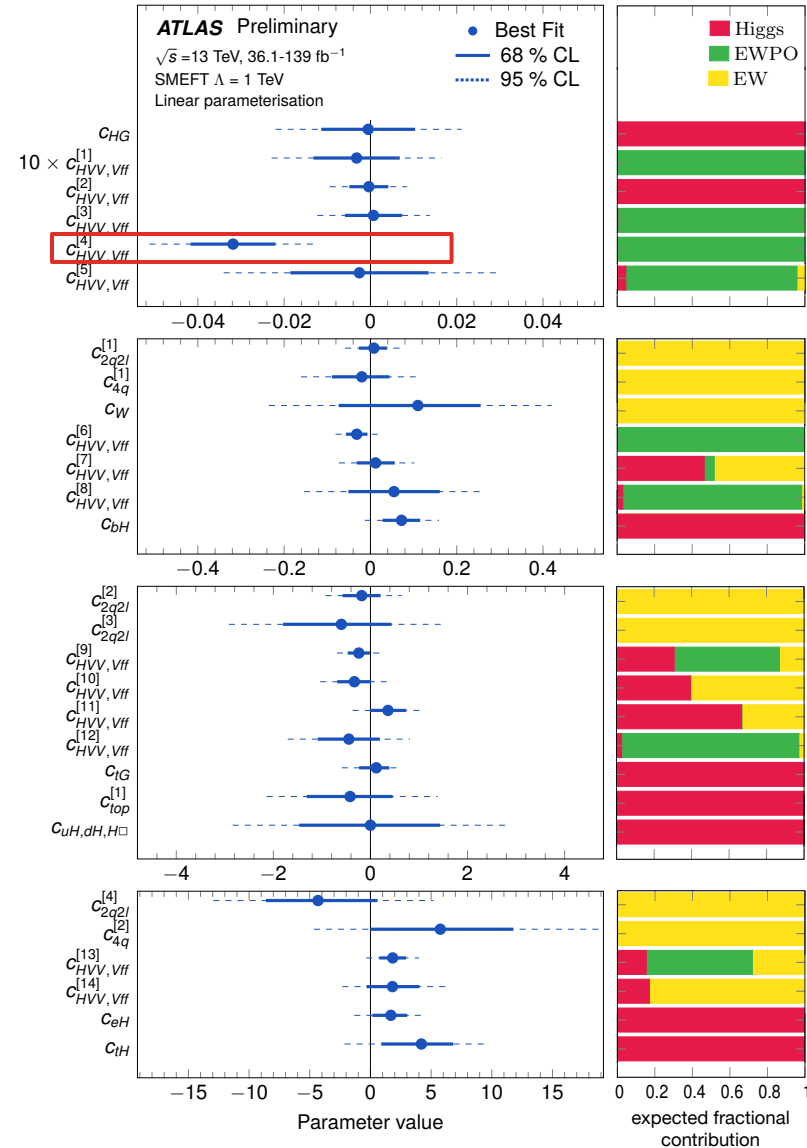
ATLAS GLOBAL COMBINATION ATL-PHYS-PUB-2022-037



GLOBAL COMBINATION

[ATL-PHYS-PUB-2022-037](#)

- Include EWPO, constrain 28 WCs
- Group of 5 WCs now tightly constrained by single observables ($gg \rightarrow H, \sigma_{had}^0, Z$ width, forward-backward asymmetries,)
- Contributions from ATLAS expected to become more important with larger dataset analyses
- Results compatible with SM except for $C_{HVV,Vff}^4$, excess driven by a well-known discrepancy between $A_{fb}^{0,b}$ and $A_{fb}^{0,c}$ measurements and the SM expectation



GLOBAL COMBINATION

[ATL-PHYS-PUB-2022-037](#)

Wilson coefficient and operator		Affected process group		
		LEP/SLD EWPO	ATLAS Higgs	ATLAS electroweak
$c_{H\Box}$	$(H^\dagger H)\Box(H^\dagger H)$		✓	
c_G	$f^{abc}G_\mu^{av}G_\nu^{bp}G_\rho^{c\mu}$		✓	✓
c_W	$\epsilon^{IJK}W_\mu^{I\nu}W_\nu^{J\rho}W_\rho^{K\mu}$		✓	✓
c_{HD}	$(H^\dagger D_\mu H)^*(H^\dagger D_\mu H)$		✓	✓
c_{HG}	$H^\dagger H G_{\mu\nu}^A G^{A\mu\nu}$		✓	
c_{HB}	$H^\dagger H B_{\mu\nu} B^{\mu\nu}$		✓	
c_{HW}	$H^\dagger H W_{\mu\nu}^I W^{I\mu\nu}$		✓	
c_{HWB}	$H^\dagger \tau^I H W_{\mu\nu}^I B^{\mu\nu}$	✓	✓	✓
c_{eH}	$(H^\dagger H)(\bar{l}_p e_r H)$		✓	
c_{uH}	$(H^\dagger H)(\bar{q} Y_u^\dagger u \tilde{H})$		✓	
c_{tH}	$(H^\dagger H)(\bar{Q} \tilde{H} t)$		✓	
c_{bH}	$(H^\dagger H)(\bar{Q} H b)$		✓	
$c_{Hl}^{(1)}$	$(H^\dagger i \overleftrightarrow{D}_\mu H)(\bar{l} \gamma^\mu l)$	✓	✓	✓
$c_{Hl}^{(3)}$	$(H^\dagger i \overleftrightarrow{D}_\mu^I H)(\bar{l} \tau^I \gamma^\mu l)$	✓	✓	✓
c_{He}	$(H^\dagger i \overleftrightarrow{D}_\mu H)(\bar{e} \gamma^\mu e)$	✓	✓	✓
$c_{Hq}^{(1)}$	$(H^\dagger i \overleftrightarrow{D}_\mu H)(\bar{q} \gamma^\mu q)$	✓	✓	✓
$c_{Hq}^{(3)}$	$(H^\dagger i \overleftrightarrow{D}_\mu^I H)(\bar{q} \tau^I \gamma^\mu q)$	✓	✓	✓
c_{Hu}	$(H^\dagger i \overleftrightarrow{D}_\mu H)(\bar{u} \gamma^\mu u)$	✓	✓	✓
c_{Hd}	$(H^\dagger i \overleftrightarrow{D}_\mu H)(\bar{d} \gamma^\mu d)$	✓	✓	✓
$c_{HQ}^{(1)}$	$(H^\dagger i \overleftrightarrow{D}_\mu H)(\bar{Q} \gamma^\mu Q)$	✓	✓	
$c_{HQ}^{(3)}$	$(H^\dagger i \overleftrightarrow{D}_\mu^I H)(\bar{Q} \tau^I \gamma^\mu Q)$	✓	✓	
c_{Hb}	$(H^\dagger i \overleftrightarrow{D}_\mu H)(\bar{b} \gamma^\mu b)$	✓		
c_{Ht}	$(H^\dagger i \overleftrightarrow{D}_\mu H)(\bar{t} \gamma^\mu t)$	✓	✓	
c_{tG}	$(\bar{Q} \sigma^{\mu\nu} T^A t) \tilde{H} G_{\mu\nu}^A$		✓	
c_{tW}	$(\bar{Q} \sigma^{\mu\nu} t) \tau^I \tilde{H} W_{\mu\nu}^I$		✓	
c_{tB}	$(\bar{Q} \sigma^{\mu\nu} t) \tilde{H} B_{\mu\nu}$		✓	
c_{ll}	$(\bar{l} \gamma_\mu l)(\bar{l} \gamma^\mu l)$	✓		✓

GLOBAL COMBINATION

[ATL-PHYS-PUB-2022-037](#)

In order to obtain a fit basis that is easy to interpret but still numerically stable, the eigenvector analysis is performed using orthogonal subsets of Wilson coefficients. The groups are constructed such that the impact from each group is distinct from the impact of the other groups. At the same time, strong similarities in the impact on observables exist within a given group. The aforementioned parameters $c_{Hq}^{(3)}$, c_{bH} , c_W , and c_{eH} can be constrained individually. The three parameters affecting $gg \rightarrow H$ (c_{HG} , c_{tG} , and c_{tH}) can also be constrained individually, albeit with a fairly strong correlation, as loop-induced ZH and $t\bar{t}H$ production offer additional constraining power. Furthermore, eight groups containing multiple operators are constructed. The groups are:

- c_{He} and $c_{Hl}^{(1)}$, which are mainly detectable by their impact on Z-boson-lepton couplings;
- $c_{Hl}^{(3)}$ and c_{ll} , which affect the strength of the electroweak coupling and thus most observables;
- c_{Hu} , c_{Hd} , and $c_{Hq}^{(1)}$, which mainly affect the high-energy tails of VH and diboson production;
- c_{uH} , c_{dH} , and $c_{H\Box}$, which have a strong effect on the rate of all Higgs boson processes (in the case of c_{uH} and c_{dH} due to their effect on the unmeasured Higgs decays into strange and charm quarks);
- c_{HB} , c_{HW} , c_{HWB} , c_{HD} , c_{tW} , and c_{tB} , which affect the $H \rightarrow \gamma\gamma$ partial width;
- $c_{lq}^{(1)}$, $c_{lq}^{(3)}$, c_{eu} , c_{ed} , c_{lu} , c_{ld} , and c_{qe} , four-fermion operators with two quark and two lepton fields, which are particularly affecting the tails of the diboson observables;
- $c_{qq}^{(1,1)}$, $c_{qq}^{(1,8)}$, $c_{qq}^{(3,1)}$, $c_{qq}^{(3,8)}$, $c_{uu}^{(1)}$, $c_{uu}^{(8)}$, $c_{dd}^{(1)}$, $c_{dd}^{(8)}$, $c_{ud}^{(1)}$, $c_{ud}^{(8)}$, $c_{qu}^{(1)}$, $c_{qu}^{(8)}$, $c_{qd}^{(1)}$, and $c_{qd}^{(8)}$, four-fermion operators with four light quarks, which are only relevant for the VBF Z measurement; and
- c_G , $c_{Qq}^{(1,1)}$, $c_{Qq}^{(1,8)}$, $c_{Qq}^{(3,1)}$, $c_{Qq}^{(3,8)}$, $c_{tu}^{(1)}$, $c_{Qu}^{(1)}$, $c_{Qu}^{(8)}$, $c_{Qd}^{(1)}$, $c_{Qd}^{(8)}$, $c_{tq}^{(1)}$, and $c_{tq}^{(8)}$, operators mainly affecting $t\bar{t}H$ production, i.e., c_G and four-quark operators coupling to the top quark.

For each of these operators groups orthogonal eigenvectors are determined from a principal component analysis that considers only operators within the group. The resulting eigenvectors are visualized in Figure 9. Again, only eigenvectors with an expected uncertainty of $\sigma < 5$ are retained. The remaining eigenvectors are fixed to zero in the maximum likelihood fit. As Wilson coefficients are expected to be at most order 1 and the new physics scale Λ is expected to be at least 1 TeV, the directions in parameter space with $\sigma > 5$ have very little impact on the measurement. The removal of these weakly constrained directions allows for measurement of the remaining coefficients simultaneously.

Eigenvector constraints are obtained from profile-likelihood fits, as described in Section 4.4. Results based on both the linear and the linear+quadratic model are presented in Figure 10. The contribution of a given measurement group i of input measurements (where i is, in this case, Higgs or LHC electroweak) to an eigenvector constraint is shown on the right-hand side. It is calculated in the Gaussian limit and using the linear model as $\frac{\sigma_i^{-2}}{\sum_j \sigma_j^{-2}}$, where σ_i is the uncertainty from the analysis of input measurement i . The correlation of fitted coefficients is shown, for the linear model, in Figure 11. In the linear+quadratic model the likelihood structure is non-Gaussian and cannot be easily represented by a correlation matrix.

The most stringent constraints are obtained for $c_{CHB,CHW,CHWB,CHD,c_{tW},c_{tB}}^{[1]}$, which modifies the rate of $H \rightarrow \gamma\gamma$ decays and c_{HG} , which modifies the $gg \rightarrow H$ production rate. These processes are loop-suppressed in the SM but can proceed at tree level in the SMEFT. Stringent constraints are also obtained for c_{bH} , which impacts the $H \rightarrow b\bar{b}$ decay rate, while the triple-gauge-coupling operator c_W and the leading

Higgs

CP TESTS IN $H \rightarrow \tau\tau$ [2205.05120](#)

- CMS full Run 2 analysis dedicated to studying anomalous couplings in ggF, VBF and VH $H \rightarrow \tau\tau$
 - Combined with $H \rightarrow \gamma\gamma$ and $H \rightarrow 4l$
- Measure effective cross-section ratios (reduce uncertainties)

$$f_{a3} = \frac{|a_3|^2 \sigma_3}{|a_1|^2 \sigma_1 + |a_2|^2 \sigma_2 + |a_3|^2 \sigma_3 + |\kappa_1|^2 \sigma_{\Lambda 1} + |\kappa_1^{Z\gamma}|^2 \sigma_{\Lambda 1}^{Z\gamma}} \operatorname{sgn} \left(\frac{a_3}{a_1} \right),$$

$$f_{a2} = \frac{|a_2|^2 \sigma_2}{|a_1|^2 \sigma_1 + |a_2|^2 \sigma_2 + |a_3|^2 \sigma_3 + |\kappa_1|^2 \sigma_{\Lambda 1} + |\kappa_1^{Z\gamma}|^2 \sigma_{\Lambda 1}^{Z\gamma}} \operatorname{sgn} \left(\frac{a_2}{a_1} \right),$$

$$f_{\Lambda 1} = \frac{|\kappa_1|^2 \sigma_{\Lambda 1}}{|a_1|^2 \sigma_1 + |a_2|^2 \sigma_2 + |a_3|^2 \sigma_3 + |\kappa_1|^2 \sigma_{\Lambda 1} + |\kappa_1^{Z\gamma}|^2 \sigma_{\Lambda 1}^{Z\gamma}} \operatorname{sgn} \left(\frac{-\kappa_1}{a_1} \right),$$

$$f_{\Lambda 1}^{Z\gamma} = \frac{|\kappa_2^{Z\gamma}|^2 \sigma_{\Lambda 1}^{Z\gamma}}{|a_1|^2 \sigma_1 + |a_2|^2 \sigma_2 + |a_3|^2 \sigma_3 + |\kappa_1|^2 \sigma_{\Lambda 1} + |\kappa_1^{Z\gamma}|^2 \sigma_{\Lambda 1}^{Z\gamma}} \operatorname{sgn} \left(\frac{-\kappa_2^{Z\gamma}}{a_1} \right),$$

Coupling	σ_i/σ_1
a_3	0.153
a_2	0.361
κ_1	0.682
$\kappa_2^{Z\gamma}$	1.746

CP TESTS IN $H \rightarrow \tau\tau$ [2205.05120](#)

- CMS full Run 2 analysis dedicated to studying anomalous couplings in ggF, VBF and VH $H \rightarrow \tau\tau$
 - Combined with $H \rightarrow \gamma\gamma$ and $H \rightarrow 4l$
- Measure effective cross-section ratios (reduce uncertainties)

$$c_{gg} = -\frac{1}{2\pi\alpha_S} a_2^{gg},$$

$$\tilde{c}_{gg} = -\frac{1}{2\pi\alpha_S} a_3^{gg},$$

$$\begin{aligned} \mu_{ggH} = & 1.1068\kappa_t^2 + 0.0082 - 0.1150\kappa_t + 2.5717\tilde{\kappa}_t^2 + 1.0298(12\pi^2 c_{gg})^2 + 2.3170(8\pi^2 \tilde{c}_{gg})^2 \\ & + 2.1357(12\pi^2 c_{gg})\kappa_t - 0.1109(12\pi^2 c_{gg}) + 4.8821(8\pi^2 \tilde{c}_{gg})\tilde{\kappa}_t. \end{aligned}$$

It is hard to distinguish between the κ and a_{gg} . The only remaining effective fractional cross section for the Hgg interaction is defined as:

$$f_{a3}^{ggH} = \frac{|a_3^{gg}|^2}{|a_2^{gg}|^2 + |a_3^{gg}|^2} \operatorname{sgn} \left(\frac{a_3^{gg}}{a_2^{gg}} \right).$$

CP TESTS IN $H \rightarrow \tau\tau$ [2205.05120](#)

Table 3: Kinematic selection requirements for the four di- τ decay channels. The trigger requirement is defined by a combination of trigger candidates with p_T over a given threshold, indicated inside parentheses in GeV. The pseudorapidity thresholds come from trigger and object reconstruction constraints. The p_T thresholds for the lepton selection are driven by the trigger requirements, except for the τ_h candidate in the $\mu\tau_h$ and $e\tau_h$ channels, and the sub-leading lepton in the $e\mu$ channel, where they have been optimized to increase the analysis sensitivity.

Channel	Trigger requirement	Year	Selection criteria		
			p_T (GeV)	η	Isolation
$\tau_h\tau_h$	$\tau_h(35) \& \tau_h(35)$	2016	$p_T^{\tau_h} > 40$	$ \eta^{\tau_h} < 2.1$	DNN τ_h ID
	$\tau_h(40) \& \tau_h(40)$	2017, 2018			
$\mu\tau_h$	$\mu(22)$	2016	$p_T^\mu > p_T^{\text{trigger}} + 1 \text{ GeV}$	$ \eta^\mu < 2.1$	$I^\mu < 0.15$
	$\mu(19) \& \tau_h(21)$	2016	$p_T^{\tau_h} > 30$	$ \eta^{\tau_h} < 2.3$	DNN τ_h ID
	$\mu(24)$	2017, 2018			
	$\mu(20) \& \tau_h(27)$	2017, 2018			
$e\tau_h$	$e(25)$	2016	$p_T^e > p_T^{\text{trigger}} + 1 \text{ GeV}$	$ \eta^e < 2.1$	$I^e < 0.15$
	$e(27)$	2017	$p_T^{\tau_h} > 30$	$ \eta^{\tau_h} < 2.3$	DNN τ_h ID
	$e(32)$	2018			
	$e(24) \& \tau_h(30)$	2017, 2018			
$e\mu$	$e(12) \& \mu(23)$	all years	$p_T^e > 15, p_T^\mu > 24$	$ \eta^e < 2.4$	$I^e < 0.15$
	$e(23) \& \mu(8)$	all years	$p_T^\mu > 15, p_T^e > 24$	$ \eta^\mu < 2.4$	$I^\mu < 0.15$

Coupling	Discriminant
a_3^{gg}	\mathcal{D}_{0-}^{ggH}
a_3	\mathcal{D}_{0-}
a_2	\mathcal{D}_{0h+}
κ_1	$\mathcal{D}_{\Delta 1}$
$\kappa_2^{Z\gamma}$	$\mathcal{D}_{\Delta 1}^{Z\gamma}$

Table 5: List of observables used in the MELA method.

Category	Observable	Goal
0-jet	$m_{\tau\tau}$	Separate H signal from backgrounds
Boosted	$p_T^{\tau\tau}, m_{\tau\tau}$	Separate H signal from backgrounds and BSM from SM HVV
VBF	\mathcal{D}_{NN}	Separate VBF-like H signal from backgrounds
VBF	$\mathcal{D}_{2\text{jet}}^{\text{VBF}}$	Separate ggH from VBF H production
VBF	$\mathcal{D}_{0-}^{\text{ggH}} (\mathcal{D}_{0-})$	Separate BSM from SM Hgg (HVV)
VBF	$\mathcal{D}_{\text{CP}}^{\text{ggH}} (\mathcal{D}_{\text{CP}}^{\text{VBF}})$	Sensitive to the interference between the CP-even and CP-odd contributions to the Hgg (HVV) coupling

CP TESTS IN $H \rightarrow \tau\tau$ [2205.05120](#)

MELA discriminants
in ggF

$$\mathcal{D}_{2\text{jet}}^{\text{VBF}} = \frac{\mathcal{P}_{\text{SM}}^{\text{ggH}} + \mathcal{P}_{0-}^{\text{ggH}}}{\mathcal{P}_{\text{SM}}^{\text{ggH}} + \mathcal{P}_{0-}^{\text{ggH}} + \mathcal{P}_{\text{SM}}^{\text{VBF}}},$$

$$\mathcal{D}_{0-}^{\text{ggH}} = \frac{\mathcal{P}_{\text{SM}}^{\text{ggH}}}{\mathcal{P}_{\text{SM}}^{\text{ggH}} + \mathcal{P}_{0-}^{\text{ggH}}},$$

$$\mathcal{D}_{\text{CP}}^{\text{ggH}} = \frac{\mathcal{P}_{\text{SM}-0-}^{\text{ggH}}}{\mathcal{P}_{\text{SM}}^{\text{ggH}} + \mathcal{P}_{0-}^{\text{ggH}}}.$$

MELA discriminants
in VBF

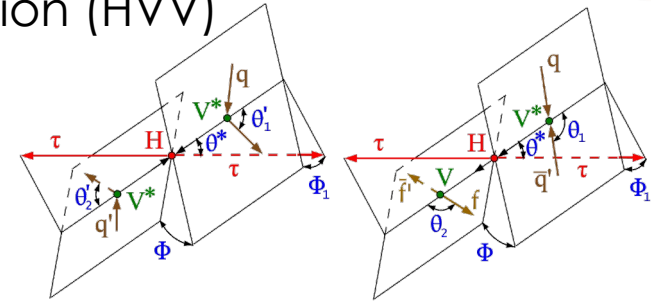
$$\mathcal{D}_{0-} = \frac{\mathcal{P}_{\text{SM}}^{\text{VBF}}}{\mathcal{P}_{\text{SM}}^{\text{VBF}} + \mathcal{P}_{0-}^{\text{VBF}}}, \quad \mathcal{D}_{0h+} = \frac{\mathcal{P}_{\text{SM}}^{\text{VBF}}}{\mathcal{P}_{\text{SM}}^{\text{VBF}} + \mathcal{P}_{a2}},$$

$$\mathcal{D}_{\Lambda 1} = \frac{\mathcal{P}_{\text{SM}}^{\text{VBF}}}{\mathcal{P}_{\text{SM}}^{\text{VBF}} + \mathcal{P}_{\Lambda 1}}, \quad \mathcal{D}_{\Lambda 1}^{\text{Z}\gamma} = \frac{\mathcal{P}_{\text{SM}}^{\text{VBF}}}{\mathcal{P}_{\text{SM}}^{\text{VBF}} + \mathcal{P}_{\Lambda 1}^{\text{Z}\gamma}}.$$

$$\mathcal{D}_{\text{CP}}^{\text{VBF}} = \frac{\mathcal{P}_{\text{SM}-0-}^{\text{VBF}}}{\mathcal{P}_{\text{SM}}^{\text{VBF}} + \mathcal{P}_{0-}^{\text{VBF}}}.$$

CP TESTS IN $H \rightarrow \tau\tau$ HIG-20-007

- Access CP -violating effects using reconstructed $H \rightarrow \tau\tau$ events
 - correlation of H and two quark jets or leptons in VBF and VH production (HVV)
 - correlation of H and two quark jets in ggH production (Hgg)
- Use a matrix element likelihood approach (MELA) and a neural network

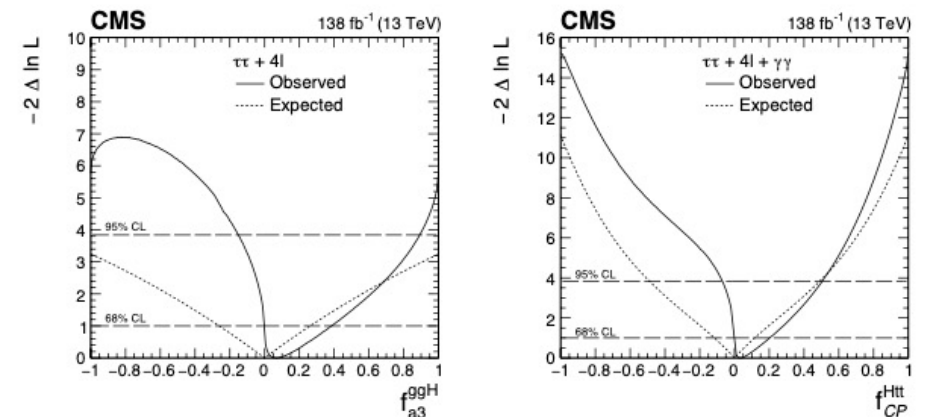


Parameter	Method	Observed		Expected	
		68% CL	95% CL	68% CL	95% CL
f_{a3}^{ggH}	MELA	$0.08^{+0.35}_{-0.08}$	$[-0.09, 0.90]$	0.00 ± 0.36	—
f_{a3}^{ggH}	$\Delta\phi_{ij}$	$0.07^{+0.59}_{-0.19}$	—	0.00 ± 0.39	—
α^{Hff}	MELA	$(11^{+18}_{-10})^\circ$	$[-11, 63]$	$(0 \pm 26)^\circ$	—
α^{Hff}	$\Delta\phi_{ij}$	$(10^{+32}_{-24})^\circ$	—	$(0 \pm 27)^\circ$	—

Parameter	Observed		Expected	
	68% CL	95% CL	68% CL	95% CL
f_{a3}^{ggH}	$0.07^{+0.32}_{-0.07}$	$[-0.15, 0.89]$	0.00 ± 0.26	—
f_{CP}^{Htt}	$0.03^{+0.17}_{-0.03}$	$[-0.07, 0.51]$	0.00 ± 0.12	$[-0.49, 0.49]$

The combined likelihood scans for the Hgg anomalous coupling measurements are shown in Fig. 13, and the allowed 68 and 95% CL intervals are listed in Table 10. The $H \rightarrow \tau\tau$ channel is

more sensitive to f_{a3}^{ggH} than the $H \rightarrow 4l$ channel is, but there is a significant improvement from including both channels in the combination. Previous measurements by the CMS and ATLAS Collaborations [21, 31] were only able to differentiate between the CP -even and CP -odd scenarios with a significance slightly less than 1 standard deviation. With the current measurement, the pure CP -odd scenario is excluded with an observed (expected) significance of 2.4 standard deviations (1.8 standard deviations), which is cross-checked with pseudo-experiments.



OFFSHELL $H \rightarrow ZZ$ IN SMEFT [ATL-PHYS-PUB-2023-012/](#)

The inclusive ggF cross-section in this framework can be calculated and normalized to the SM prediction to yield [6]:

$$\frac{\sigma^{\text{SMEFT}}(c_t, c_g)}{\sigma^{\text{SM}}} \simeq (c_t + c_g)^2 \left(1 - \frac{7}{15} \frac{c_g}{c_t + c_g} \frac{m_H^2}{4m_t^2} \right) \quad (3)$$

In the on-shell Higgs boson region, the mass-dependent term can be neglected, yielding

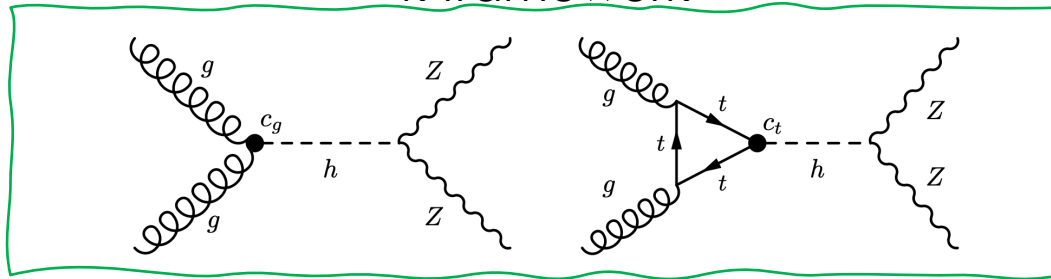
$$\frac{\sigma_{\text{on-shell}}^{\text{SMEFT}}(c_t, c_g)}{\sigma_{\text{on-shell}}^{\text{SM}}} \simeq (c_t + c_g)^2 \quad (4)$$

This is the source of the coupling degeneracy: as the SMEFT on-shell signal strength is only dependent on the sum of c_t and c_g , they cannot be measured separately in the on-shell regime. However, for the off-shell Higgs production, for which $m_{ZZ} > m_t$, the mass term in Equation 3 can no longer be ignored. Therefore, measurements using off-shell events can probe c_t and c_g separately.

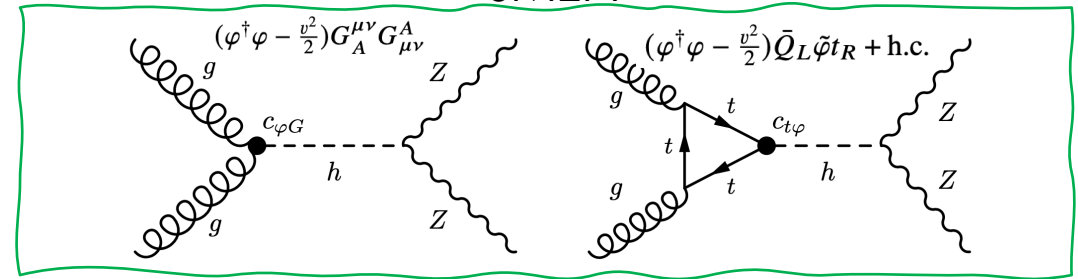
OFFSHELL $H \rightarrow ZZ$ IN SMEFT [ATL-PHYS-PUB-2023-012/](#)

- $ZZ \rightarrow 4l$ and $ZZ \rightarrow 2l2\nu$ final states, with $l = e$ or μ

k-framework



SMEFT

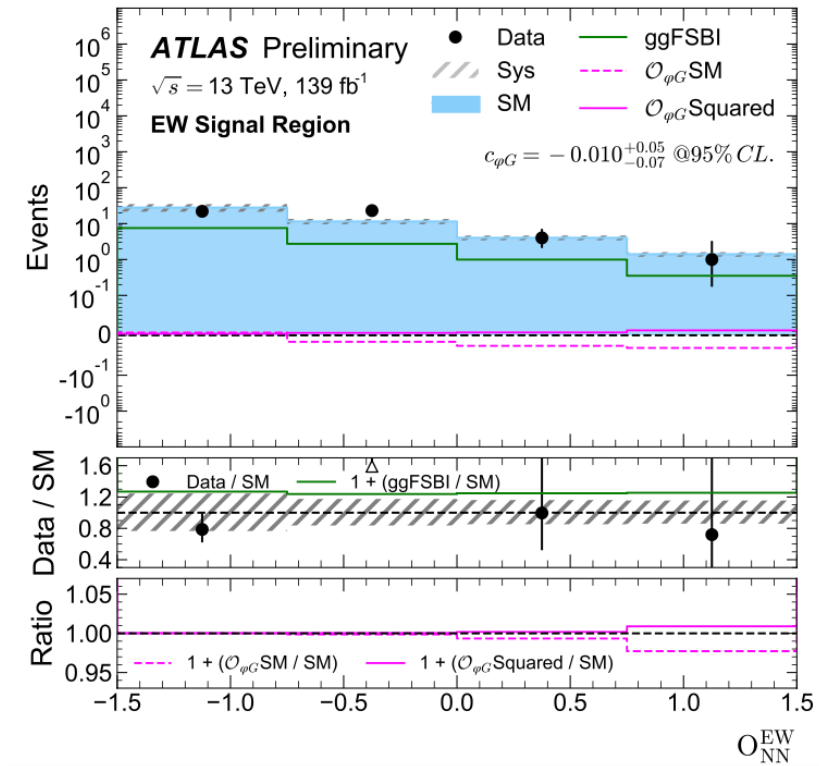
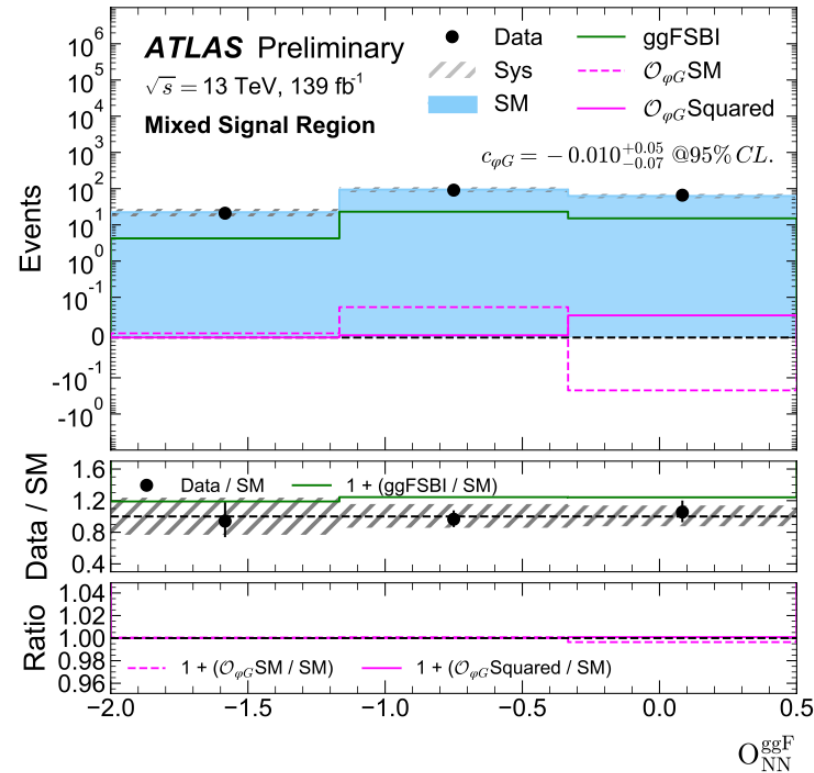
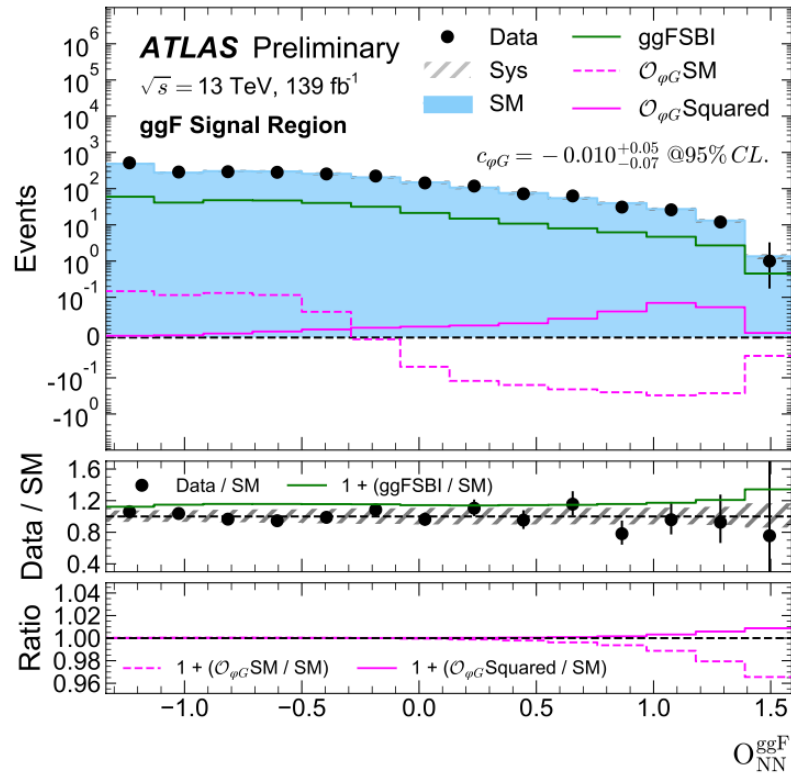


$$c_{t\varphi} = -\frac{y_t \Lambda^2}{v^2} (c_t - 1)$$

$$c_{\varphi G} = \frac{g_s^2 \Lambda^2}{48\pi^2 v^2} c_g$$

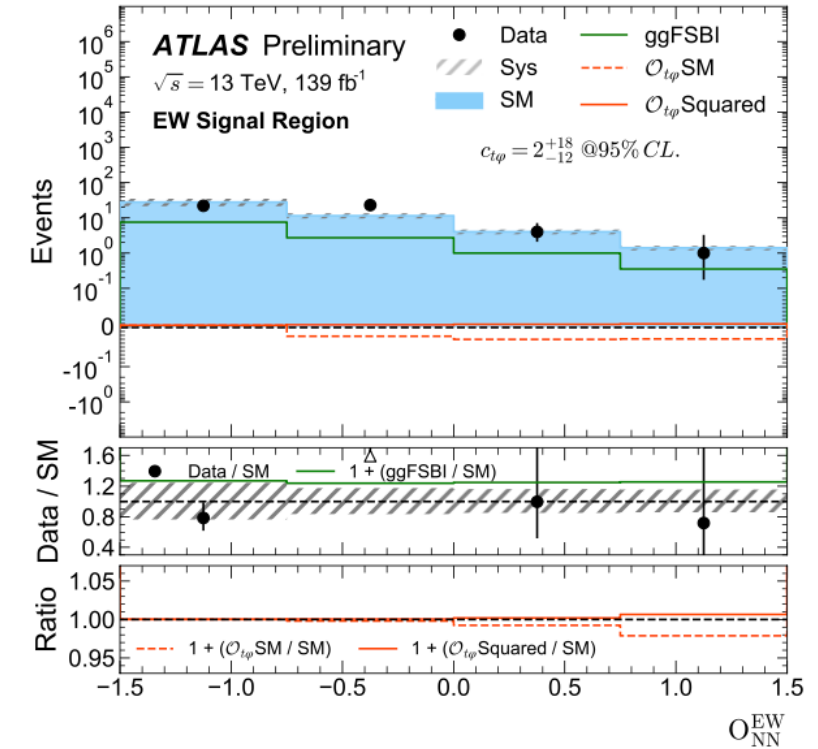
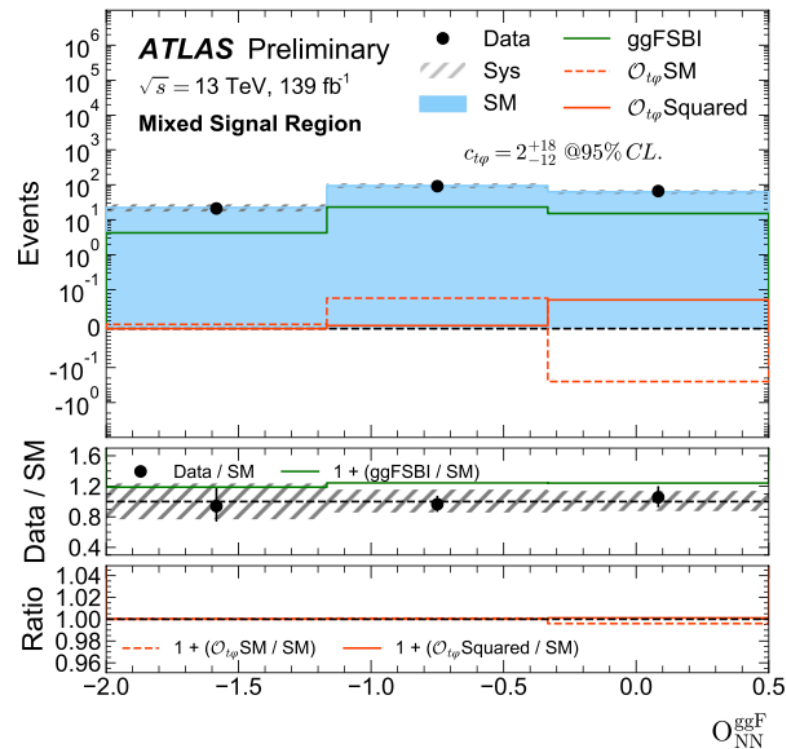
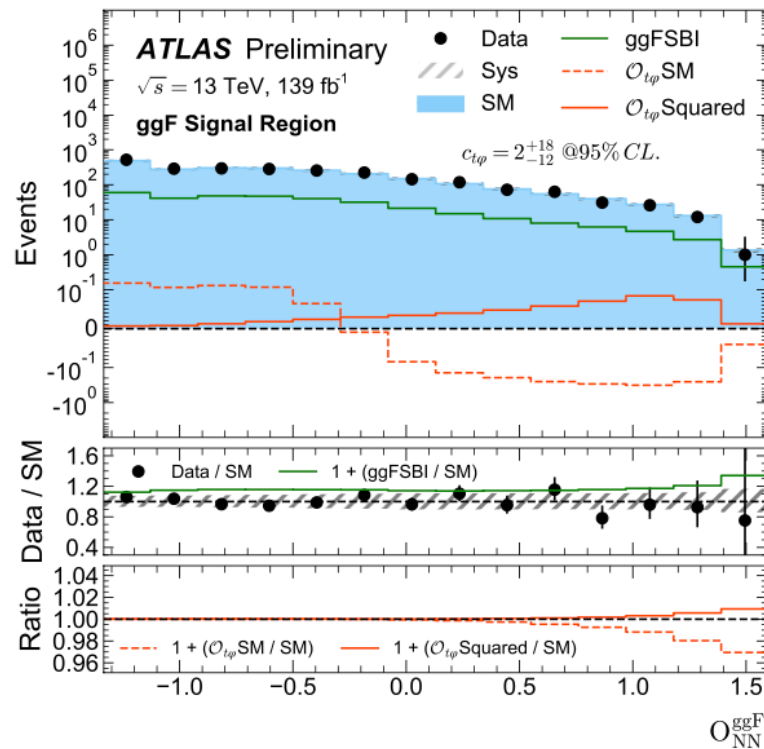
OFFSHELL $H \rightarrow ZZ$ IN SMEFT [ATL-PHYS-PUB-2023-012/](#)

$$ZZ \rightarrow 4l \quad \mathcal{O}_{NN} = \log_{10} \frac{P_S}{P_B + P_{NI}}$$



OFFSHELL $H \rightarrow ZZ$ IN SMEFT ATL-PHYS-PUB-2023-012/

$ZZ \rightarrow 4l$ $O_{NN} = \log_{10} \frac{P_S}{P_B + P_{NI}}$ Signal, back-ground and non interfering bkg

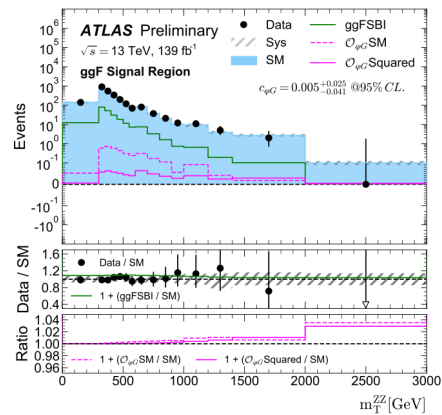


OFFSHELL $H \rightarrow ZZ$ IN SMEFT

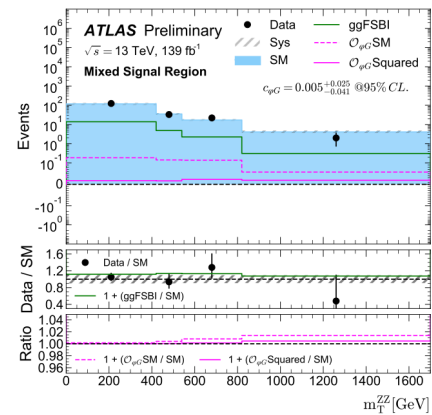
ATL-PHYS-PUB-2023-012/

$ZZ \rightarrow 2l2\nu$

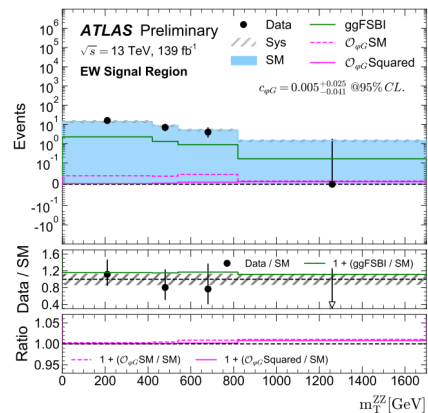
$$m_T^{ZZ} \equiv \sqrt{\left[\sqrt{m_Z^2 + (p_T^{\ell\ell})^2} + \sqrt{m_Z^2 + (E_T^{\text{miss}})^2} \right]^2 - \left| \vec{p}_T^{\ell\ell} + \vec{E}_T^{\text{miss}} \right|^2}$$



(a)



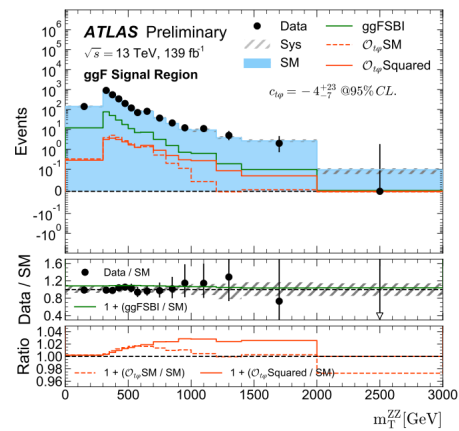
(b)



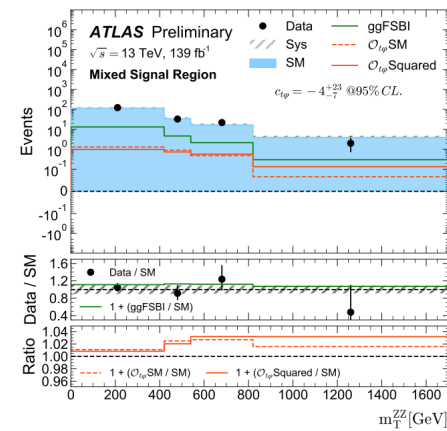
OFFSHELL $H \rightarrow ZZ$ IN SMEFT

[ATL-PHYS-PUB-2023-012/](#)
 $ZZ \rightarrow 2\ell 2\nu$

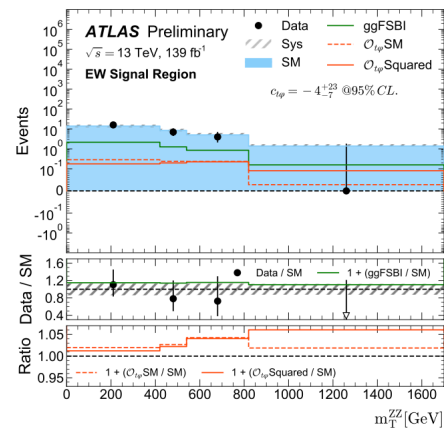
$$m_T^{ZZ} \equiv \sqrt{\left[\sqrt{m_Z^2 + (p_T^{\ell\ell})^2} + \sqrt{m_Z^2 + (E_T^{\text{miss}})^2} \right]^2 - \left| \vec{p}_T^{\ell\ell} + \vec{E}_T^{\text{miss}} \right|^2}$$



(a)

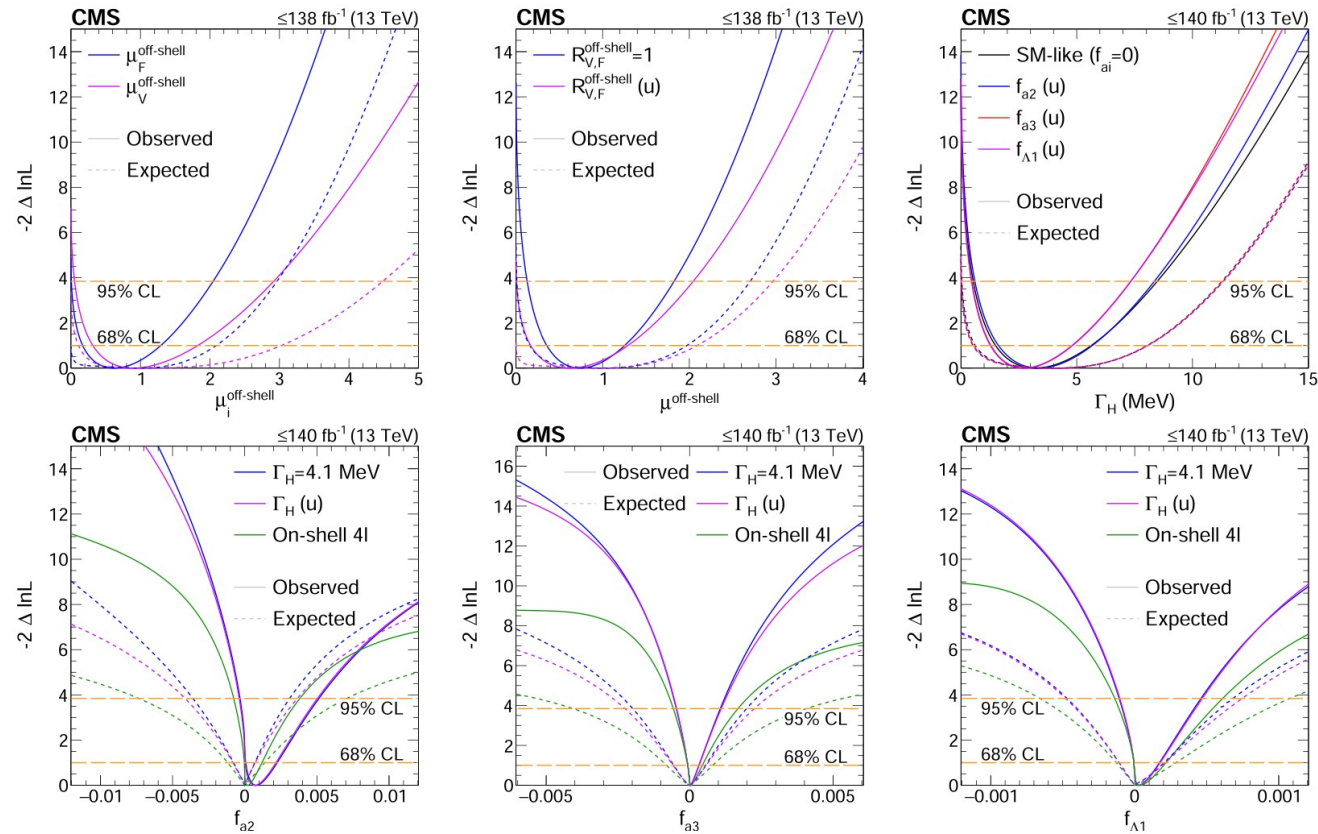


(b)



OFFSHELL $H \rightarrow ZZ$

<https://www.nature.com/articles/s41567-022-01682-0>

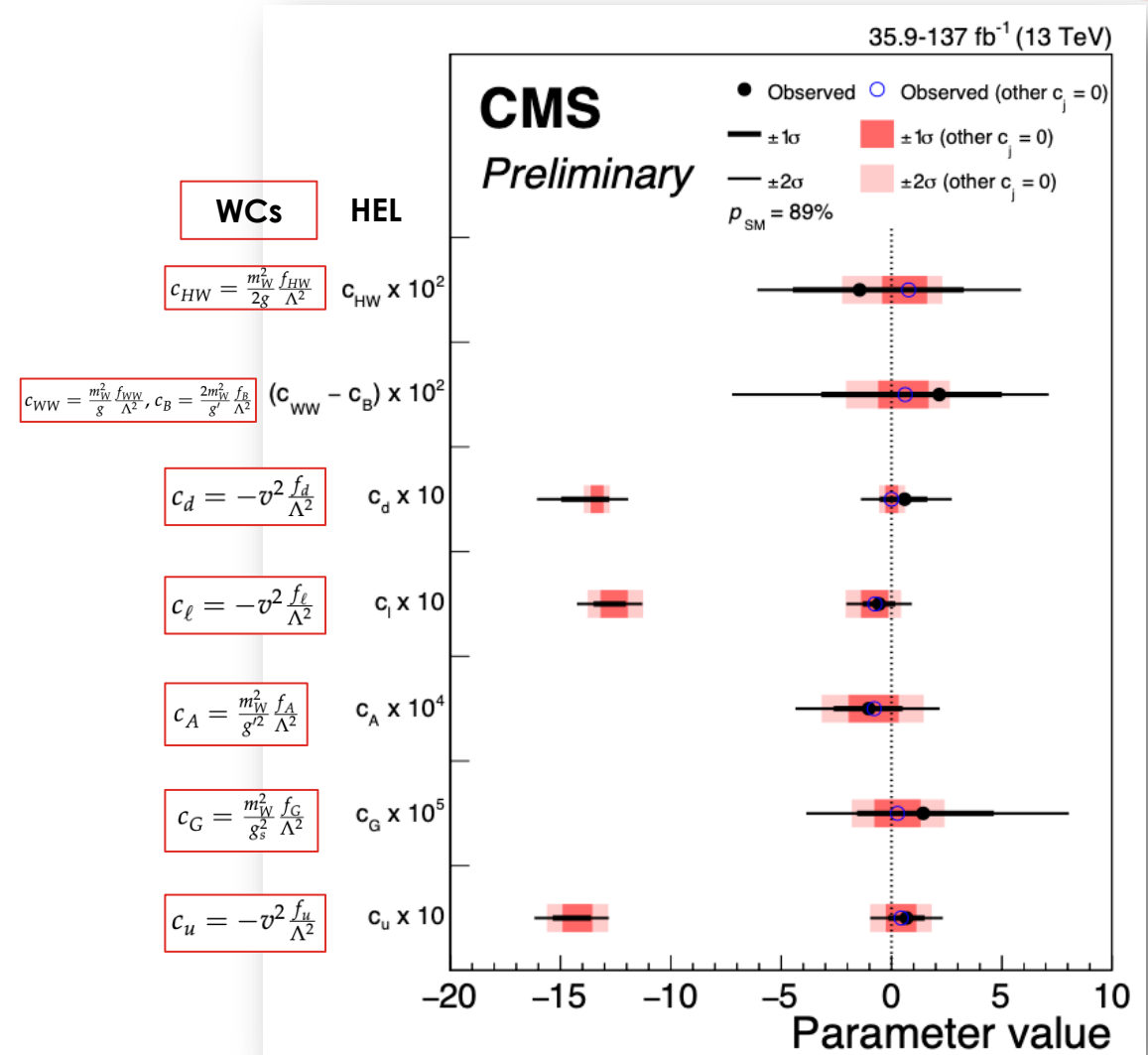


Extended Data Fig. 8 | Log-likelihood scans of the off-shell signal strengths, Γ_H and f_{ai} . Top panels: The likelihood scans are shown for $\mu_F^{\text{off-shell}}$ or $\mu_V^{\text{off-shell}}$ (left), $\mu^{\text{off-shell}}$ (middle), and Γ_H (right). Scans for $\mu_F^{\text{off-shell}}$ (blue) and $\mu_V^{\text{off-shell}}$ (magenta) are obtained with the other parameter unconstrained. Those for $\mu^{\text{off-shell}}$ are shown with (blue) and without (magenta) the constraint $R_{V,F}^{\text{off-shell}} (= \mu_V^{\text{off-shell}} / \mu_F^{\text{off-shell}}) = 1$. Constraints on Γ_H are shown with and without anomalous HVV couplings. Bottom panels: The likelihood scans of the anomalous HVV coupling parameters f_{a2} (left), f_{a3} (middle), and $f_{\lambda 1}$ (right) are shown with the constraint $\Gamma_H = \Gamma_H^{\text{SM}} = 4.1$ MeV (blue), Γ_H unconstrained (magenta), or based on on-shell $4l$ data only (green). Observed (expected) scans are shown with solid (dashed) curves. The horizontal lines indicate the 68% ($-2\Delta \ln \mathcal{L} = 1.0$) and 95% ($-2\Delta \ln \mathcal{L} = 3.84$) CL regions. The integrated luminosity reaches up to 138 fb^{-1} when only off-shell information is used, and up to 140 fb^{-1} when on-shell $4l$ events are included.

CMS HIGGS COMBINATION

[HIG-19-005-pas](#)

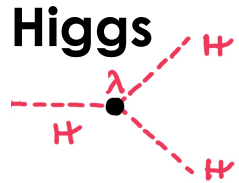
- Interpretation of **Higgs boson production and decay rates** in terms of simultaneous constraints on EFT couplings in the **Higgs Effective Lagrangian (HEL) model**
- Included Higgs boson decays to $\gamma\gamma, ZZ, WW, \tau\tau, bb$ (*non boosted*) @ 13 TeV, 35.9–137 fb^{-1} depending on the analysis



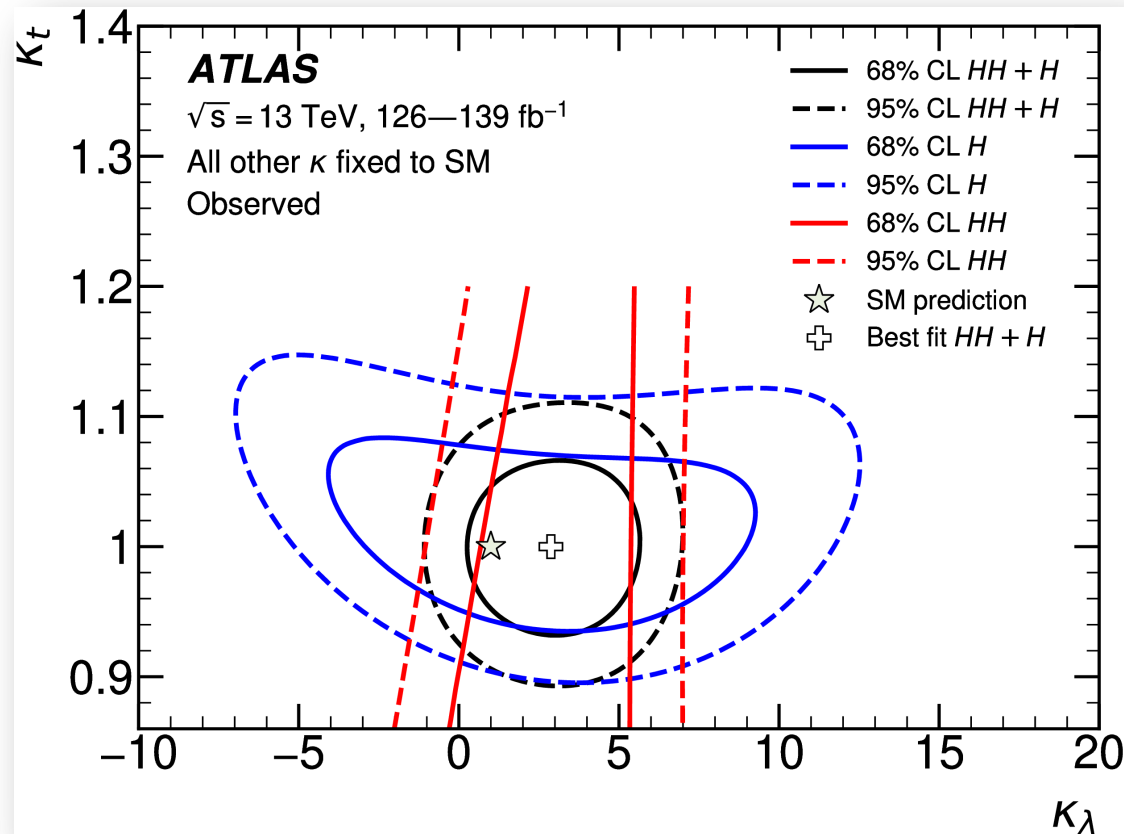
Higgs Pairs

WHY HH? AND WHY IN EFT?

Higgs pairs produced by means of various interactions at the LHC, including the **self-coupling**, λ , giving us *direct* access to its measurement when searching for HH



Complementarity between H & HH clear
already from k framework [i.physletb.2023.137745](https://arxiv.org/abs/2303.13774)



EFT FOR HH

[HiggsPairs-2022_Scyboz.pdf](#)

► SMEFT:

- $H \equiv \text{SU}(2)_L \times U(1)_Y$ doublet
- Canonical dimension counting ($\sim 1/\Lambda^n$)

$$\mathcal{L}_{\text{SMEFT}} = \mathcal{L}_{\text{SM}} + \sum_i \frac{C_i^{(6)}}{\Lambda^2} \mathcal{O}_i^{(6)} + \mathcal{O}\left(\frac{1}{\Lambda^3}\right)$$

► HEFT:

- $H \equiv \text{EW}$ singlet
- Chiral dimension counting d_χ (\equiv loop counting)

$$\mathcal{L}_{\text{HEFT}} = \mathcal{L}_{(d_\chi=2)} + \sum_{L=1}^{\infty} \sum_i \left(\frac{1}{16\pi^2}\right)^L c_i^{(L)} \mathcal{O}_i^{(L)}$$

<https://arxiv.org/pdf/2304.01968.pdf>

$$\begin{aligned} \Delta\mathcal{L}_{\text{Warsaw}} = & \frac{C_{H,\square}}{\Lambda^2} (\phi^\dagger \phi) \square (\phi^\dagger \phi) + \frac{C_{HD}}{\Lambda^2} (\phi^\dagger D_\mu \phi)^* (\phi^\dagger D^\mu \phi) + \frac{C_H}{\Lambda^2} (\phi^\dagger \phi)^3 \\ & + \left(\frac{C_{uH}}{\Lambda^2} \phi^\dagger \phi \bar{q}_L \tilde{\phi} t_R + \text{h.c.} \right) + \frac{C_{HG}}{\Lambda^2} \phi^\dagger \phi G_{\mu\nu}^a G^{\mu\nu,a} \\ & + \frac{C_{uG}}{\Lambda^2} (\bar{q}_L \sigma^{\mu\nu} T^a G_{\mu\nu}^a \tilde{\phi} t_R + \text{h.c.}) . \end{aligned}$$

$$\begin{aligned} \Delta\mathcal{L}_{\text{HEFT}} = & -m_t \left(c_t \frac{h}{v} + c_{tt} \frac{h^2}{v^2} \right) \bar{t} t - c_{hhh} \frac{m_h^2}{2v} h^3 \\ & + \frac{\alpha_s}{8\pi} \left(c_{ggh} \frac{h}{v} + c_{gghh} \frac{h^2}{v^2} \right) G_{\mu\nu}^a G^{a,\mu\nu} . \end{aligned}$$

EFT FOR HH

<https://arxiv.org/pdf/2304.01968.pdf>

Such a translation is given in Table 2.1. However, it has to be used with great care, as the different EFT descriptions rely on different assumptions and therefore are not necessarily translatable into each other. As a consequence, an anomalous coupling configuration which is perfectly valid in HEFT can lie outside the validity range of SMEFT upon such a naive translation. Examples are given in Chapter 3.

HEFT	SILH	Warsaw
c_{hhh}	$1 - \frac{3}{2}\bar{c}_H + \bar{c}_6$	$1 - 2\frac{v^2}{\Lambda^2}\frac{v^2}{m_h^2}C_H + 3\frac{v^2}{\Lambda^2}C_{H,\text{kin}}$
c_t	$1 - \frac{\bar{c}_H}{2} - \bar{c}_u$	$1 + \frac{v^2}{\Lambda^2}C_{H,\text{kin}} - \frac{v^2}{\Lambda^2}\frac{v}{\sqrt{2}m_t}C_{uH}$
c_{tt}	$-\frac{\bar{c}_H+3\bar{c}_u}{4}$	$-\frac{v^2}{\Lambda^2}\frac{3v}{2\sqrt{2}m_t}C_{uH} + \frac{v^2}{\Lambda^2}C_{H,\text{kin}}$
c_{ggh}	$128\pi^2\bar{c}_g$	$\frac{v^2}{\Lambda^2}\frac{8\pi}{\alpha_s}C_{HG}$
c_{gggh}	$64\pi^2\bar{c}_g$	$\frac{v^2}{\Lambda^2}\frac{4\pi}{\alpha_s}C_{HG}$

Table 2.1: Leading order translation between different operator basis choices.

Eq. (2.8)	Ref. [22]	Ref. [64]
c_{hhh}	κ_λ	c_3
c_t	κ_t	c_t
c_{tt}	c_2	$c_{tt}/2$
c_{ggh}	$\frac{2}{3}c_g$	$8c_g$
c_{gggh}	$-\frac{1}{3}c_{2g}$	$4c_{gg}$

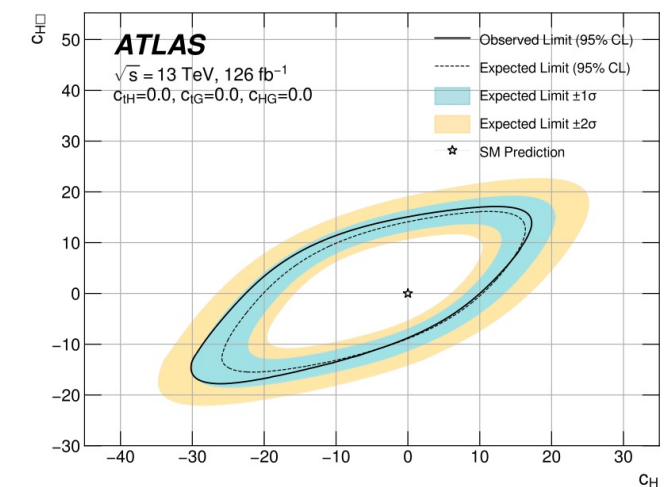
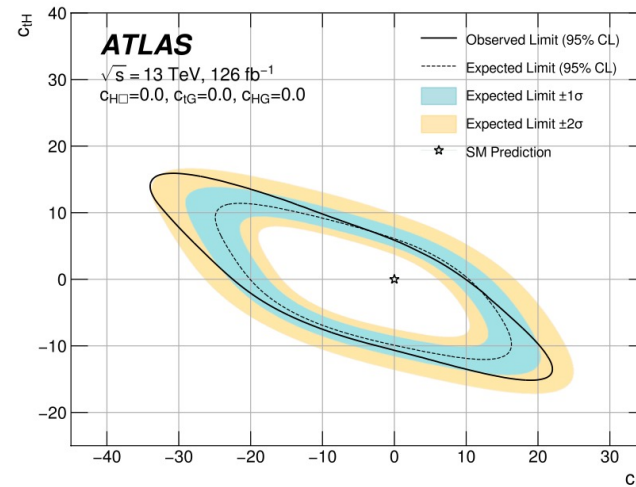
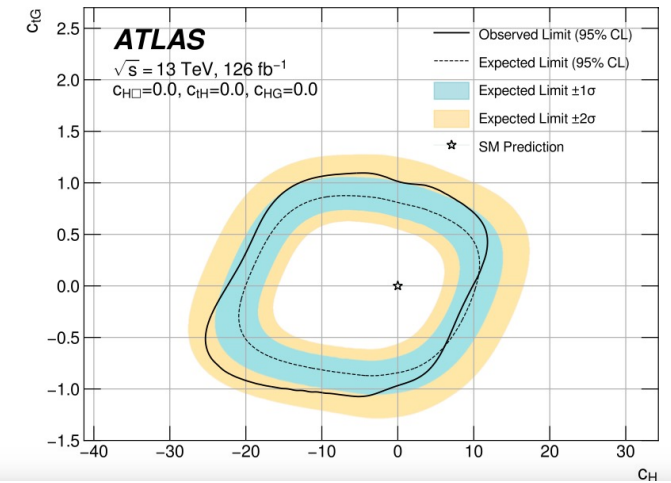
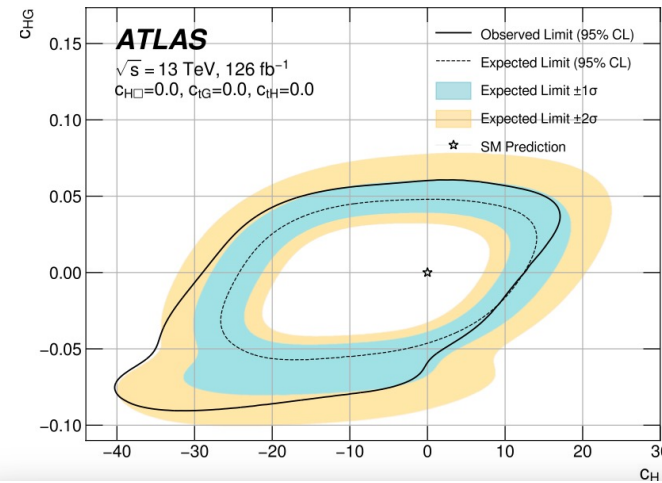
Table 3.1: Translation between different conventions for the definition of the anomalous couplings.

HIGGS PAIRS IN SMEFT [2301.03212](#)

$$\mathcal{L}_{\text{SMEFT}} = \mathcal{L}_{\text{SM}} + \frac{1}{\Lambda^2} \sum_k c_k^{(6)} O_k^{(6)}$$

Wilson Coefficient	Operator
c_H	$(H^\dagger H)^3$
$c_{H\Box}$	$(H^\dagger H)\Box(H^\dagger H)$
c_{tH}	$(H^\dagger H)(\bar{Q}\tilde{H}t)$
c_{HG}	$H^\dagger H G_{\mu\nu}^A G^{\mu\nu}_A$
c_{tG}	$(\bar{Q}\sigma^{\mu\nu}T^A t)\tilde{H}G_{\mu\nu}^A$

ATLAS $HH \rightarrow 4b$



HIGGS PAIRS IN SMEFT [2301.03212](#)

$$\mathcal{L}_{\text{SMEFT}} = \mathcal{L}_{\text{SM}} + \frac{1}{\Lambda^2} \sum_k c_k^{(6)} O_k^{(6)}$$

ATLAS $HH \rightarrow 4b$

Wilson Coefficient	Operator
c_H	$(H^\dagger H)^3$
$c_{H\Box}$	$(H^\dagger H)\Box(H^\dagger H)$
c_{tH}	$(H^\dagger H)(\bar{Q}\tilde{H}t)$
c_{HG}	$H^\dagger H G_{\mu\nu}^A G_A^{\mu\nu}$
c_{tG}	$(\bar{Q}\sigma^{\mu\nu}T^A t)\tilde{H}G_{\mu\nu}^A$

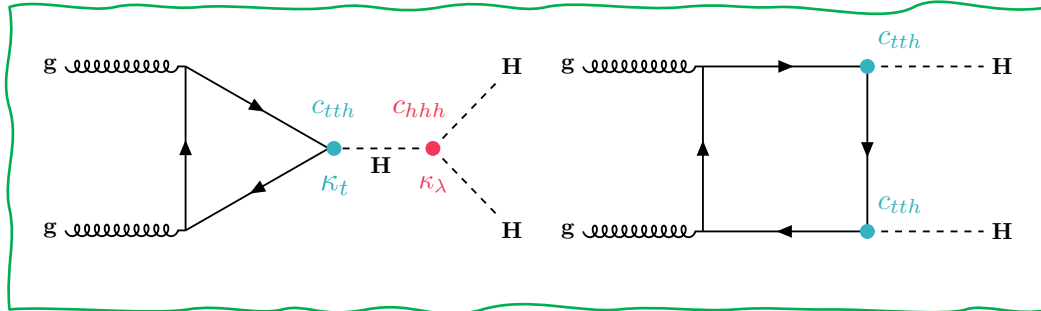
Table 10: The extracted upper and lower limits on the SMEFT parameters to which the analysis is sensitive. For each parameter, the constraints are provided assuming the other parameters are fixed to 0. The VBF HH process is ignored for this result.

Parameter	Expected Constraint		Observed Constraint	
	Lower	Upper	Lower	Upper
c_H	-20	11	-22	11
c_{HG}	-0.056	0.049	-0.067	0.060
$c_{H\Box}$	-9.3	13.9	-8.9	14.5
c_{tH}	-10.0	6.4	-10.7	6.2
c_{tG}	-0.97	0.94	-1.12	1.15

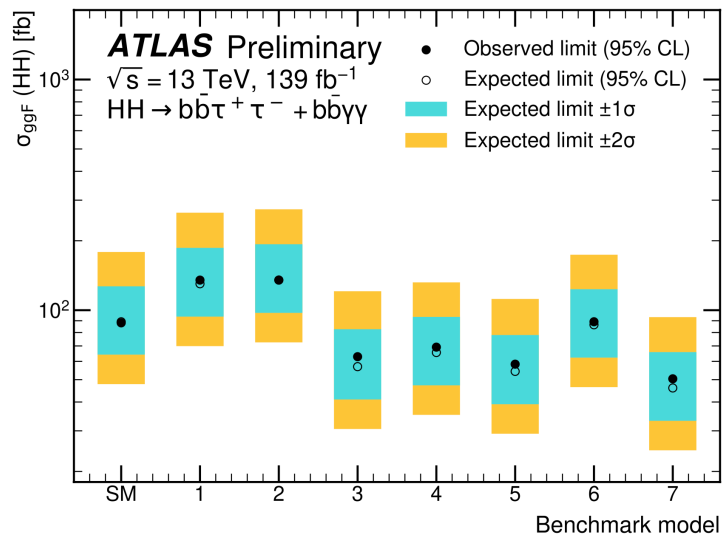
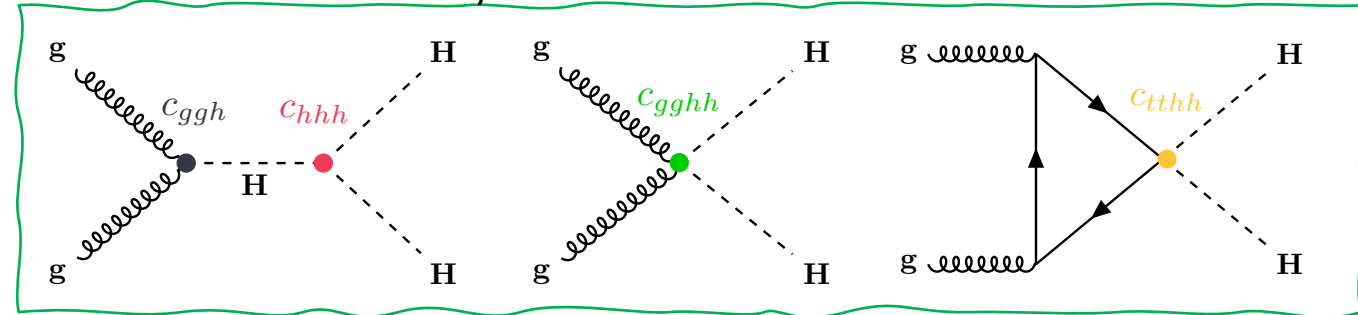
HIGGS PAIRS IN HEFT HDBS-2019-29, ATL-PHYS-PUB-2022-019/

- ATLAS $HH \rightarrow \gamma\gamma bb$ and $HH \rightarrow bb\tau\tau$ combined, results available also from $HH \rightarrow 4b$
- In HEFT, anomalous single-Higgs-boson and HH couplings defined separately

Standard Model



Beyond Standard Model



Benchmark model	C_{hhh}	C_{tth}	C_{ggh}	C_{gghh}	C_{tthh}
SM	1	1	0	0	0
BM 1	3.94	0.94	1/2	1/3	-1/3
BM 2	6.84	0.61	0.0	-1/3	1/3
BM 3	2.21	1.05	1/2	1/2	-1/3
BM 4	2.79	0.61	-1/2	1/6	1/3
BM 5	3.95	1.17	1/6	-1/2	-1/3
BM 6	5.68	0.83	-1/2	1/3	1/3
BM 7	-0.10	0.94	1/6	-1/6	1

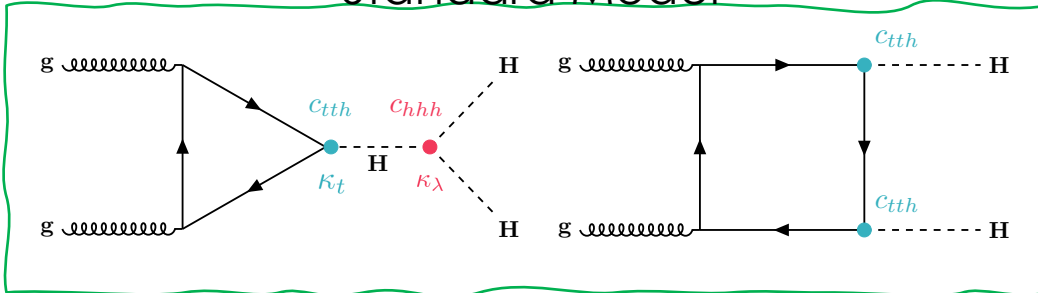
M. Capozzi and G. Heinrich,
*Exploring anomalous couplings in
 Higgs boson pair production through
 shape analysis, JHEP 03 (2020) 091,*
 arXiv: [1908.08923 \[hep-ph\]](https://arxiv.org/abs/1908.08923).

HIGGS PAIRS IN HEFT

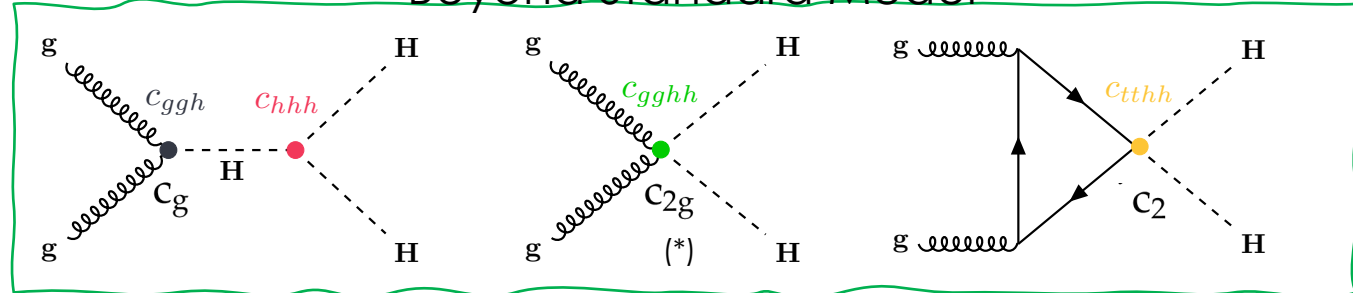
[2301.03212](#), [ATL-PHYS-PUB-2022-019](#), [JHEP 03 \(2021\) 257](#)

In HEFT, anomalous **single-Higgs couplings** \neq **HH couplings** ($c_{ggHH} \neq c_{ggH}, c_{ttHH} \neq c_{tth}$)

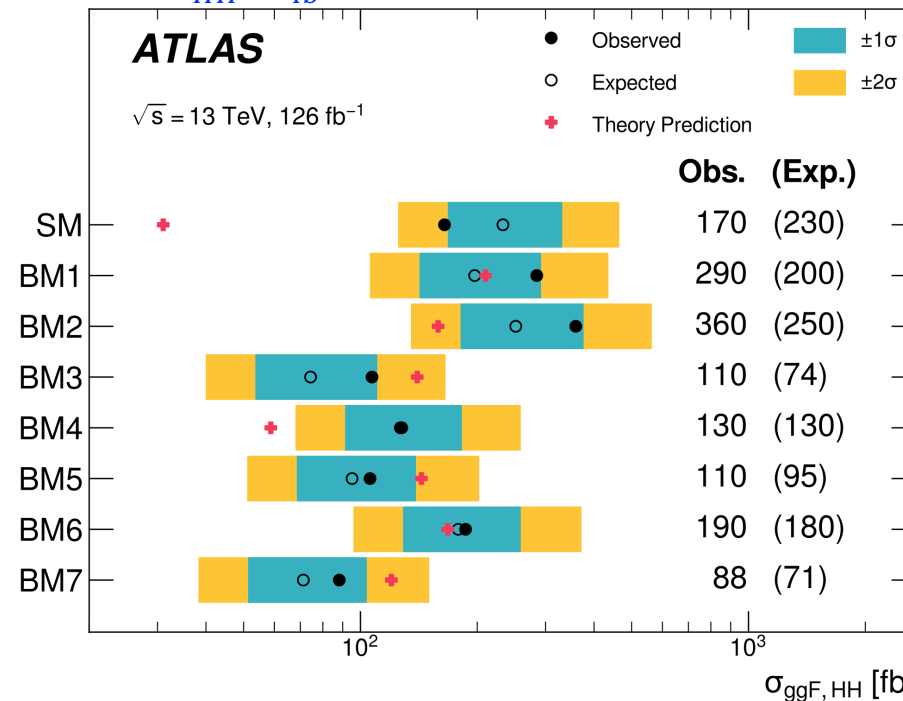
Standard Model



Beyond Standard Model



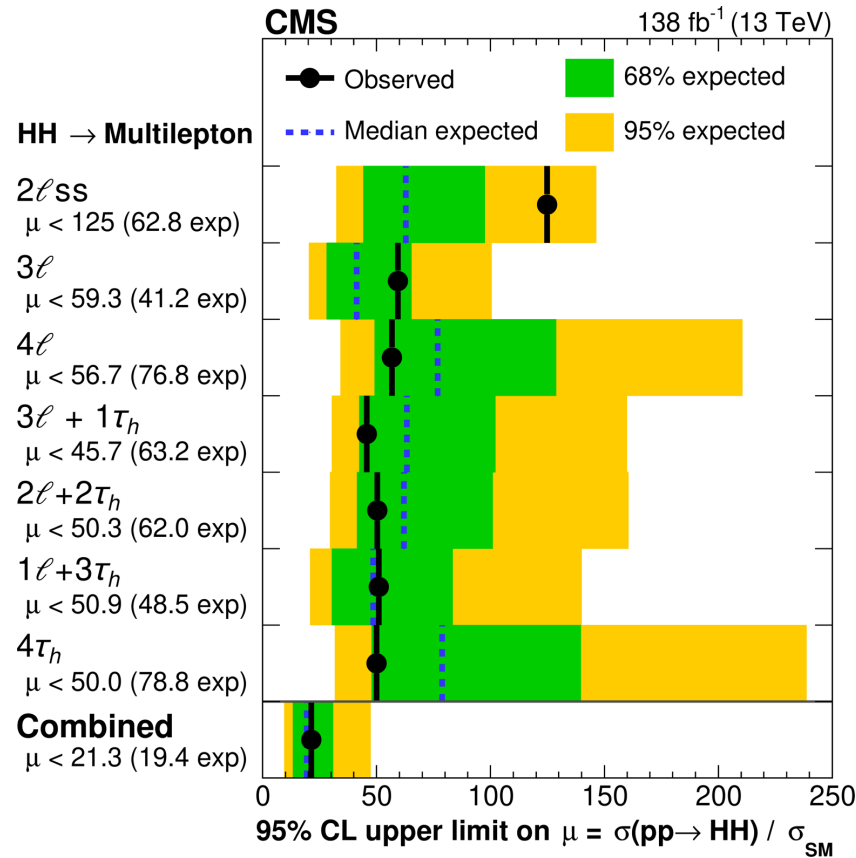
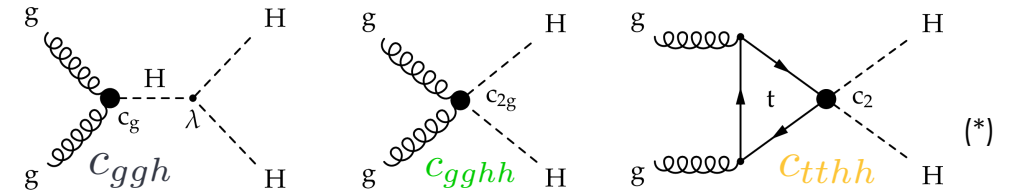
$HH \rightarrow 4b$



(*) In black the CMS WCs convention, in colors the ATLAS one

HIGGS PAIRS IN HEFT 2206.10268

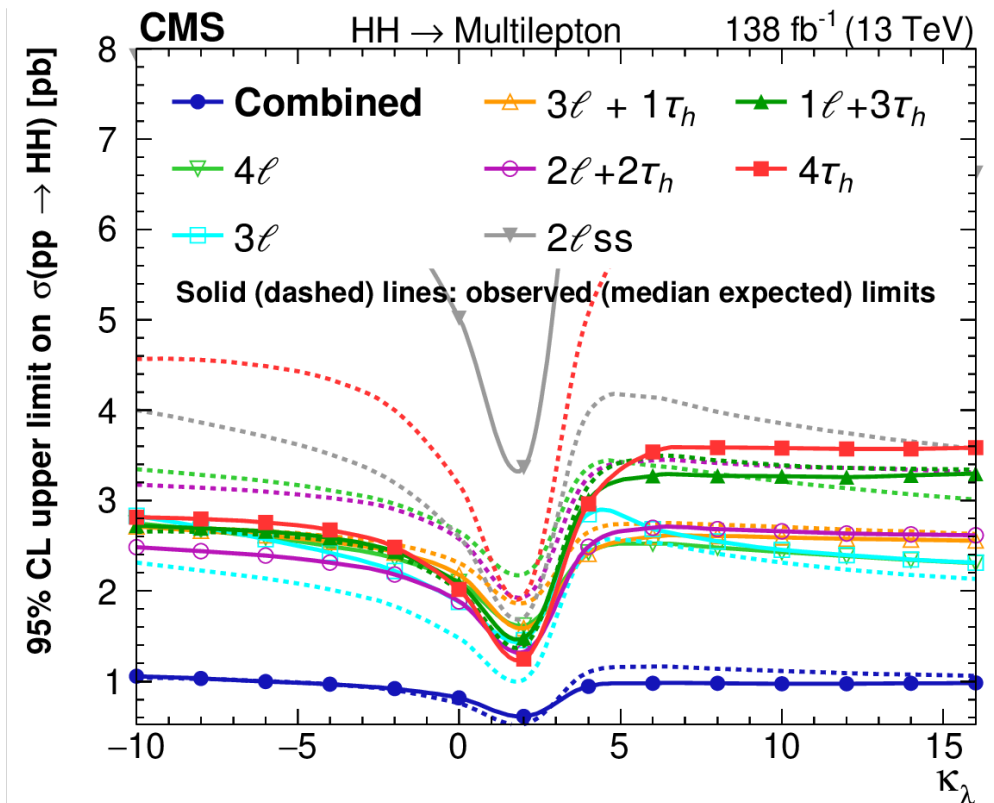
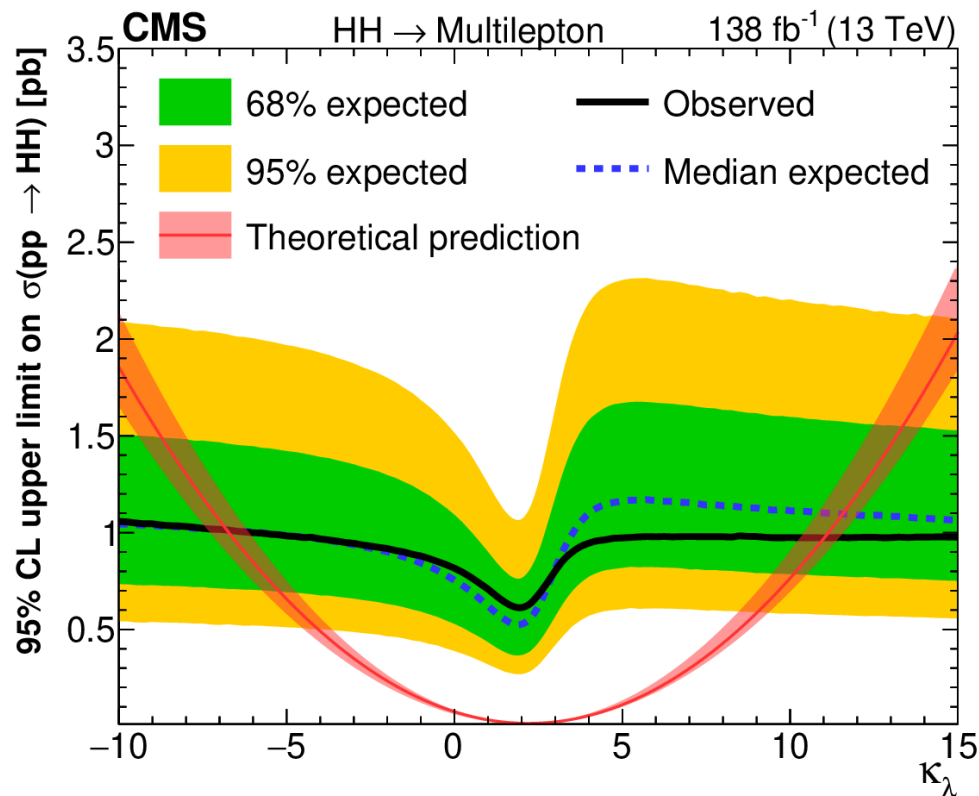
- CMS full Run 2 search for $HH \rightarrow WWWW, WW\tau\tau, \text{ and } \tau\tau\tau$
- Require multi-leptons (e, μ, τ_{had}) in the final state



(*) In black the CMS WCs convention, in colors the ATLAS one

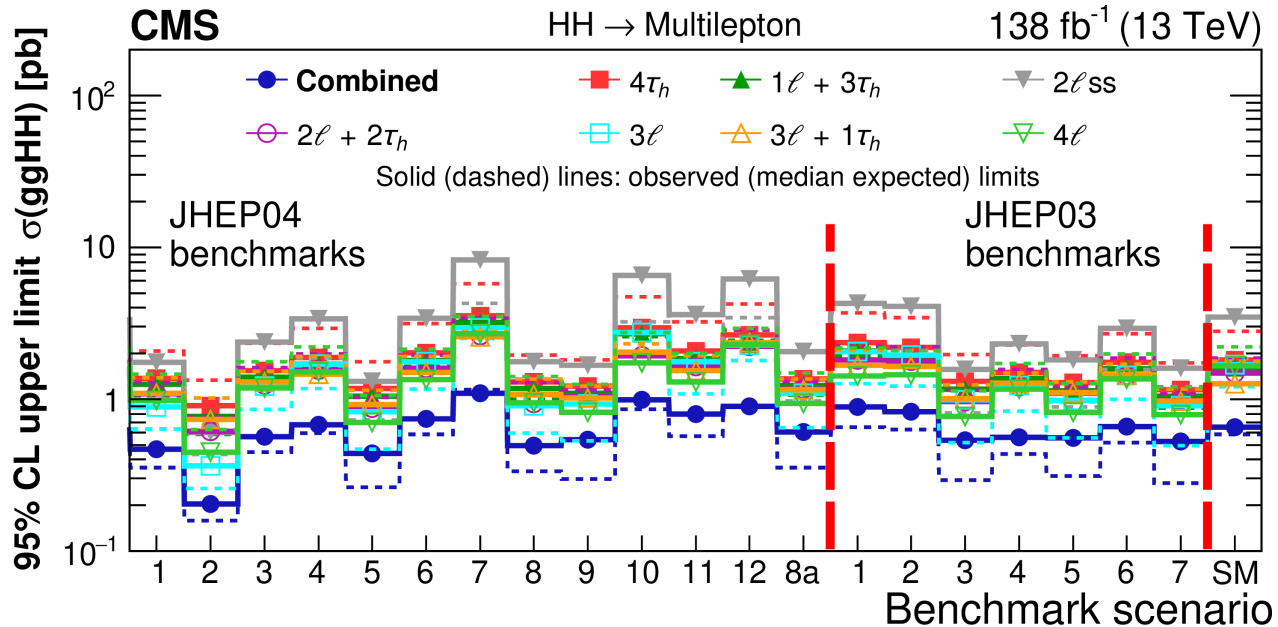
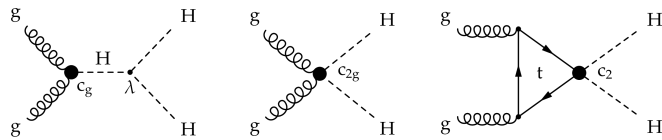
HIGGS PAIRS IN HEFT HIG-21-002

- CMS full Run 2 search for $HH \rightarrow WWWW, WW\tau\tau, \text{ and } \tau\tau\tau\tau$
- Require 2, 3, or 4 leptons (e, μ, τ_{had})
- Observed (expected) upper limit on cross section at 95% confidence level (CL) is 21.3 (19.4) x SM



HIGGS PAIRS IN HEFT HIG-21-002

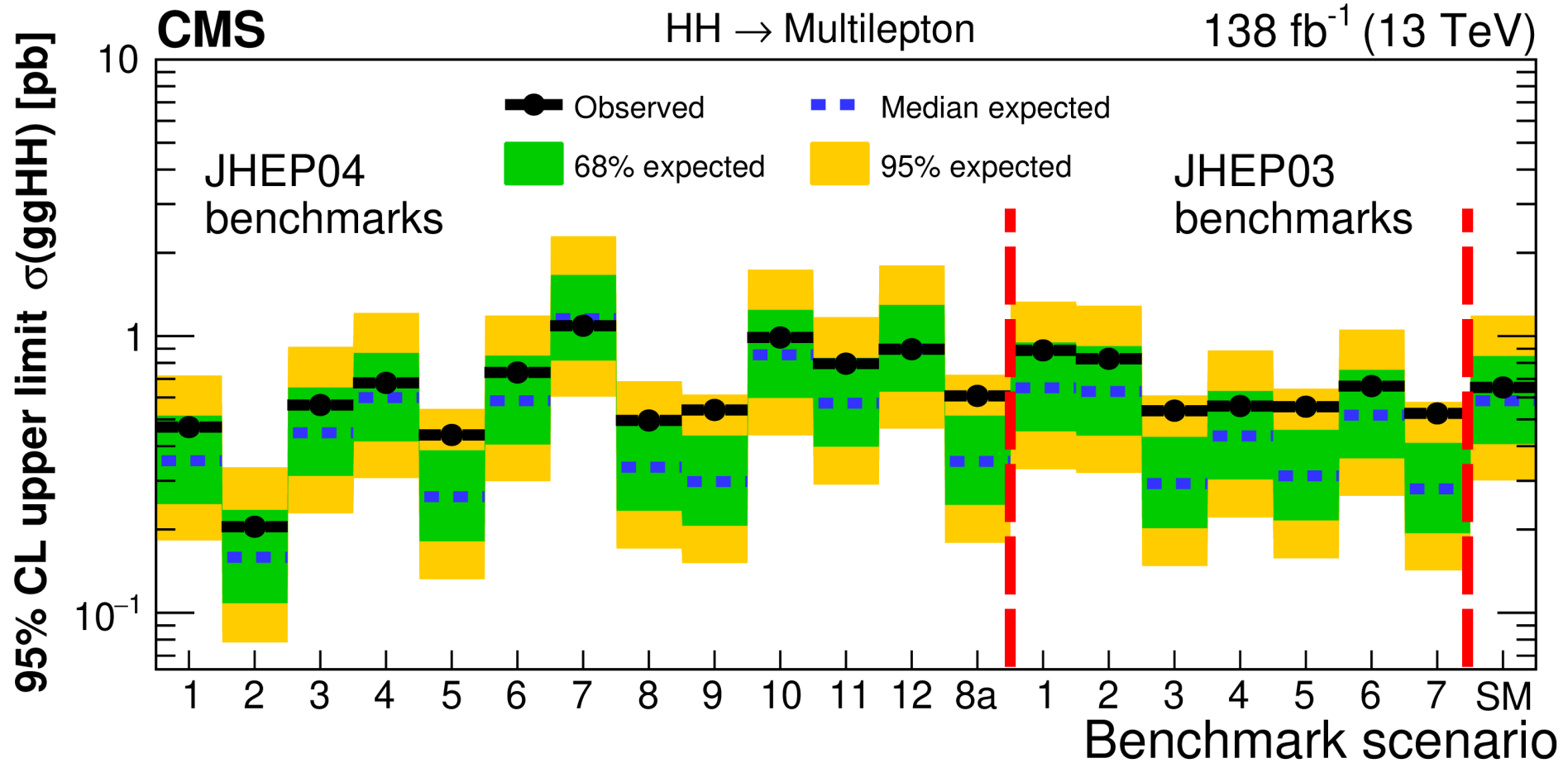
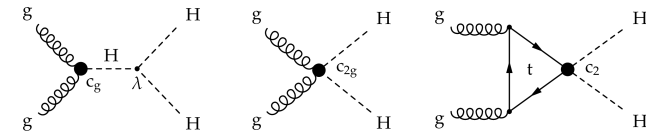
- CMS full Run 2 search for $HH \rightarrow WWWW, WW\tau\tau, \text{ and } \tau\tau\tau\tau$
- Require 2, 3, or 4 leptons (e, μ, τ_{had})
- Observed (expected) upper limit on cross section at 95% confidence level (CL) is 21.3 (19.4) x SM



Benchmark	κ_λ	κ_t	c_2	c_g	c_{2g}
JHEP04 BM1	7.5	1.0	-1.0	0.0	0.0
JHEP04 BM2	1.0	1.0	0.5	-0.8	0.6
JHEP04 BM3	1.0	1.0	-1.5	0.0	-0.8
JHEP04 BM4	-3.5	1.5	-3.0	0.0	0.0
JHEP04 BM5	1.0	1.0	0.0	0.8	-1.0
JHEP04 BM6	2.4	1.0	0.0	0.2	-0.2
JHEP04 BM7	5.0	1.0	0.0	0.2	-0.2
JHEP04 BM8	15.0	1.0	0.0	-1.0	1.0
JHEP04 BM8a	1.0	1.0	0.5	4/15	0.0
JHEP04 BM9	1.0	1.0	1.0	-0.6	0.6
JHEP04 BM10	10.0	1.5	-1.0	0.0	0.0
JHEP04 BM11	2.4	1.0	0.0	1.0	-1.0
JHEP04 BM12	15.0	1.0	1.0	0.0	0.0
JHEP03 BM1	3.94	0.94	-1/3	0.75	-1
JHEP03 BM2	6.84	0.61	1/3	0	1
JHEP03 BM3	2.21	1.05	-1/3	0.75	-1.5
JHEP03 BM4	2.79	0.61	1/3	-0.75	-0.5
JHEP03 BM5	3.95	1.17	-1/3	0.25	1.5
JHEP03 BM6	5.68	0.83	1/3	-0.75	-1
JHEP03 BM7	-0.10	0.94	1	0.25	0.5
SM	1.0	1.0	0.0	0.0	0.0

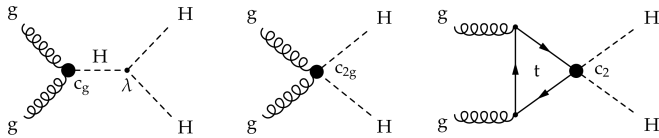
HIGGS PAIRS IN HEFT 2206.10268

- CMS full Run 2 search for $HH \rightarrow WWWW, WW\tau\tau, \text{ and } \tau\tau\tau$
- Require multi-leptons (e, μ, τ_{had}) in the final state



HIGGS PAIRS IN HEFT [HIG-21-002](#)

- CMS full Run 2 search for $HH \rightarrow WWWW, WW\tau\tau, \text{ and } \tau\tau\tau\tau$
- Require 2, 3, or 4 leptons (e, μ, τ_{had})
- Observed (expected) upper limit on cross section at 95% confidence level (CL) is 21.3 (19.4) x SM



JHEP04 benchmark	Observed (expected) limit [fb]
BM1	469 (354)
BM2	205 (159)
BM3	563 (447)
BM4	677 (600)
BM5	439 (263)
BM6	739 (584)
BM7	1090 (1156)
BM8	495 (336)
BM9	541 (298)
BM10	988 (855)
BM11	795 (572)
BM12	897 (898)
BM8a	608 (353)

JHEP03 benchmark	Observed (expected) limit [fb]
BM1	888 (650)
BM2	828 (632)
BM3	538 (293)
BM4	559 (436)
BM5	556 (313)
BM6	660 (518)
BM7	525 (280)